

Regulation of transcriptional intermediary factor 1 γ by adenovirus

Pól Ó Catnaigh

Report of work submitted for the MSc in Cancer Cell and Molecular Biology in
the Department of Biochemistry, University of Leicester, July 2011

Regulation of transcriptional intermediary factor 1 γ by adenovirus

Pól Ó Catnaigh

Abstract

The transcriptional repressor, E3 ubiquitin ligase and putative tumour suppressor TIF1 γ /TRIM33/Ectodermin is involved in embryological development and haematopoiesis. It antagonises the TGF- β pathway by preventing downstream signalling through SMAD4. Recent observations suggested that absolute cellular levels of TIF1 γ fall dramatically post-infection with different adenoviral serotypes, including Ad5 and Ad12. Given the functional similarities between the usurpation of the cellular machinery by adenovirus and the cellular reprogramming that occurs in cancer, it was considered useful to investigate adenoviral regulation of TIF1 γ .

Western blot findings confirmed a reduction in cellular TIF1 γ levels following Ad5 or Ad12 infection. TIF1 β /TRIM28 levels did not fall, however, suggesting selective regulation of TIF1 γ . TIF1 γ interacted with the adenoviral E1B-55kDa oncoprotein in adenoviral transformed cells and immunofluorescence microscopy implied that they co-localised in cytoplasmic aggresome-like structures.

As E1B-55kDa and E4orf3 can cooperatively mediate protein degradation, further work examined the role of Ad5 E4orf3 in the regulation of TIF1 γ . Confocal microscopy revealed that TIF1 γ co-localised with PML in nuclear tracts in adenovirus-infected cells. Similar nuclear co-localisation of TIF1 γ with Ad5 E4orf3 was shown 18 hours post-infection and with Ad12 E4orf3 in transfected HeLa cells.

E4orf3- mutant Ad5 infection failed to abate TIF1 γ levels, implying a necessary role for E4orf3 in the process. Interestingly, the adenoviral E3 ubiquitin ligase remained functional as p53 was still degraded. Ad5 E4orf3 transcriptional repression of p53-dependent gene expression was shown not to be required to attenuate TIF1 γ levels.

To identify novel E4orf3-interactors, immunoprecipitation followed by mass spectrometry was performed. The data suggested UBE4A as a promising potential regulator of TIF1 γ .

To conclude, E4orf3 plays a necessary role reducing cellular TIF1 γ levels during Ad5 infection, although it remains to be seen if this phenomenon involves the Ad5 E3 ubiquitin ligase or a novel mechanism.

Keywords: adenovirus, transcriptional intermediary factor 1 γ , tripartite motif containing protein 33, transcriptional repressor, tumour suppressor, protein regulation.

Acknowledgements

I owe a special debt of gratitude to my supervisor, Dr. Andrew Turnell, who provided me with continuous support and encouragement throughout my time at Birmingham. I was also fortunate enough to have recourse to the practical expertise of Dr. Roger Grand when Andy was not available. I also wish to thank the other members of my lab for their friendship, helpful advice and practical insights, without which my days would have been much longer and less enjoyable.

I greatly appreciated being able to call upon Dr. Ashley Martin's technical knowledge and computing acumen during the periods I spent in his lab obtaining and interpreting mass spectrometry data.

Away from Birmingham, I wish to thank all the helpful academic and administrative staff in the Department of Biochemistry at Leicester. Finally, a special mention is due to Dr. Sally Prigent for kindly arranging this project for me at Birmingham and being available to provide me with helpful advice and information throughout its duration.

Contents

Title Page.....	i
Abstract.....	ii
Acknowledgements.....	iii
Contents Page.....	iv
List of Figures.....	vii
List of Tables.....	ix
List of Abbreviations.....	x
Chapter 1: Introduction.....	1
1.1 Adenovirus and cancer – an overview.....	1
1.2 Adenoviral genome.....	2
1.3 Prevention of adenoviral genome concatemerisation	3
1.4 Promyelocytic leukaemia protein oncogenic domains.....	3
1.5 Ubiquitin-proteasome pathway of protein degradation.....	3
1.6 Adenoviral oncogenic and transformation potential.....	5
1.7 Function of proteins encoded by selected early region transcription units.....	8
1.7.1 E1A.....	8
1.7.2 E1B.....	9
1.7.3 E4orf3.....	10
1.7.4 E4orf6.....	11
1.8 Transcriptional Intermediary Factor 1 (TIF1).....	13
1.9 TIF1 γ	14
1.10 Aims.....	16
Chapter 2: Materials and methods.....	18
2.1 Materials.....	18
2.1.1 Suppliers of chemicals, reagents and media.....	18
2.1.2 Human cell lines used	20
2.1.3 Viruses and plasmids.....	20
2.1.4 Antibodies.....	21
2.2 Methods.....	22
2.2.1 Cell culture.....	22
2.2.2 Generation of E4orf3-expressing clonal cell lines.....	23
2.2.3 Transfections with calcium chloride.....	24

2.2.4	Viral infections.....	24
2.2.5	Cell lysis.....	24
2.2.6	Sonication and centrifugation.....	25
2.2.7	Protein quantification.....	25
2.2.8	Sodium dodecylsulphate polyacrylamide gel electrophoresis (SDS-PAGE)..	25
2.2.9	Gel transfer.....	26
2.2.10	Confirmation that proteins had transferred onto the membrane.....	27
2.2.11	Blocking.....	27
2.2.12	Probing with antibodies for Western blotting.....	27
2.2.13	Developing blots.....	27
2.2.14	Immunoprecipitation.....	28
2.2.15	Immunofluorescence.....	28
2.2.16	Mass spectrometry.....	29
2.2.16.i	Preparation of samples.....	29
2.2.16.ii	Analysis of data.....	32
Chapter 3: Results.....		33
3.1	Effect of adenoviral infection on absolute levels of certain cellular proteins.....	33
3.2	Interaction of E1B-55kDa with TIF1 γ and other cellular proteins.....	35
3.3	Demonstration of TIF1 γ and E1B-55kDa co-localisation using immunofluorescence microscopy.....	37
3.4	Demonstration of TIF1 γ and PML/E4orf3 co-localisation using immunofluorescence microscopy.....	39
3.5	E4orf3 is necessary for the reduction in TIF1 γ levels seen following Ad5 infection in A549 cells.....	42
3.6	Repression of p53-dependent transcription by Ad5 E4orf3 is not necessary to instigate the reduction in TIF1 γ levels seen following infection.....	44
3.7	Mass spectrometry data suggests that Ad5 E4orf3 interacts with a ubiquitin E3/E4 ligase that could potentially mediate TIF1 γ degradation.....	46
3.8:	Summary of results.....	51
Chapter 4: Discussion.....		52
4.1:	Initial observations and considerations.....	52
4.2:	Reflections on the TIF1 γ -E1B-55kDa protein interaction.....	53
4.3:	Considerations following immunofluorescence findings.....	54

4.4:	Implications of mutant virus data.....	55
4.5:	E4orf3-dependent regulation of TIF1 γ is p53-independent.....	56
4.6:	Discussion of mass spectrometry results.....	57
4.6.1:	Validity of data.....	57
4.6.2:	Function of putative E4orf3 interacting proteins/protein complexes.....	61
4.6.2.i:	Ubiquitin conjugation factor E4 A (UBE4A).....	61
4.6.2.ii:	Conserved Oligomeric Golgi Complex.....	62
4.6.2.iii:	Eukaryotic translation initiation factor 3 (eIF3).....	62
4.6.2.iv:	Exportin 7.....	63
4.6.2.v:	Tyrosine-protein phosphatase non-receptor type 13 (FAP-1).....	63
4.6.2.vi:	Kinase D-interacting substrate of 220 kDa (Kidins220).....	63
4.6.2.vii:	Prolow-density lipoprotein receptor-related protein 1 (LRP1).....	63
4.6.2.viii:	LETM1 and EF-hand domain-containing protein 1 (LETM1).....	64
4.6.3:	Conclusions from mass spectrometry data.....	64
4.7:	Overall conclusions and suggestions for further work.....	65
References.....		67
Appendices.....		80

List of Figures

Chapter 1

1.1: Schematic representation of the approximate location of the early region transcription units of the adenoviral genome.....	2
1.2: Schematic diagram to represent the structure of a protein covalently attached to a lysine-48 linked polyubiquitin chain.....	4
1.3: Schematic representation of adenovirus-transformed cell lines used in this investigation showing their expressed complement of viral proteins.....	7
1.4: Schematic representation of the proteins involved in the Von Hippel-Lindau (VHL)-containing cullin-RING E3 ubiquitin ligase.....	12
1.5: Schematic representation of the proteins involved in the Ad5 and Ad12 cullin-RING E3 ubiquitin ligases.....	13
1.6: Schematic representation showing the major conserved domains found in all TIF1 family proteins.....	14
1.7: Simplified schematic representation of signalling through SMAD4 to show the points at which TIF1 γ is postulated to act.....	15

Chapter 2

2.1: Western blot showing expression of Ad5 or Ad12 HA-tagged E4orf3 (as stated) in clonal lines generated from transfected HEK293 cells.....	23
2.2: Schematic representation of the composition of a Western blotting transfer cassette.....	26
2.3A: Processing of proteins for trypsinisation to generate peptides for analysis by mass spectrometry.....	30
2.3B: Processing of peptides for analysis by mass spectrometry.....	31

Chapter 3

3.1 (A and B): Western blots showing the absolute levels of specified proteins over time following Ad5, Ad12, or mock infection of A549 cells at time=zero.....	34/35
--	--------------

3.2: Co-immunoprecipitation of named proteins with; A) Ad5 large E1B in HEK293 cells, or B) Ad12 large E1B in HER2 cells.....	36
3.3 (A and B): Immunofluorescence confocal microscopy images showing staining for either Ad5 or Ad12 E1B-55kDa in conjunction with either p53 or TIF1 γ in adenoviral transformed cells.....	38/39
3.4i: Immunofluorescence confocal microscopy images of HeLa cells showing staining for PML and TIF1 γ	41
3.4ii: Immunofluorescence confocal microscopy images of HeLa cells showing staining for TIF1 γ or FLAG and either Ad5 E4orf3 or HA, respectively.....	41
3.5: Western blots showing the absolute levels of specified proteins over time following wild type Ad5, E4orf3- mutant Ad5, E4orf3-/E4orf6- mutant Ad5 or mock infection of A549 cells at time=zero.....	44
3.6: Western blots showing the absolute levels of specified proteins over time following Ad5, Ad12, or mock (serum free DMEM) infection of H1299 cells at time=zero.....	46
3.7A: Western blot to confirm the continued expression of HA-tagged E4orf3 in the clonal cell lines generated previously (section 2.2.2).....	47
3.7B: Image of gel used in mass spectrometry experiment following destaining.....	48
3.7C: MS/MS spectra generated following the fragmentation of a peptide of sequence IFLITLDNSDPSLK.....	50

Chapter 4

4.1: Effects of different experiments on the hypothetical ability of p53 to stabilise TIF1 γ levels in a transcription-dependent manner.....	56
--	-----------

List of Tables

Chapter 1

1.1: List of Human Adenovirus species by serotype.....	1
1.2: Classes of enzyme involved in protein ubiquitylation.....	5
1.3: Major effects of the adenoviral proteins expressed in HEK293 and HER2/10 cells.....	7

Chapter 2

2.1: A list of suppliers of chemicals, reagents and media used in this investigation.....	18
2.2: A list of chemicals, reagents and media not supplied by Sigma.....	19
2.3: Cell lines used during the course of this investigation.....	20
2.4A: Primary antibodies sourced in-house or from other academic laboratories.....	21
2.4B: Antibodies sourced commercially.....	21
2.4C: Horseradish peroxidase (HRP)-conjugated secondary antibodies used for Western blotting.....	22
2.4D: Alexa Fluor dye-conjugated secondary antibodies for use in immunofluorescence confocal microscopy.....	22
2.5: Composition of solutions referred to in Figure 2.3.....	29

Chapter 3

3.1A: Putative Ad5 E4orf3 interacting proteins suggested by mass spectrometry....	49
3.1B: Putative Ad12 E4orf3 interacting proteins suggested by mass spectrometry...	49

Chapter 4

4.1: Possible SUMOylation sites within the TIF1 γ protein.....	53
4.2: Effect of E4orf3/p53 status on TIF1 γ levels 24 hours post-Ad5 infection.....	57

List of Abbreviations

3'	3-prime hydroxyl end of a DNA molecule
TEMED	1,2-bis(dimethylamino)ethane
DAPI	4',6-diamidino-2-phenylindole (DNA binding stain)
HEPES	4-2-hydroxyethyl-1-piperazineethanesulphonic acid
5'	5-prime phosphate end of a DNA molecule
ATCC	American Tissue Culture Collection
APS	ammonium persulphate
α - (as in α -E1B)	antibody (e.g. anti-E1B antibody)
BMP	bone morphogenic protein
BSA	bovine serum albumin
CBP – as Rb	cAMP response element binding protein binding protein
CR3	conserved region 3 (within adenoviral E1A protein)
Cul	cullin
DMEM	Dulbecco's modified Eagle's medium
E1-4 (adenovirus)	early region transcription units 1-4
E1-4 (ubiquitylation pathway)	enzyme classes involved in ubiquitylation (see Table 1.2)
eIF3	eukaryotic translation initiation factor 3
FCS	foetal calf serum
FAM	fat facets in mammals
G76	glycine-76 residue in ubiquitin
GFP	green fluorescent protein
HPLC	high performance liquid chromatography
H3K9	Histone H3, residue lysine-9
HRP	horseradish peroxidase
Ad	human adenovirus (subsequent number refers to serotype)
HER(2/10?)	human embryo retinoblasts
HEK (as in HEK293)	human embryonic kidney (HEK293 cell line)
HPV	human papillomavirus
IP	immunoprecipitation
IMM	inner mitochondrial membrane
Kidins220	kinase D-interacting substrate of 220 kDa
LETM1	LETM1 and EF-hand domain-containing protein 1
K48	lysine-48 residue in ubiquitin
MHC	major histocompatibility complex
MS	mass spectrometry
MOMP	mitochondrial outer membrane permeabilisation
MDM2	mouse double minute
MRN	Mre11/Rad50/Nbs1 complex
R (as in 243R/289R)	number of amino acid residues (in E1A splice variants)
orf (e.g. adenovirus E4orf3)	open reading frame (genetic) and the protein it encodes
PBS	phosphate buffered saline

PIPES	piperazine-N,N'-bis(2-ethanesulphonic acid
PHD	plant homeodomain
pfu	plaque forming units
POD	PML oncogenic domains
LRP1	prolow-density lipoprotein receptor-related protein 1
PML (a.k.a. TRIM19)	promyelocytic leukaemia protein
RET	rearranged during transfection tyrosine kinase
Rb	retinoblastoma protein
rpm	revolutions per minute
SDS-PAGE	SDS-polyacrylamide gel electrophoresis
SUMO	small ubiquitin-like modifier
SDS	sodium dodecylsulphate
S (12S/13S/26S)	Svedburg units (sedimentation coefficient)
MS/MS	tandem mass spectrometry
TP	terminal protein
TopBP1 (capitals???)	topoisomerase II- β binding protein 1
TIF (as in TIF1 γ)	transcriptional intermediary factor
TGF- β	transforming growth factor beta
TRIM (as in TRIM33)	tripartite motif containing protein
Tris	tris(hydroxymethyl)aminomethane
TBST	Tris-buffered saline Tween-20
TNF α	tumour necrosis factor alpha
FAS-1	tyrosine-protein phosphatase non-receptor type 13
VHL	von Hippel-Lindau
wt	wild type

As abbreviated single letter amino acid codes are used in the text, they are all listed here for completeness:

A	alanine	N	asparagine
B	aspartate/asparagine	P	proline
C	cysteine	Q	glutamate
D	aspartate	R	arginine
E	glutamate	S	serine
F	phenylalanine	T	threonine
G	glycine	V	valine
H	histidine	W	tryptophan
I	isoleucine	X	any/unknown/non-standard
K	lysine	Y	tyrosine
L	leucine	Z	glutamate/glutamine
M	methionine		

Chapter 1: Introduction

1.1 Adenovirus and cancer – an overview

Adenoviruses were first recorded in 1953 after having been isolated from human adenoid tissue following adenoidectomy (Rowe *et al.*, 1953).

Human adenoviruses form a subset of six species within the mammal host specific mastadenovirus genus, designated human adenovirus A-F (Davison *et al.*, 2003). Each of these species contain one or more serotypes, of which there are over 50 shared between the six species as shown in Table 1 (Turnell, 2008).

Table 1.1: List of Human Adenovirus species by serotype

Human Adenoviral Species	Serotypes*
A	12, 18, 31
B	3, 7, 11, 14, 16, 21, 34-35, 50
C	1, 2, 5, 6
D	8-10, 13, 15, 17, 19, 20, 22-30, 32-33, 36-39, 42-49, 51
E	4
F	40-41

* As listed in Turnell (2008). Further serotypes have since been discovered. For example, 54 are mentioned in Ferreyra *et al.* (2010) which also points to the possibility of serotype 52 representing a possible new species (G), but these have been omitted due to conflict in the literature.

Human adenoviruses exhibit a lytic lifecycle in their human cell hosts. Clinically, they tend to infect the respiratory, urinary bladder, gastrointestinal or ocular epithelium resulting in a variety of site of infection-specific symptoms in non-immunosuppressed individuals. In immunocompromised patients, however, adenoviral infections can be life-threatening (Lenaerts *et al.*, 2008).

In order to allow for the replication of its genome prior to the assembly and release of new virions, adenovirus suppresses the host cell's ability to respond to DNA damage and hijacks its protein synthesis machinery. In these respects, adenovirus manipulates the cell into acting in a way akin to a cancer cell. For example, the virus generates a cellular environment that is conducive to the replication of its genome (Turnell, 2008). This is much like a cancer cell inappropriately inducing S-phase in the absence of appropriate exogenous growth signals – one of the six classic hallmarks of cancer (Hanahan and Weinberg, 2000). Adenovirus confers at least two other hallmarks onto host cells, namely insensitivity to anti-growth signals and evasion of apoptosis. There is some evidence that at least one adenoviral serotype encodes a

protein that can greatly increase human cell lifespan in culture (Gallimore *et al.*, 1997), linking up with another hallmark – limitless replicative potential.

Avoiding immune destruction is one of four “emerging hallmarks” of cancer that Hanahan and Weinberg propose in a recent update to their seminal 2000 paper (Hanahan and Weinberg, 2011). The adenoviral E3 transcription unit, for example, encodes proteins that interfere with the ability of the host to launch an immune response against infected cells (Wold and Gooding, 1991) with at least one acting by multiple mechanisms (Bennett *et al.*, 1999).

1.2 Adenoviral genome

Adenovirus has a linear double stranded DNA genome. The length of the genome is serotype-specific, ranging between 26-45 kb (Davison *et al.*, 2003). Both strands contain coding sequences (Figure 1.1). The 5-prime (5') ends of the DNA molecules are covalently capped with a virally-encoded protein termed terminal protein (TP).

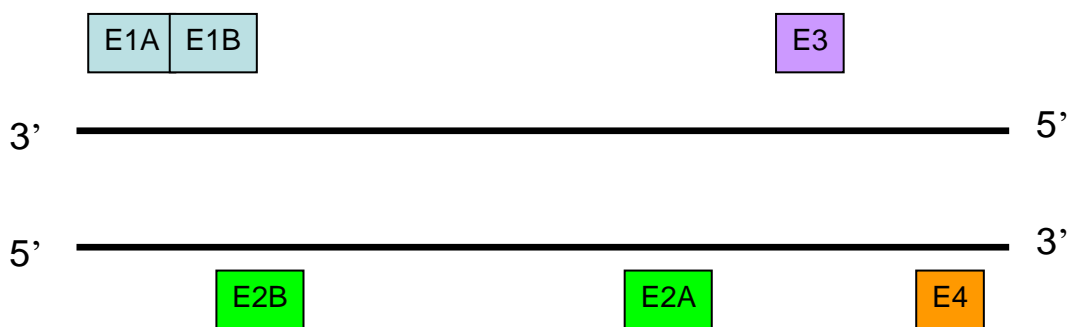


Figure 1.1: A schematic representation of the approximate location of the early region transcription units of the adenoviral genome. The intermediate and late region transcription units, some of which share base sequences with early region transcription units, were excluded for clarity. The sequence lengths are not to scale. As with other genes, these are read in the 3'-5' direction.

Adenoviral DNA replication uses a combination of at least three virally encoded proteins (a 5'-3' DNA polymerase, a DNA binding protein and a protein primer that is later cleaved to generate the 5' terminal protein cap) and a variety of host proteins. For a review of this topic, see de Jong *et al.* (2003).

Transcription of adenoviral early region transcription units is choreographed in a time-dependent manner (Nevins *et al.*, 1987). The transcription units are assigned to one of three groups depending on relative time of the onset of their transcription. These groups are:

- 1) Early region, consisting of six transcription units (E1A, E1B, E2A, E2B, E3, E4)
- 2) Intermediate region
- 3) Late region

The intermediate (e.g. Lutz *et al.*, 1997) and late (Logan and Shenk, 1982) regions mainly encode viral structural proteins and will not be examined further here.

1.3 Prevention of adenoviral genome concatemerisation

As adenovirus has a short linear double stranded genome, it risks being recognised as genomic DNA containing double stranded breaks. The presence of multiple copies of the viral genome can cause the host cell DNA damage response machinery to ligate them together, thereby preventing the formation of viral progeny. Mechanistically, this was shown to involve the Mre11/Rad50/Nbs1 (MRN) complex-induced non-homologous end-joining following the removal of TP using the Mre11 endonuclease domain (Stracker *et al.*, 2002).

Clearly genome concatemerisation is a process that adenovirus must prevent and both its E4orf3 and E4orf6 proteins have been implicated as functioning in such a capacity (Weiden and Ginsberg, 1994; Stracker *et al.*, 2002; see sections 1.7.3 and 1.7.4).

1.4 Promyelocytic leukemia protein oncogenic domains

Mre11 is one of many cellular targets for adenoviral proteins that are found in nuclear structures known as promyelocytic leukemia protein (PML) oncogenic domains (PODs) (Lombard and Guarente, 2000). PODs are nuclear protein structures formed around assemblies of PML covalently modified by small ubiquitin-like modifier (SUMO) (Muller *et al.*, 1998). The SUMOylated PML proteins then interact with a variety of proteins with SUMO-interacting motifs (Lallemand-Breitenbach and de Thé, 2010). PODs also contain a variety of non-SUMOylated proteins whose localisation is determined by other covalent modifications (Lallemand-Breitenbach and de Thé, 2010). Many of the constituent proteins are known tumour suppressors (e.g. p53 and retinoblastoma (Rb) protein) or proto-oncogenes (e.g. protein kinase B) (Lallemand-Breitenbach and de Thé, 2010).

1.5 Ubiquitin-proteasome pathway of protein degradation

The ultimate fate of Mre11 in cells infected with the human adenovirus (Ad), species C, serotype 5 (Ad5) is degradation by the 26S proteasome (Stracker *et al.*, 2005) – a large (Hough *et al.*, 1986), barrel shaped multi-subunit protein complex (Walz *et al.*, 1998) that is involved in degrading proteins that are predominately covalently attached to lysine 48 connected polyubiquitin chains (Figure 1.2).

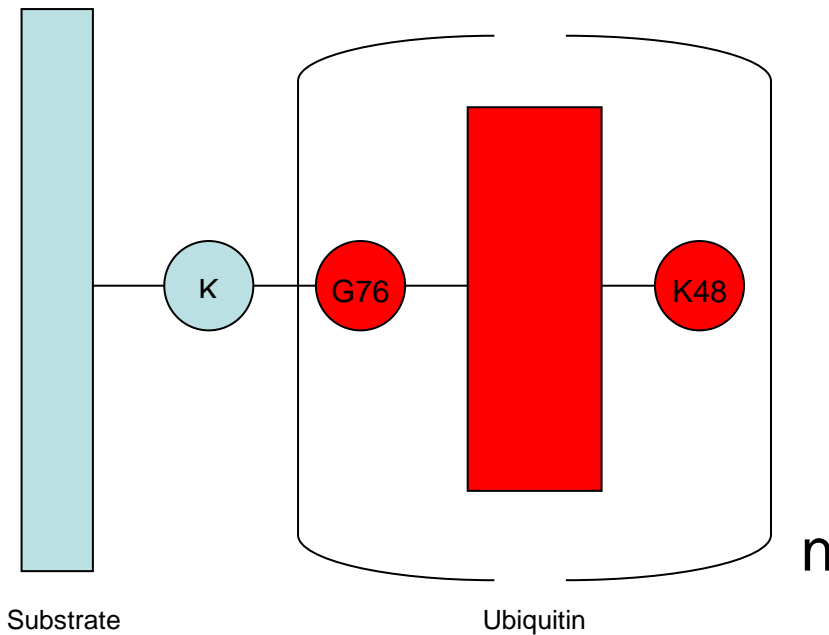


Figure 1.2: A schematic diagram representing the structure of a protein covalently attached to a lysine-48 linked polyubiquitin chain. Circles represent amino acid residues and rectangles represent whole proteins. n must be at least 4 for a protein (blue) to be targeted for proteasomal degradation (Thrower *et al.*, 2000). Polyubiquitin chains formed with lysine 11 and lysine 63 linkages have also been linked to proteasomal degradation (Li and Ye, 2008; Matsumoto *et al.*, 2010), although these and other non-K48 linked chains tend to be associated with other cellular functions (Chen and Sun, 2009).

The ubiquitylation cascade involves a number of different classes of enzyme (Table 1.2):

Table 1.2: Classes of enzyme involved in protein ubiquitylation

E1 ubiquitin activating enzymes	These transfer AMP from ATP onto ubiquitin. They then bind to the ubiquitin via an E1 cysteine residue in a process that removes AMP from ubiquitin. There is only one E1 enzyme in mammals.
E2 ubiquitin conjugating enzymes	These accept ubiquitin from an E1 and prepare it for transfer to a substrate in conjunction with an E3 ligase.
E3 ubiquitin ligases*	These mediate the transfer of one, or a series, of ubiquitin monomers from E2 conjugating enzymes to a substrate. There are three main classes of E3 ligase, of which the RING box and U-box containing varieties are of importance in this investigation.
E4 polyubiquitin ligases	These multifunctional proteins can catalyse the addition of ubiquitin to substrates already ubiquitylated by an E3 ligase (Koegl <i>et al.</i> , 1999). These proteins are not always required for polyubiquitylation. They may also act independently as E3 ligases (Hatakeyama <i>et al.</i> , 2001).

* 'E3 ligase' and 'E3 ubiquitin ligase' are used interchangeably in the text.

1.6 Adenoviral oncogenic and transformation potential

Notwithstanding the close similarities between adenoviral strategies for self-replication and human cancer cells, there has been no substantiated report in the literature of any human adenovirus serotype leading to cancer in man.

Certain human adenoviruses have shown oncogenic potential in rodents however. Human adenovirus, species A, serotype 12 (Ad12) was shown to cause tumours in neonate Syrian hamsters whereas representative members of species B, C and D did not (Trentin *et al.*, 1962). When Ad12 infects non-permissive hamster cells little viral DNA reaches the nucleus and both viral DNA replication and late transcription are inhibited (Doerfler, 2007). Loss of late transcription prevents the formation of viral progeny as late region genes encode most of the viral structural proteins (see below). Ad12 DNA integrates randomly into the hamster cell genome (Hilger-Eversheim and Doerfler, 1997), and retains expression of early region proteins.

Whilst Ad2 was shown to be non-oncogenic in neonate Syrian hamsters, both Ad12 (McBride and Wiener, 1964) and Ad2 (Freeman *et al.*, 1967) were able to transform primary rodent cells *in vitro*. Further study led to further complexity. Ad2 transformed hamster embryo cells were, for example, shown to have oncogenic potential when inoculated into newborn hamsters but not into adult hamsters (Lewis and Cook, 1982). It was further shown that

tumours generated in newborn hamsters could be cultivated to develop oncogenic potential in congenic adult hamsters, but not in adults of a different strain of the same species (Lewis and Cook, 1982).

In another study, rat cells were transformed with combinations of Ad5 and Ad12 E1A and E1B proteins. These cells were then injected into congenic rats and immunodeficient congenic rats and/or immunodeficient mice (Bernards *et al.*, 1983). These experiments showed a number of interesting facts. Cells transformed with any combination of Ad5 and Ad12 E1A and E1B were oncogenic in immunodeficient animals. In congenic rats, only cells transformed with Ad12 E1A had oncogenic potential and this was greatly enhanced (from 10%-100%) when Ad12 E1B was used as opposed to the Ad5 variety. Possibly most importantly, when cells were transformed with Ad 12 E1B and both Ad12 and Ad5 E1A, these did not possess any oncogenic potential in congenic rats. They went on to provide a partial explanation for some of these differences by showing that major histocompatibility complex (MHC) class 1 antigens are massively downregulated in cells transformed with Ad12 E1A, but not Ad5 E1A. They also show that the Ad5 phenotype is dominant when both are present.

Ad12 E1A was later shown to reduce MHC class 1 presentation at the transcriptional level, whereas Ad5 E1A was not (Ge *et al.*, 1992). As stated above, such immune evasion is considered an emerging hallmark of cancer (Hanahan and Weinberg, 2011).

It was much more difficult to transform human primary cells with human adenovirus, however. Graham and colleagues describe the generation of the transformed human embryonic kidney (HEK) 293 cell line following transfection with sheared Ad 5 DNA (Graham *et al.*, 1977).

HEK293 cells were derived from embryonic kidney tissue although it is believed that they are of a neuroectodermal, as opposed to mesenchymal, lineage (Shaw *et al.*, 2002). A wide range of neuronal receptor agonists were shown to elicit calcium transients in HEK293 cells (Vetter and Lewis, 2010), providing strong pharmacological evidence for the theory.

There are also examples of human embryo retinoblasts (HER) cells being transformed following transfection with plasmid encoded Ad12 E1 region transcription units (Byrd *et al.*, 1982). These cells are neuroepithelial in origin (Grabham *et al.*, 1988). Interestingly, it was suggested that human adenoviruses preferentially transform neuronal cells (Shaw *et al.*, 2002).

HEK293 cells and HER2/10 cells express the E1A and E1B proteins of the virus with which they were transformed (Nevins, 1982; Grand and Gallimore, 1986; Figure 1.3).

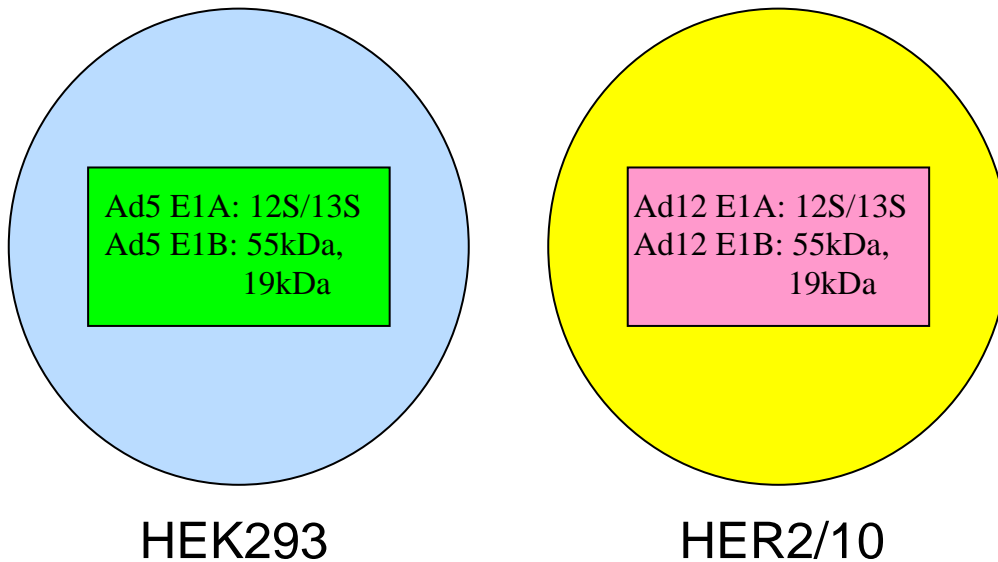


Figure 1.3: A schematic representation of adenovirus-transformed cell lines used in this investigation showing their expressed complement of viral proteins. Other E1B splice variants may be expressed, although this has not been investigated.

The Ad5 and Ad12 E1 transcription units encode proteins that are sufficient for cellular transformation to occur (Table 1.3). Certain E4 genes can also promote transformation in conjunction with E1 proteins. These include E4 open reading frame (orf) 6 (Moore *et al.*, 1996) and E4orf3 (Nevels *et al.*, 1999), both of which are discussed below. One other example of an oncogenic adenoviral protein is the product of the Ad9 E4orf1. This protein is responsible for the generation of mammary tumours in rats (Javier, 1994).

Table 1.3: Major effects of the adenoviral proteins expressed in HEK293 and HER2/10 cells.

Adenoviral proteins	Major effect on host cell	Effects on apoptosis
E1A	Transcriptional modulation Possesses transforming potential	pro-apoptotic
E1B	Protein synthesis and post-translational modulation Cooperates with E1A in cellular transformation	anti-apoptotic

(see section 1.7 for further details)

1.7 Function of proteins encoded by selected early region transcription units

1.7.1 E1A

The E1A transcription unit has two major protein products, formed by differential splicing, that are important in transformation (Boulanger and Blair, 1991). These proteins are termed 13S and 12S after their mRNA sedimentation coefficients or 243R and 289R after their number of amino acids (for Ad5 proteins). The proteins differ with respect to the presence or absence of the conserved region 3 (CR3) sequence. This region encodes a zinc finger transcription factor domain and functions as a transactivator in human adenoviral serotypes of all species (Ablack *et al.*, 2010).

As well as this, both E1A proteins are known to interact with a large number of cellular proteins. These include a number of transcription factors such as c-Jun, the cell cycle regulating transcriptional repressor Rb (Whyte *et al.*, 1988), and the closely related transcriptional co-activators and p53 E4 ubiquitin ligases (Shi *et al.*, 2009) 3'-5' cyclic adenosine monophosphate response element binding protein binding protein (CBP) and p300 (Gallimore and Turnell, 2001). p300 was first discovered as an E1A interacting protein (Banerjee *et al.*, 1994). Another important tumour suppressor initially discovered as being an E1A interacting protein is the transcriptional co-repressor, C-terminal binding protein (CtBP) (Boyd *et al.*, 1993).

The net effect of these, and other, interactions is to allow the adenovirus to manipulate the cell into acting as if it had received growth signals encouraging it to enter S phase (Turnell, 2008). For example, the ability of E1A to sequester the Rb protein allows for the liberation of E2F transcription factors that lead to the upregulation of genes that push the cell through the restriction (G1-S) checkpoint and commit itself to passing through the cell cycle (Weinberg, 2006).

Such S-phase promoting transcriptional modulation as mentioned above determines E1A's transforming ability. This is only part of the picture however, and E1A has only been shown to be weakly transforming when transfected into cells in the absence of some other co-operating oncogene (Turnell, 2008). Such oncogenes include constitutively activated Harvey (H-) *ras* (Lin *et al.*, 1995), adenoviral proteins such as those encoded by the E1B transcription unit (see below) and others, some of which are mentioned above. This has been put down to E1A also demonstrating potent pro-apoptotic properties. Much evidence in the literature

suggests that E1A can induce apoptosis in a p53-dependent manner and Ad5 E1A has been shown to stabilise p53 (Lowe and Ruley, 1993).

One protein that may be important in p53 stabilisation in E1A transformed cells is the p14^{ARF} protein that inhibits HDM2 binding to p53 (Sherr, 2001). HDM2 is the human homologue of the mouse double minute (MDM2) protein that acts as an E3 ubiquitin ligase for p53. The mouse homolog of p14^{ARF}, p19^{ARF}, was shown as necessary to facilitate the stabilisation of p53 by E1A in mouse cells (de Stanchina *et al.*, 1998).

Other evidence implies that the pro-apoptotic activity of E1A may be at least in some cases, p53-independent (Teodoro *et al.*, 1995).

Irrespective of the precise biological explanation for the pro-apoptotic side effects of E1A in any given cellular environment, it is obvious that adenoviruses must be able to counteract them.

1.7.2 E1B

The E1B transcription unit generates a single mRNA that generates a number of proteins by alternative splicing (Sieber and Dobner, 2007). Of these, it encodes two major proteins with properties well documented in the literature – a larger, approximately 55kDa, protein and a smaller 19kDa protein (Turnell, 2008). There are also known to be at least three other smaller E1B encoded proteins consisting of 156, 93 and 84 amino acids respectively (Sieber and Dobner, 2007).

E1B-55kDa and E1B-19kDa have been shown to independently cooperate with E1A in the transformation of rodent cells, by different anti-apoptotic mechanisms.

- 1) E1B-55kDa has been shown to bind p53 on promoters and repress its transcriptional activity (Yew *et al.*, 1994). Moreover, evidence implies that it can act as a substrate recruitment molecule that targets p53 and other substrates to a E4-orf6 dependent cullin-RING E3 ubiquitin ligase complex that is formed by many adenoviral serotypes including Ad5 and Ad12 (Cheng *et al.*, 2011; Forrester *et al.*, 2011). This in turn targets p53 for proteasomal degradation (Blanchette *et al.*, 2004).

Ad5 E1B-55kDa also causes the proteasomal degradation of the Daxx protein in an E4orf6-independent fashion (Schreiner *et al.*, 2010). Daxx exhibits a variety of functions, among them being:

- i) Aiding in the instigation of the extrinsic pathway of apoptosis by binding to the cytosolic side of activated Fas receptors (Yang *et al.*, 1997).
- ii) Increasing sensitivity to Fas signalling at the transcriptional level. The pool responsible for this resides in PODs (Torii *et al.*, 1999).

E1B-55kDa has also recently been suggested to act independently as an E3 SUMO ligase for p53, causing its relocalisation to PODs prior to nuclear export, thereby inhibiting its ability to activate transcription (Pennella *et al.*, 2010).

- 2) The E1B-19kDa protein has been shown to be functionally equivalent to the anti-apoptotic B cell lymphoma 2 (BCL2) protein in baby rat kidney cells (Rao *et al.*, 1992). BCL2 functions by binding to the direct effectors of apoptosis (BAK and BAX), preventing their oligomerisation. This avoids mitochondrial outer membrane permeabilisation (MOMP) occurring (Chipuk *et al.*, 2010). MOMP leads to cytochrome c release, apoptosome formation and activation of the initiator caspase, caspase 9 (Riedl and Salvesen, 2007).

Interestingly, as well as its BCL2-like anti-intrinsic pathway effects, E1B-19kDa has also been shown to protect cells from certain extrinsic pathway mediators such as tumour necrosis factor α (TNF α) (White *et al.*, 1992).

Ad5 E1B has also been shown to be involved in the inhibition of host cell protein synthesis (Babiss and Ginsberg, 1984). Ad5 E1B carries out this function, as well as increasing late viral protein synthesis, at the level of mRNA export in conjunction with the adenoviral E3 ubiquitin ligase complex (Woo and Berk, 2007).

1.7.3 E4orf3

E1B-55kDa is known to reduce p53 transcriptional activity (see above). Nevertheless, a recent study showed that E1B-55kDa is not necessary for p53 transcriptional repression in adenoviral infection as E4orf3 is capable of selectively silencing p53 responsive genes by

mediating the methylation of histone H3 lysine 9 (H3K9) and chromatin remodelling in promoter regions (Soria *et al.*, 2010).

E4orf3 is known to cause a dramatic morphological change in PODs, leading to the generation of track structures that sequester proteins away from viral replication centres. At least in the case of Ad5 E4orf3, the PODs must contain the PML-II for this effect to be seen (Hoppe *et al.*, 2006). Ad5 E4orf3 is localised with E1B-55kDa in the restructured PODs (Leppard and Everett, 1999). It has also been shown to cause the relocalisation of Mre11 within PODs, although this does not occur with Ad12 E4orf3 (Stracker *et al.*, 2005). Other proteins relocalised to the E4orf3 tracks include the PML-related transcriptional modulator TRIM24/transcriptional intermediary factor (TIF) 1 α (Yondola and Hearing, 2007).

The MRN complex can associate with Ad5 E1B-55kDa within PODs and, in the presence of either E4orf3 or E4orf6, can later become relocalised to cytoplasmic inclusion bodies akin to aggresomes (Liu *et al.*, 2005). Aggresomes are pericentriolar structures containing protein aggregates (Johnston *et al.*, 1998). These can sequester misfolded proteins prior to their degradation via the autophagy pathway (Wileman, 2007). In the case of Ad5 E1B-55kDa mediated MRN sequestration, however, the end point is increased proteasomal degradation (Liu *et al.*, 2005). Recent evidence suggests that biochemically genuine aggresomes are formed in Ad5 infection, whereas representative serotypes from other adenoviral species may form pseudo-aggresomes that lack γ -tubulin (Greer *et al.*, 2011).

One interesting point is that baby rat kidney cells can be transformed with Ad5 E1A together with E4orf3 or E4orf6, in most cases the transformed cell lines do not express the E1A viral proteins and expression of the E4 protein is either absent (E4orf3), or very low (E4orf6) (Nevels *et al.*, 2001). This is in contrast to cell lines transformed with E1A and E1B, where both proteins are well expressed (Figure 1.3), and led to a model of “hit and run” transformation (Nevels *et al.*, 2001).

1.7.4 E4orf6

As well as transforming cells in cooperation with E1A, E4orf6 has been shown to interact with specific host cullins (Cul) to generate adenovirus-regulated cullin-RING E3 ubiquitin ligases (Querido *et al.*, 2001). These E3 ligases are structurally similar to cellular ligases such as the Von Hippel-Lindau E3 ligase (Figure 1.4 versus Figure 1.5) and, like them, they can target a range of proteins for degradation by the proteasome. There are a number of serotype specific differences in structure and substrate specificity. Ad5 E4orf6 uses a Cul5 scaffold

whereas Ad12 E4orf6 uses a Cul2 scaffold. Ad16 E4orf6 can form an E3 ligase complex using Cul2 or Cul5 as a scaffold (Cheng *et al.*, 2011).

Both the Ad5 and Ad12 E3 ubiquitin ligases cause the polyubiquitylation and subsequent proteasomal degradation of p53 (Querido *et al.*, 2001; Blackford *et al.*, 2010) whereas the Ad12 ligase, but not the Ad5 ligase, targets the ataxia telangiectasia mutated and Rad3 related (ATR) activator, topoisomerase II β binding protein 1 (TopBP1) for proteasomal degradation (Blackford *et al.*, 2010).

Not all serotypes with E4orf6 containing E3 ubiquitin ligases target p53 (Cheng *et al.*, 2011) nor Mre11 (Forrester *et al.*, 2011), but E3 ligases from all serotypes examined targeted DNA ligase IV (Cheng *et al.*, 2011).

The different complement of cellular proteins targeted by each serotype exemplifies a different evolutionary strategy by which to subjugate the host cell's cell cycle control mechanisms and DNA damage response pathways.

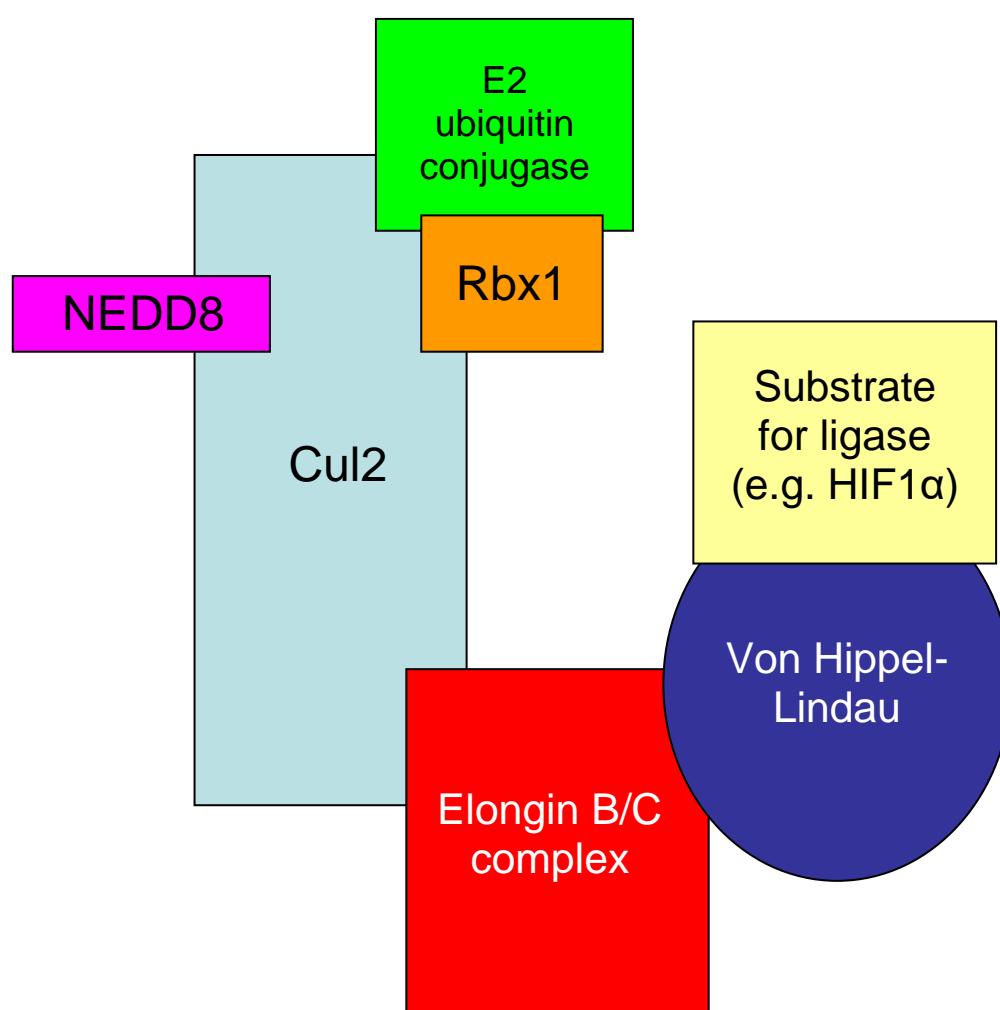


Figure 1.4: A schematic representation of the proteins involved in the Von Hippel-Lindau (VHL)-containing cullin-RING E3 ubiquitin ligase. VHL recruits substrates, such as HIF1 α , to the ligase. The RING finger containing Rbx1 protein then mediates the transfer of ubiquitin from an E2 conjugase to the substrate that is then targeted for degradation by the 26S proteasome. NEDDylation of Cul2 greatly enhances ligase activity (Ohh *et al.*, 2002).

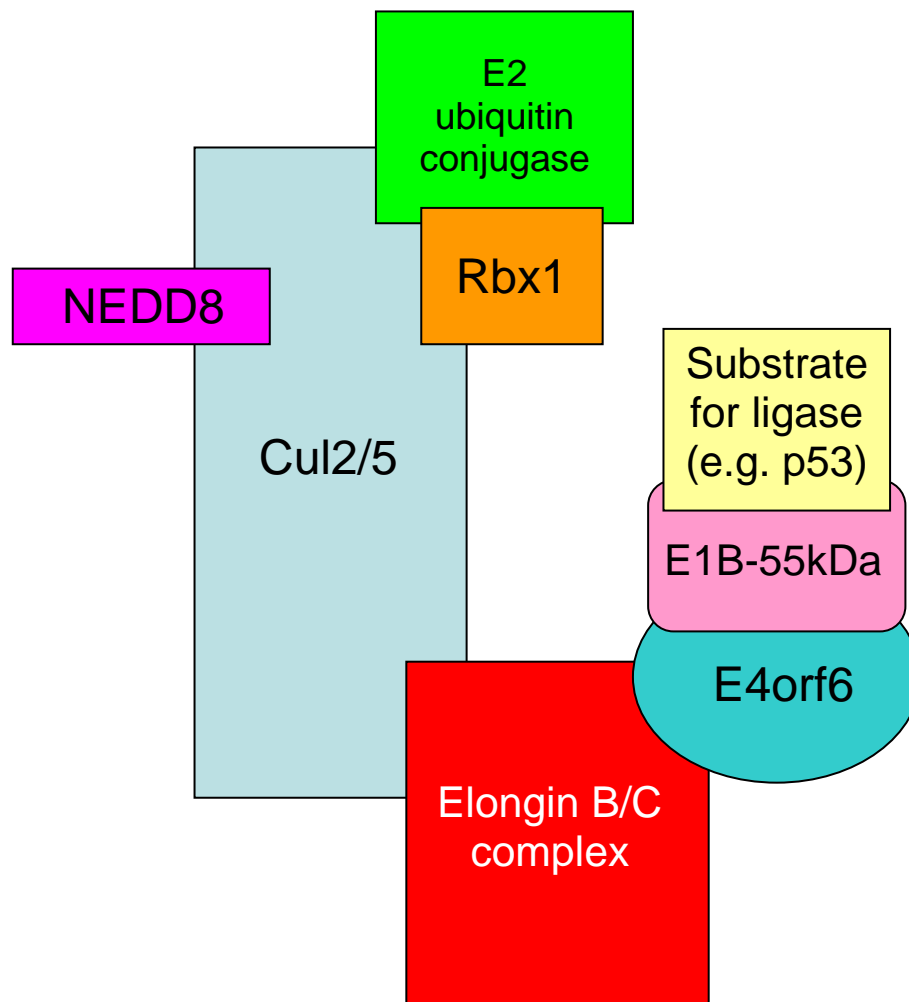


Figure 1.5: A schematic representation of the proteins involved in the Ad5 and Ad12 cullin-RING E3 ubiquitin ligases. E1B-55kDa can recruit substrates, such as p53, to the ligase. The RING finger containing Rbx1 protein then mediates the transfer of ubiquitin from an E2 conjugase to the substrate that is then targeted for degradation by the 26S proteasome. There is some evidence showing that E1B-55kDa is not required for the polyubiquitylation of all ligase substrates (see section 1.7.4 for further details).

1.8 Transcriptional Intermediary Factor 1 (TIF1)

TIF1 encompasses a group of transcriptional corepressors within the larger family of tripartite motif-containing (TRIM) proteins that include, for example, the PML protein (also known as TRIM19).

Four mammalian TIF1 proteins are currently documented in the literature; TRIM24/TIF1 α , TRIM28/TIF1 β , TRIM33/TIF1 γ and TRIM66/TIF1 δ (Khetchoumian *et al.*, 2004). These proteins all share a common basic structure (Figure 1.6).

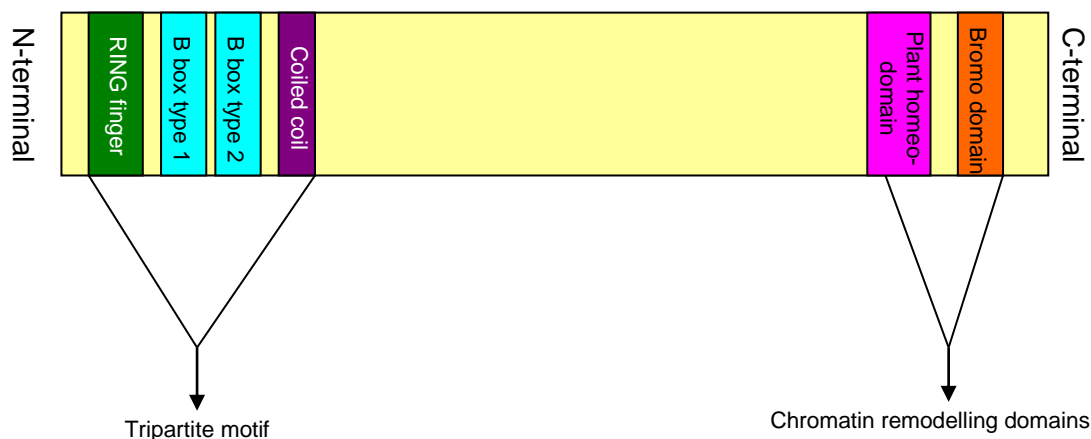


Figure 1.6: A schematic representation showing the major conserved domains found in all TIF1 family proteins (not to scale).

The N-terminal tripartite motif of many TRIM family members, including TIF1 γ , has been shown to be involved in the ubiquitylation pathway, functioning as an E3 ligase (Meroni and Diez-Roux, 2005).

1.9 TIF1 γ

TIF1 γ /TRIM33, also known as Ectodermin after its *Xenopus laevis* homologue, has been shown to interact with SMAD proteins in a variety of developmental and adult settings, including haematopoiesis (Ransom *et al.*, 2004; Dupont *et al.*, 2005; He *et al.*, 2006; Morsut *et al.*, 2010). TIF1 γ was shown to inhibit transforming growth factor-beta (TGF- β) and bone morphogenic protein (BMP) signalling by decreasing the nuclear:cytoplasmic ratio of SMAD4 via ubiquitylation (Dupont *et al.*, 2005). Further work by the same group showed TIF1 γ mediated monoubiquitylation of SMAD4 that is antagonised by the FAM deubiquitylase, an enzyme they show to be essential for signalling through SMAD4 (Dupont *et al.*, 2009). Other work has implied that TIF1 γ prevents TGF- β signalling by interacting with phospho-SMAD2/3 in such a way as to prevent interaction with SMAD4 (He *et al.*, 2006). Whilst these findings need not be mutually exclusive, they do point to an unresolved conflict in the literature and show that more work is required to properly elucidate the mechanism(s) by which TIF1 γ inhibits TGF- β signalling (Figure 1.7).

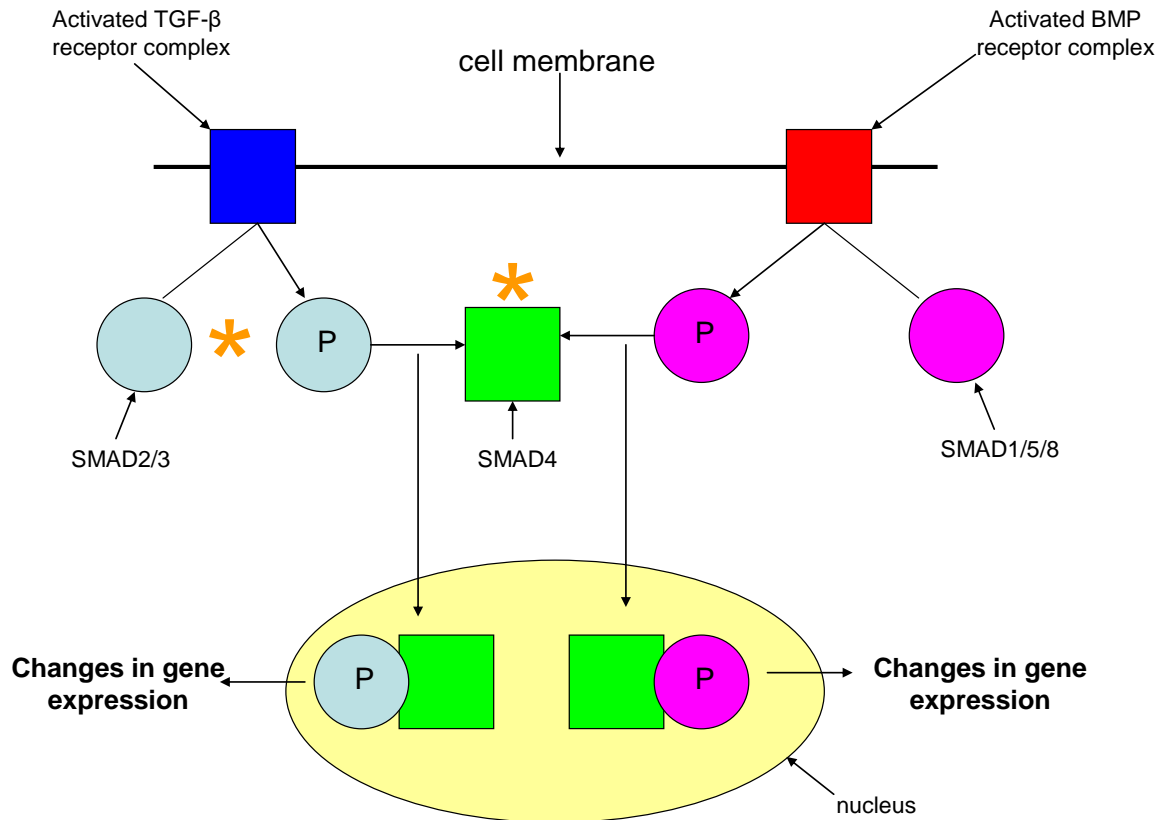


Figure 1.7: A simplified schematic representation of signalling through SMAD4 to show the points at which TIF1 γ is postulated to act. Activated receptors phosphorylate receptor SMADs (light blue/pink circles) and this allows them to associate with their common mediator SMAD4. The ensuing complex can then migrate to the nucleus where it functions as a transcription factor and modulates gene transcription. Orange asterisks signify points at which TIF1 γ is suggested to function. By sequestering SMAD2/3 or inactivating SMAD4, TIF1 γ can reduce signalling through the TGF- β side of the diagram. Inactivation of SMAD4 can also prevent signalling through the BMP side of the diagram.

Conflict aside, there is agreement that links do exist between TIF1 γ and decreased TGF- β signalling. This could imply a possible role in oncogenesis. An initial role in cancer was demonstrated when TIF1 γ was found as a fusion protein with the Rearranged During Transfection (RET) tyrosine kinase in papillary thyroid carcinomas (Klugbauer and Rabes, 1999). Since then, an increasing number of papers have suggested that TIF1 γ functions as a tumour suppressor in a variety of histological settings (Vincent *et al*, 2009; Aucagne *et al*, 2011; Herquel *et al.*, 2011). Interestingly, FAM has also been shown to demonstrate proto-oncogene properties (Schwickart *et al.*, 2010).

The C-terminal region of TIF1 γ contains a plant homeodomain (PHD) and a bromodomain, both of which have been shown to be involved in binding to acylated lysine residues on

histone proteins (Mellor, 2006). Such interactions with chromatin offer a direct mechanism by which transcriptional modulation can occur.

Importantly, as far as this current project is concerned, the Turnell group has recently shown that Ad5 and Ad12 infection results in a reduction in the cellular levels of the TIF1 γ protein. Other exciting preliminary mass spectrometry data suggested that the fat facets in mammals (FAM) deubiquitylating enzyme co-immunoprecipitated with E1B-55kDa from both Ad5 and Ad12 (Forrester and Turnell, unpublished observations).

1.10 Aims

Whilst many interesting facts had been discovered concerning the effect of adenoviral proteins on TRIM family proteins, both in isolation and in infection, many questions remain unanswered.

E1B-55kDa was known to interact with TIF1 γ in Ad5 and Ad12 transformed cells and both Ad5 and Ad12 infection of cultured cells had been shown to lead to a reduction in cellular levels of TIF1 γ . The function of the E1B-55kDa-TIF1 γ interaction remains enigmatic, however. E1B-55kDa was known to ferry cellular proteins to the adenoviral E3 ubiquitin ligase and thereby target them for degradation by the 26S proteasome. The possibility that TIF1 γ is degraded by a similar mechanism will be considered.

Ad5 E4orf3 has been shown to co-localise to nuclear tracks with other TRIM family proteins, such as PML and TIF1 α . This investigation will examine whether or not it also co-localises with TIF1 γ , potentially modulating its function or turnover rate.

E4orf3 has also recently been shown to act as a transcriptional repressor by modulating methylation at p53 responsive promoters. The possibility that it could also repress transcription of TIF1 γ will also be considered, as this would offer a putative mechanism by which TIF1 γ levels could fall post-infection. To further investigate a potential role for E4orf3 in the regulation of TIF1 γ I also aimed to identify novel E4orf3 interacting proteins by mass spectrometry.

Many proteins are targeted to the proteasomal degradation pathway following ubiquitylation by the adenoviral E4orf6 containing cullin-RING E3 ligase. This could be the mechanism by which TIF1 γ levels fall during adenoviral infection. Mutant Ad5 viruses that lack E4orf3, or

both E4orf3 and E4orf6, expression will be used to dissect the relative importance of E4orf3 and E4orf6.

In summary, this investigation aims to explore the regulation of the tumour suppressor protein TIF1 γ by adenovirus, using Ad12 and Ad5 as exemplars.

Chapter 2: Materials and methods

2.1 Materials

2.1.1 Suppliers of chemicals, reagents and media

With the exception of certain antibodies (section 2.1.4), all chemicals, reagents and media used during the course of this investigation were sourced from the suppliers listed in Table 2.1. Sigma was the default supplier, supplying all such products unless stated otherwise below (Table 2.2 and footnote).

Table 2.1: A list of suppliers of chemicals, reagents and media used in this investigation

Supplier	Details
BDH	BDH Laboratory Supplies, Poole, England
Bio-Rad	Bio-Rad, Munich, Germany
Fisher	Fisher Scientific, Loughborough, England
Invitrogen	Invitrogen Limited, Paisley, Scotland
KPL	KPL, Gaithersburg, USA
Melford	Melford Laboratories, Ipswich, England
PAA	PAA Laboratories, Pasching, Austria
PALL	PALL Corporation, Pensacola, USA
Promega	Promega, Madison, USA
Severn	Severn Biotech, Kidderminster, England
Sigma	Sigma-Aldrich, Gillingham, England
Vector	Vector Labs, Peterborough, England
VWR	VWR International, Fontenay-sous-Bois, France

Table 2.2: List of chemicals, reagents and media not supplied by Sigma

Supplier	Product
On-site	Deionised water (for gels)
On-site	Gel running markers
On-site	Phosphate buffered saline (PBS)
On-site	Saline
On-site	Tris-Buffered Saline Tween-20 (TBST)
BDH	Hydrogen peroxide
Bio-Rad	Protein assay solution
Fisher	Acetic acid
Fisher	Acetonitrile
Fisher	Paraformaldehyde
Invitrogen	Trypsin (for cell culture)
KPL	Protein G on agarose beads
Melford	1,2-bis(dimethylamino)ethane (TEMED)
Melford	Bicine
Melford	Glycine
Melford	Sodium Chloride
Melford	Tris(hydroxymethyl)aminomethane (Tris)
PAA	Foetal calf serum (FCS)
PALL	Nitrocellulose membrane
Promega	Trypsin (Mass spectrometry) and associated resuspension buffer
Severn	Sodium dodecylsulphate (SDS)
Vector	Vectashield Mounting Medium containing DAPI
VWR	Mass spectrometry grade water (Chromanorm brand)

Reconstituted Marvel® branded powdered milk was also used. It is widely available in English grocery shops.

2.1.2: Human cell lines used

All cell lines used during this investigation are presented in Table 2.3.

Table 2.3: Cell lines used during the course of this investigation.

Cell line	Cell type	Cell origin	Notes
A549	Epithelial	Small cell lung carcinoma	wild type p53
HeLa	Epithelial	Cervical carcinoma	transformed with HPV16* E6** and E7**
HEK293	Neural	Embryonic kidney	Ad5 E1 region-transformed
HER2/HER10	Neural	Embryonic retina	Ad12 E1 region-transformed
U2OS	Epithelial	Osteosarcoma	wild type p53
H1299	Epithelial	Non-small cell lung carcinoma	p53 null

N.B. not all cell lines are necessarily referred to in the text due to the data obtained from certain experiments being unusable for this thesis. * = Human papillomavirus (HPV) serotype 16. ** = protein products of the HPV Early Region (E) 6/7 genes.

2.1.3: Viruses and plasmids

Ad5, and Ad12 Huie *wt* viruses were obtained from the American Tissue Culture Collection (ATCC). Ad5 mutant E4orf3- and E4orf3-/6- viruses, and pcDNA3 Ad5/ Ad12 HA-E4orf3 plasmids were made in the lab of Prof. Thomas Dobner (University of Hamburg, Germany). FLAG-tagged TIF1 γ was a gift from Prof. Stefano Piccolo (University of Padua, Italy).

2.1.4: Antibodies

All primary and secondary antibodies used in the course of this investigation are shown in Table 2.4 (A-D).

Table 2.4A: Primary antibodies sourced in-house or from other academic laboratories

Antibody targeting	Name	Raised in	Used for	Source
Ad12 E1A	5D02	Mouse	WB	In-house
Ad12 E1B-55kDa	XPH9	Mouse	WB, IF, IP	In-house
Ad5 E1A	M58	Mouse	WB	In-house
Ad5 E1B-55kDa	2A6	Mouse	WB, IF, IP	In-house
HA tag	12CA5	Mouse	WB, IP	In-house
p53	DO-1	Mouse	WB	In-house
TIF1 γ	197	Rabbit	WB, IF, IP	In-house
TOPBP1	(5H)52	Rabbit	WB	Iain Morgan *
Ad5 E4orf3	6A11	Mouse	WB, IF	Thomas Dobner **
Ad5 E4orf6	RSA3	Rat	WB	Thomas Dobner **

* University of Glasgow

** University of Hamburg

WB – Western blotting

IF – Immunofluorescence microscopy

IP – immunoprecipitation

Table 2.4B: Antibodies sourced commercially

Antibody target	Name	Raised in	Used for	Source
HA tag	AB9110	Rabbit	IF	Abcam *
None - control IgG	AB37355	Mouse	IP	Abcam *
TIF1 β	A300-274A	Rabbit	WB	Bethyl **
FAM	A301-351A	Rabbit	WB	Bethyl **
Mre11	12D7	Mouse	WB	GeneTex ***
PML	PG-M3	Mouse	IF	Santa Cruz #
FLAG tag	M2	Mouse	WB, IF	Sigma ##
β -actin	A2228	Mouse	WB	Sigma ##
p53	CM1	Rabbit	IF	Vector ##

* Abcam, Cambridge, England

** Bethyl Laboratories Inc., Montgomery, USA

*** GeneTex Inc., Irvine, USA

Santa Cruz Biotechnology, Inc., Santa Cruz, USA

See Table 2.1 for contact details

Table 2.4C: Horseradish peroxidase (HRP)-conjugated secondary antibodies used for Western blotting.

Antibody	Raised in	Source
Anti-mouse immunoglobulin G (IgG)	Goat	DAKO*
Anti-rabbit IgG	Swine	DAKO*
Anti-rat IgG	Rabbit	DAKO*
Protein G **	Bacteria	Bio-Rad***

* DAKO, Glostrup, Denmark

** Not strictly an antibody, but it functions like a secondary antibody by binding to primary antibodies raised in many species; including mouse, rat and rabbit. It was only used for IP-Western blots. As it does not recognise denatured antibodies, it was used to detect proteins around the mass of the IgG heavy or light chains when they would otherwise be seen. It was also used as default in place of anti-rabbit secondary antibodies following IPs with an antibody raised in rabbit and probing with a primary antibody also raised in rabbit.

*** See Table 2.1 for contact details

Table 2.4D: Alexa Fluor dye-conjugated secondary antibodies for use in immunofluorescence confocal microscopy.

Antibody	Raised in	Optimal excitation wavelength of dye (nm) *
Anti-mouse IgG	Goat	488
Anti-mouse IgG	Donkey	594
Anti-rabbit IgG	Donkey	488
Anti-rabbit IgG	Goat	594

* - wavelength refers to the conjugated Alexa Fluor dye. All antibodies were sourced from Invitrogen (see Table 2.1 for contact details).

2.2: Methods

2.2.1: Cell culture

All cell lines were maintained in Dulbecco's modified Eagle's medium (DMEM) containing 8% foetal calf serum (FCS). The medium was stored at 4°C when not in use.

Antibiotics were not used. All plasmids used contained a G418 selection marker and their medium was supplemented with G418 (final concentration of 200µg/ml) where stated.

All cell lines were maintained in 10cm diameter Petri dishes housed in one of two humidified incubators at 37°C supplied with 5% carbon dioxide. They were split or fed twice a week. When splitting, cells were washed twice with phosphate buffered saline (PBS, in house) warmed to 37°C in a water bath. After the removal of the second wash, 1ml of trypsin solution (strength as supplied by Sigma) was added per dish and the dishes were re-placed in

an incubator for sufficient time for the cells to detach (usually between 3 and 5 minutes). At least 5ml of DMEM containing 8% FCS was then added to inactivate the trypsin and the solution was transferred to tubes for centrifugation at 1500 revolutions per minute (rpm) for 3 minutes. The supernatant was discarded and the cell pellet resuspended in DMEM containing 8% FCS. This was then divided by plating out onto fresh dishes with additional DMEM containing 8% FCS added to make a final volume of 8-12ml. The splitting ratio varied between cell type and experimental requirements. When cells were fed, they had their old medium removed and fresh DMEM containing 8% FCS was added.

2.2.2: Generation of E4orf3-expressing clonal cell lines

A 10cm dish of HEK293 cells was split into a 15ml tube and cell density was measured using a haemocytometer. The cells were then diluted to a concentration of $8 \times 10^6 \text{ml}^{-1}$. Aliquots of 200 μl of this suspension were then added to 200 μl of a solution made of 100 μl of 2xDMEM, 96 μl sterile deionised water and 4 μl of either Ad5, Ad12 HA-E4orf3 or empty vector (pcDNA3) plasmid constructs that also included a G418 resistance marker (=6 μg of DNA).

Electroporation of plasmid DNA into cells was achieved using a Bio-Rad Gene Pulsar (settings 220V, 960 μF). The cell solutions were then split onto 10cm dishes at a density of around 400 cells per dish in DMEM medium containing 8% (v/v) FCS.

After 48 hours the medium was changed to 200 $\mu\text{g}/\text{ml}$ G418-containing medium. Cells were then fed with the selection medium every few days over two weeks. At the end of this period a dozen or so colonies were picked from each dish using a sterile 200 μl pipette and transferred to 6cm dishes containing selection medium. After around a week each of these was split onto two 10cm dishes each. Once confluent, one dish each was tested for HA-E4orf3 expression.

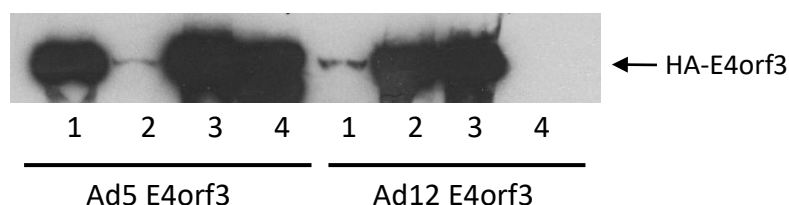


Figure 2.1: Representative Western blot testing for expression of Ad5 or Ad12 HA-tagged E4orf3 (as stated) in clonal lines generated from transfected HEK293 cells. A selection marker conferring resistance to G418 was included on the E4orf3-containing plasmid and used to select for cells that had taken up plasmid.

All clonally derived cell lines were tested for expression of the HA-tag for both Ad5 and Ad12 E4orf3 transfected cells. Clone 3, as presented in Figure 3.7a, was selected in both cases, and was maintained for use in future experiments.

2.2.3 Transfections with calcium chloride

For the immunofluorescence experiment requiring Ad12 HA-E4orf3 and FLAG-tagged TIF1 γ transfected HeLa cells, a dish of HeLa cells was split 1 in 10 onto a new dish and left in incubator overnight. The next morning 61 μ l of 1M calcium chloride was added to 10 μ l of mixed plasmid DNA (around 15 μ g DNA) and made up to 0.5ml with sterile deionised water. A further 0.5ml of 2x HEPES [4-2-hydroxyethyl-1-piperazineethanesulfonic acid]-buffered saline (40mM HEPES, 300mM sodium chloride) was then added and the suspension was left for 30mins. The cells were then fed with 9ml of fresh DMEM containing 8% FCS and the plasmid solution was added dropwise. The cells were fed the next day and returned to the incubator. The following day they were placed in G418 selection medium and were then maintained in this until used.

2.2.4: Viral infections

10cm dishes at around 70-80% confluence were washed in serum free DMEM prior to submersion in 2ml of serum free DMEM containing 10 plaque forming units (pfu) per cell of Ad5, Ad12 or mock (serum free DMEM). The dishes were placed in an incubator for 2 hours, during which time they were swirled every 15mins to ensure even distribution of virus. After the 2 hours, 8ml of DMEM containing 8% FCS was added to the dishes.

The same procedure was used when cells in microscope slide mini-wells were infected, with correspondingly reduced volumes, except that the dishes were not swirled.

2.2.5: Cell lysis

Dishes of cells being used for straight Western blots were lysed in urea buffer (9M urea, 50mM Tris (pH 7.2), 150mM β -mercaptoethanol). Dishes of cells being used for immunoprecipitations (IPs) were lysed in HiLo buffer (50mM Tris at pH 7.4, 0.825M sodium chloride, 1% v/v NP-40). 1ml of cold lysis buffer was used per confluent 10cm dish and 300 μ l per 6cm dish. Volumes were reduced correspondingly for sub-confluent dishes. Dishes were left a 4 $^{\circ}$ C for at least one minute before the dishes were scraped with a cell scraper and the lysates aspirated up in a 1ml Gilson pipette, transferred to a suitable container and stored on ice until required.

2.2.6: Sonication and centrifugation

Cell lysates were sonicated for around 15s in 1.5ml tubes to shear DNA and were then centrifuged at 13,000rpm for 20mins at 4°C. The lysates were then aspirated into a syringe through a 25G needle, taking care to leave precipitated material and the upper lipid layer, and transferred to a suitable container. Subsequent rounds of spinning down for 10 minutes under the same conditions were carried out until a sufficient amount of purified lysate was obtained. The lysates were kept on ice when not being used.

2.2.7: Protein quantification

4µl aliquots of lysate were added to 1ml of protein assay solution diluted 1 in 5 in deionised water. These were then assayed for protein concentration spectrophotometrically at 595nm against standard solutions of bovine serum albumin (BSA) containing 5, 10, 20 and 30µg protein. Lysate volumes equating to 50µg protein were calculated.

2.2.8: Sodium dodecylsulphate polyacrylamide gel electrophoresis (SDS-PAGE)

Typically 12% (w/v) acrylamide gels were set to resolve the lysate proteins by SDS-PAGE. These gels were formed using 12% acrylamide, made up with deionised water, containing 0.1M Tris, 0.1M bicine and 0.1% w/v SDS, to which 0.3% v/v TEMED and 0.06% w/v APS were added to instigate polymerisation.

Gels were run at a constant current of between 8 and 30mA per gel depending on the duration for which they were to be running and the size of proteins of interest.

Gel markers were made by the lab and included proteins of 77, 66 and 45kDa. Two smaller proteins were also present (18.5 and 14.5kDa), but these were usually allowed to run off the gel unless E4orf3 was being resolved for Western blotting.

50µg protein, as calculated above, was added to 1.5ml tubes followed by 15µl loading buffer (stock contains 1 part 10% SDS, 2 parts urea buffer and sufficient bromophenol blue to give an intense blue colour, to which 5%v/v β-mercaptoethanol was added immediately prior to use). Tubes were then spun down for one minute at 13000rpm prior to heating for 10mins in a heating block set to 80°C. The liquid was then spun down for a further minute at 13000rpm and loaded onto a gel for resolution by SDS-PAGE.

2.2.9: Gel transfer

Gels were transferred onto nitrocellulose membrane by assembling a transfer cassette as in Figure 2.2. The sponges, 3MM Whatman filter paper, gel and membrane were all pre-soaked in transfer buffer (0.05M Tris, 0.19M glycine and 20% v/v methanol) during assembly. A blunt metal roller was used to remove any air pockets between the gel and the membrane after the second piece of filter paper was applied. The cassette was finally fully submerged in a transfer tank containing transfer buffer. A constant current was passed through the tank depending on the length of time allocated for the transfer, typically 180mA overnight or 280mA for 6 hours.

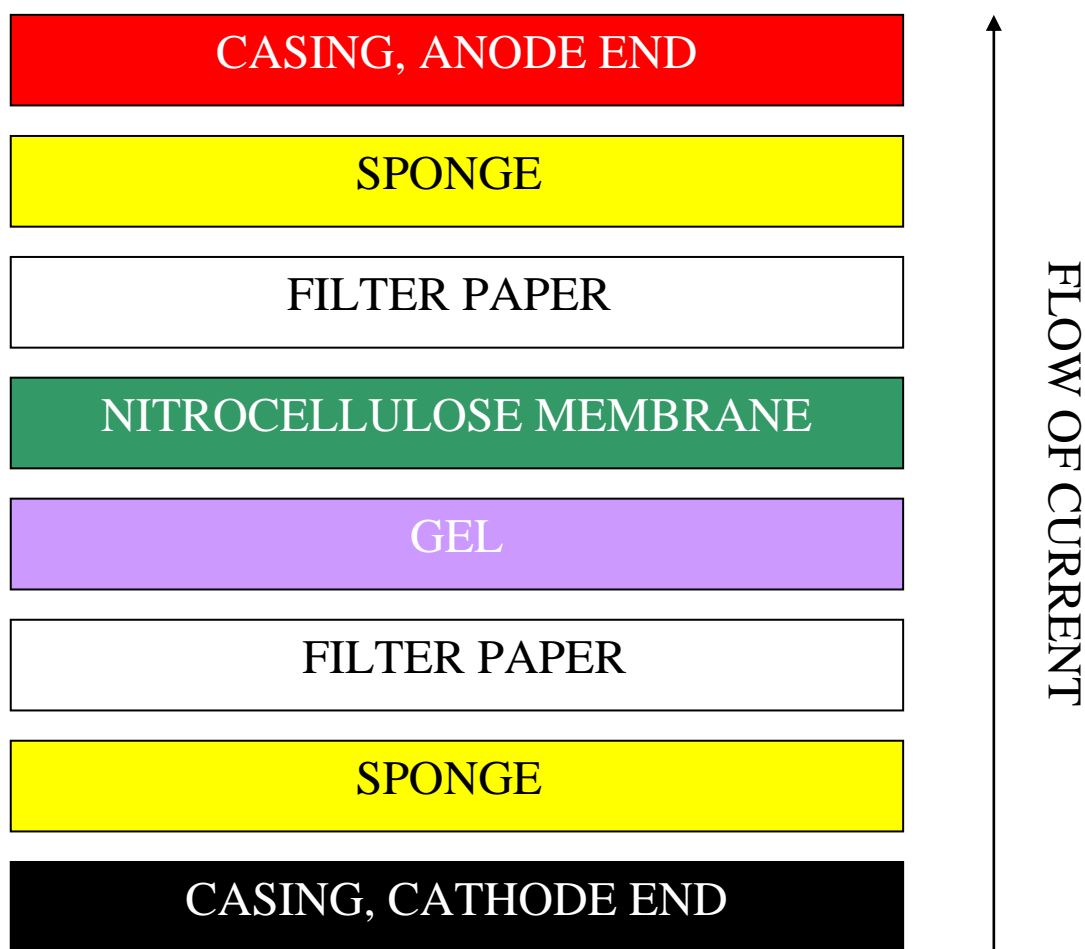


Figure 2.2: A schematic representation of the composition of a transfer cassette, as seen from above looking into the transfer tank. N.B. the diagram is not to scale and each layer was pressed firmly against its neighbours leaving no gaps.

2.2.10: Confirmation that protein had transferred onto the membrane

After the membrane was removed from the transfer cassette it was placed into a plastic tray protein end up and 1% (w/v) Ponceau S in 3% (w/v) trichloroacetic acid solution was poured onto it. After swirling for around a minute, excess solution was removed and the membrane was then washed in deionised water. Pink staining indicated the presence of protein and the staining process also indicated if air pockets had adversely affected the transfer procedure. When transfer had been shown to have occurred successfully, the membrane was then cut as required. The stain was washed off by covering the membrane with TBST (50 mM Tris [pH = 7.6], 150 mM NaCl, 0.05% Tween 20) and placing on a rotating platform for 10mins.

2.2.11: Blocking

The stained TBST solution was then poured off and replaced with a 5% w/v powdered milk solution (milk) that had been reconstituted in TBST. This was then placed back onto a rotating platform and left for at least 30mins.

2.2.12: Probing with antibodies for Western blotting

Suitable primary and secondary antibodies were selected for each blot and dissolved to their respective working concentrations in milk.

Sufficient primary antibody to cover individual blots was added within plastic pockets that were heat sealed to size. These were left on a rocking platform at room temperature for between 2 and 6 hours depending on the antibody, or overnight on a rocking platform at 4°C.

After the designated time the pockets were opened and the primary antibody was removed. The blots were then washed in TBST for around 5mins after which the secondary antibody was added in the same way as the primary had been. The pockets were placed on a rocking platform at room temperature for between 2 and 4 hours.

After that time the secondary antibody was removed and the blots were then subjected to a series of 5 separate washes in TBST over a period of at least 45mins.

2.2.13: Developing blots

After sufficient washing, the blots were swirled for 1min in around 30ml of 0.1M Tris, pH=8.5 to which 125µl of 250mM luminol, 75µl of 150mM coumaric acid and 100µl of hydrogen peroxide had been added. The solution was then poured off and the blots were wrapped in Sarin wrap. These were placed protein side up inside a photographic cassette in a

dark room and a photographic plate was placed on top and locked in the cassette for varying amounts of time before being removed and developed using an X-ray developer imaging machine.

2.2.14: Immunoprecipitations

Cells lysates were divided into two equal volumes for each IP, typically around 1.2ml for IP-Westerns and around 8-10ml in IPs for mass spectrometry. An equal volume of HiLo buffer was placed into a third tube.

Suitable antibodies were selected and added to one tube containing lysate and to the HiLo tube. Typically around 10µg of antibody were added per tube for IP-Westerns and proportionally more for IPs for mass spectrometry. All tubes were placed on a rotator overnight.

The next day a 50% slurry of Protein G on agarose beads in HiLo buffer was added to all tubes. Around 40µl of slurry was added for IP-Westerns and proportionally more for IPs for mass spectrometry. The tubes were then replaced on the rotator for 2 hours.

The tubes were then spun down at 4000rpm for 1 minute to sediment out the beads. The supernatant was removed with a needle and the beads were then resuspended in 500µl of HiLo buffer, and transferred to a 1.5ml tube in the case of IPs for mass spectrometry. The washing procedure was repeated 5 times after which the beads were either frozen down at -80°C for later use or had 30µl of fresh loading buffer added prior to heating, as in section 2.2.8.

Care was taken to aspirate up as much liquid as possible, which was then loaded onto a gel for SDS-PAGE. A control lane, containing a volume of original lysate equating to 50µg protein processed with loading buffer, was also run to confirm the presence of the protein of interest in the original lysate.

2.2.15: Immunofluorescence

A549 cells were split and seeded at around 3000 cells per well onto 12 well slides on 10cm dishes and incubated overnight. The cells were washed twice with PBS the next day and then infected with mock (serum-free DMEM), Ad5 or Ad12. After 2 hours the dishes were flooded with 15ml of serum-containing medium and incubated overnight. The next day the medium was removed and the slides were dried by placing on a paper towel. They were then washed

twice with PBS prior to being placed in pre-extraction buffer (10mM piperazine-N,N'-bis(2-ethanesulfonic acid) [PIPES, pH=6.8], 20mM sodium chloride, 300mM sucrose, 3mM magnesium chloride, 0.5% Triton X-100) for 5mins. The cells were then fixed in 4%w/v paraformaldehyde for 10mins. After washing with PBS, the 10µl of blocking solution containing 10% (w/v) BSA in PBS was added to each well and the slides were left in a humid box for 1 hour. Following washing in PBS, selected combinations of primary antibodies made up in 0.1% (w/v) BSA in PBS were added per well. The slides were replaced in the humid box and placed in an incubator for 2 hours. Then, following three PBS washes, suitable secondary antibodies were added and left for 90mins (Table 2.4D). After a final set of washes in the dark, the slides were mounted with coverslips using Vectashield mounting medium. This contains the blue nuclear 4',6-diamidino-2-phenylindole (DAPI) stain. Slides were then wrapped in foil and frozen at -20°C until required. They were later observed using software associated with an LSM 510 Meta laser scanning microscope (Zeiss).

2.2.16: Mass spectrometry

2.2.16.i Preparation of samples

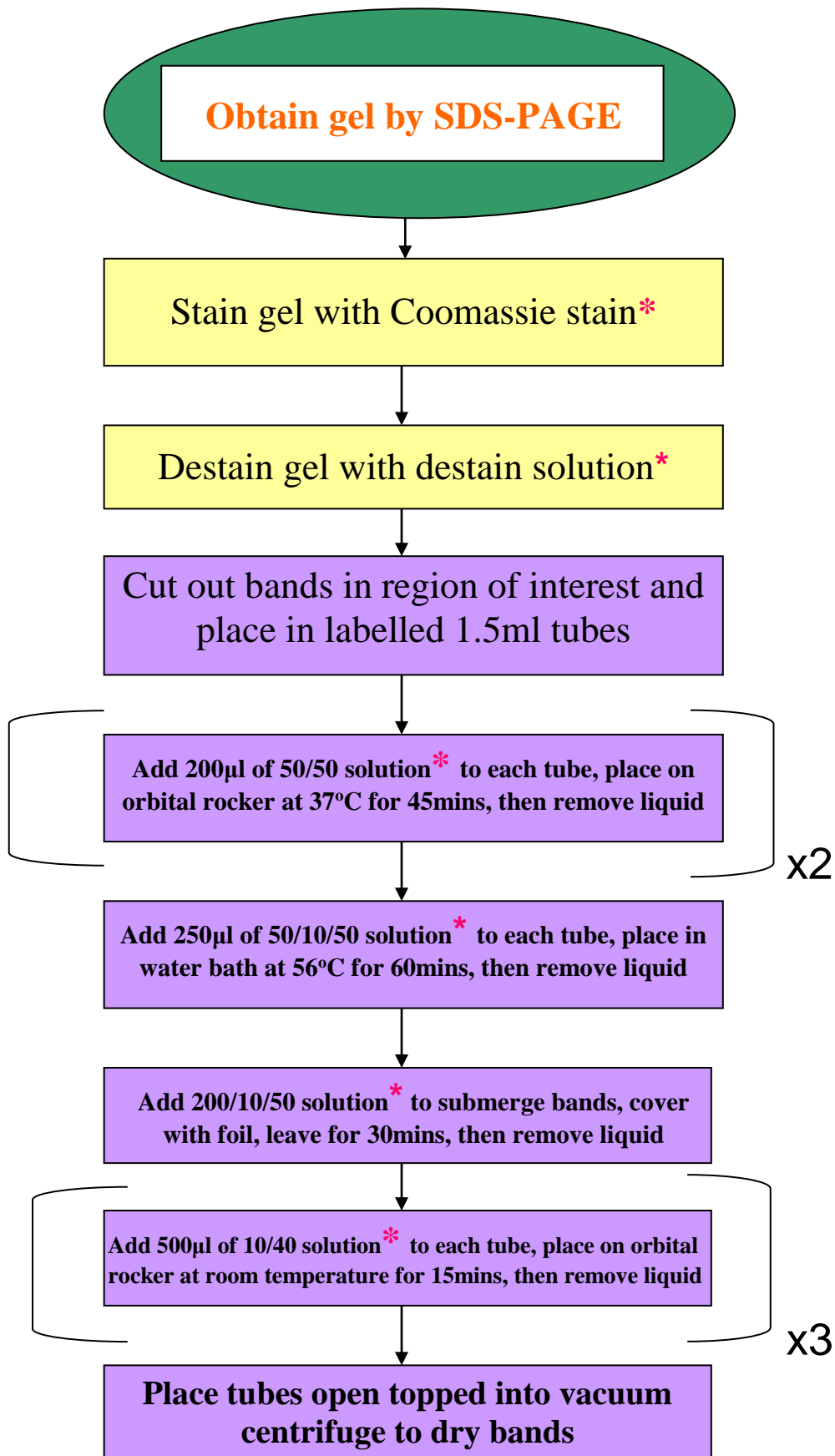
The steps in the preparation of samples for mass spectroscopy are laid out in Figure 2.3. There are four stages:

- 1) Obtaining the gel as for IP-Westerns (v.s., green in Figure 2.3A)
- 2) Selectively staining protein bands on the gel (yellow in Figure 2.3A)
- 3) Preparing the proteins in the gel bands for trypsinisation (purple in Figure 2.3A)
- 4) Trypsinising and preparing the peptides for analysis (Figure 2.3B)

Table 2.5: Composition of solutions referred to in Figure 2.3

Solution	Composition
Coomassie stain	0.1% w/v Coomassie G-250 dye in 1.6%(v/v) phosphoric acid,
Destain solution	8% (w/v) ammonium sulphate and 20% (v/v) methanol
50/50 solution	1% (v/v) acetic acid
50/10/50 solution	50% v/v acetonitrile and 50mM ammonium bicarbonate
200/10/50 solution	50mM dithiothreitol, 10% v/v acetonitrile,
10/40 solution	50mM ammonium bicarbonate
Reconstituted trypsin	200mM iodoacetamide, 10% v/v acetonitrile and
	50mM ammonium bicarbonate
	10% v/v acetonitrile and 40mM ammonium bicarbonate
	1 part (20µg vial of sequencing grade trypsin in 200µl
	of resuspension buffer):7 parts 10/40 solution

A



B

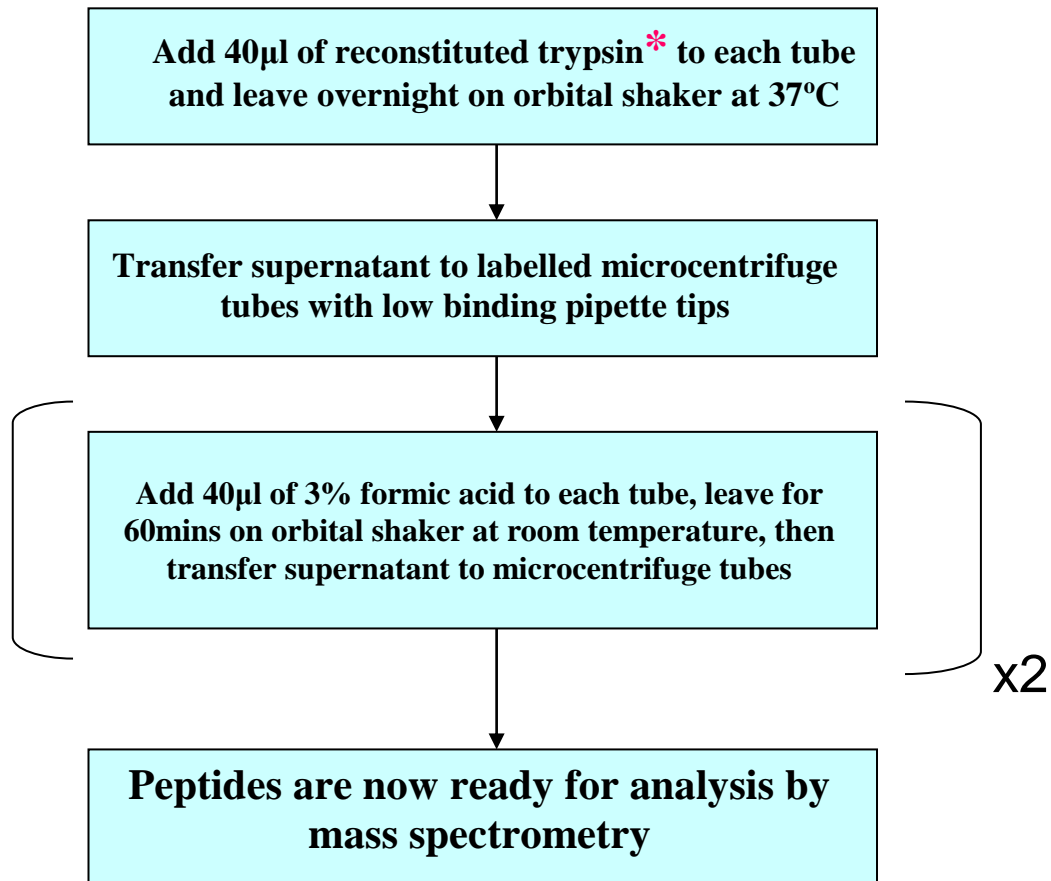


Figure 2.3: Flow diagram showing the steps involved in processing gels for analysis by mass spectrometry. Boxes in parenthesis are repeated as indicated. A) Preparation of proteins for trypsinisation, B) preparation of peptides for analysis by mass spectrometry. The composition of solutions marked with a red asterisk (*) are given in Table 2.5.

2.2.16.ii Analysis of data

Portions of the peptide solutions previously obtained by trypsinisation (Figure 2.3B) were initially separated by reversed phase high performance liquid chromatography (HPLC) using a Dionex 3000 system.

- 1) peptides loaded onto a C18 Pepmap reverse phase trap
- 2) peptides eluted at 350nl/min onto a 15cm Dionex Pepman reverse phase resolving column
- 3) peptides directly infused into the mass spectrometer by electrospray ionisation

The Bruker 4G maXis time of flight/time of flight tandem mass spectrometer initially selected the three most abundant ions from each sample and fragmented them by collision induced dissociation before subjecting the fragments to analysis. The mass/charge range for both the initial mass spectrometry (MS) of the proteins and the subsequent MS/MS analysis of peptides was 250-2900Da/electronic charge units.

The ProteinScape software associated with the mass spectrometer was used to carry out a Mascot search of the SwissProt protein database to identify the peptides it had selected for fragmentation. The mass tolerance was set at 0.05Da and a minimum Mascot score of 20 was set as a significance criterion.

Chapter 3: Results

3.1 Effect of adenoviral infection on cellular protein levels

Preliminary observations from the Turnell lab had indicated that TIF1 γ levels fall during the course of viral infection with Ad5 or Ad12 (Forrester and Turnell, unpublished observations). Initially, therefore, it was decided to ascertain the magnitude of any change in the absolute levels of TIF1 γ and other selected proteins post-infection with Ad5 or Ad12.

To do this, dishes of A549s were infected with Ad5, Ad12, or mock (serum free DMEM) and harvested at 24, 48 and 72 hours. The resultant lysates were then subjected to protein quantification, SDS-PAGE and Western blotting (Figure 3.1A).

Blots were carried out with suitable antibodies for the E1A and E1B-55kDa proteins from both serotypes in order to confirm that the infections had worked (Figure 3.1A, Panels 5-8).

In keeping with expectations, p53 levels fell following infection with Ad5 or Ad12 (Figure 3.1A, Panel 4).

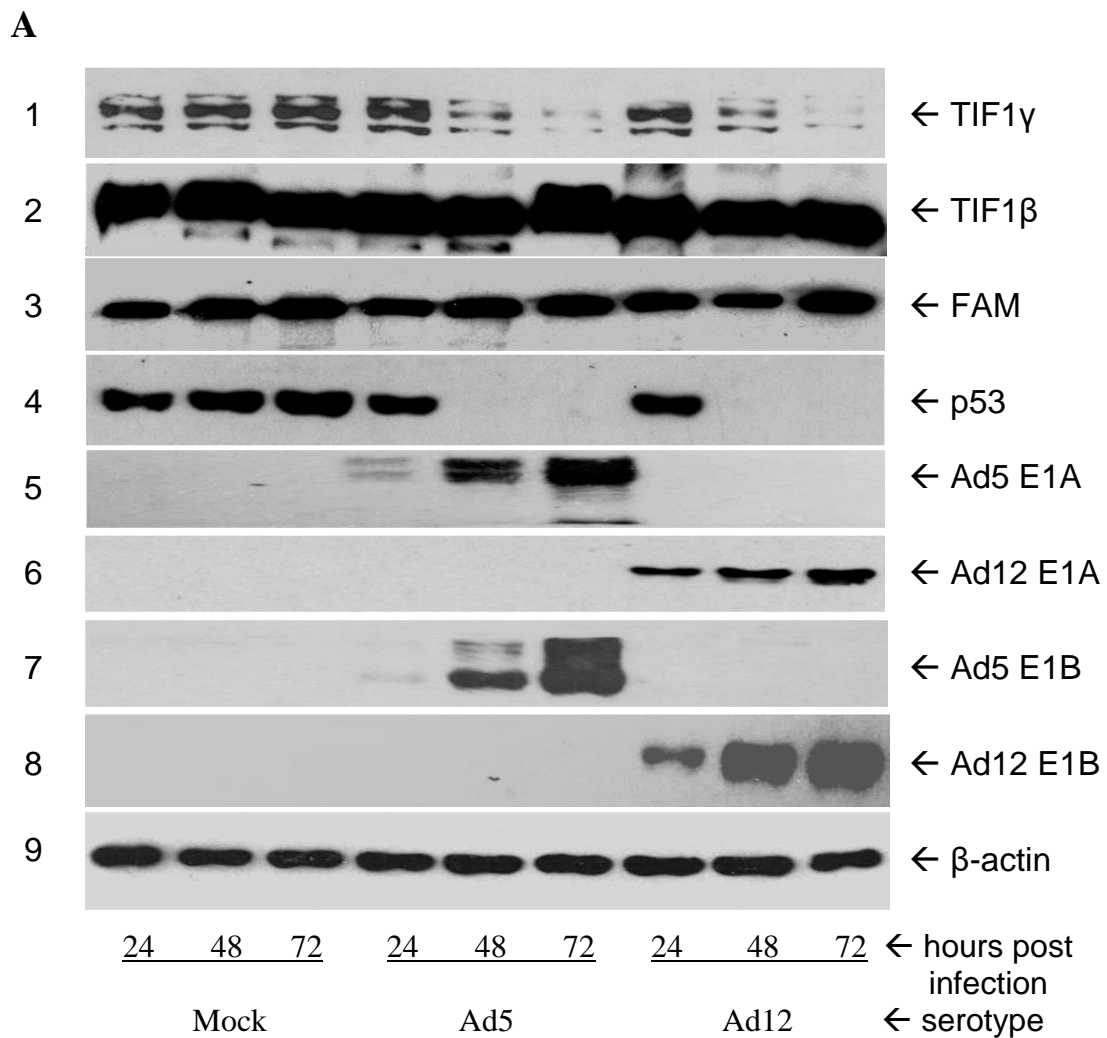
Confident that the data were reliable based on the above findings, it was encouraging to note that TIF1 γ levels decline following Ad5 or Ad12 infection (Figure 3.1A, Panel 1). Owing to the fundamental importance of that finding to the further course of this investigation, these blots were repeated a number of times with the same result being obtained on each occasion.

To compare the effects of infection between TIF1 γ and other closely related proteins, blots were also carried out for TRIM28/TIF1 β . Neither Ad5 nor Ad12 infection resulted in an appreciable change in absolute levels of this protein (Figure 3.1A, Panel 2), implying that TIF1 γ was selectively targeted.

Given that FAM had been shown to co-immunoprecipitate with both Ad5 and Ad12 E1B-55kDa following infection with the respective serotype, it was also investigated. As with TIF1 β , Western blotting failed to demonstrate a significant change in absolute levels following infection with either serotype (Figure 3.1A, Panel 3).

Absolute levels of TOPBP1 were also investigated in a later experiment as it had previously been shown to be a substrate for the Ad12 Cul2-containing E3 ubiquitin ligase, but not for the

Ad5 Cul5-containing E3 ubiquitin ligase. In agreement with earlier findings absolute levels of TOPBP1 fell following Ad12 infection although they increased slightly within 24 hours post-infection with Ad5 before reducing towards basal levels over the next 24 hours (Figure 3.2B, Panel 1). Other blots confirmed that the infections had been successful and that the virus was competent to reduce protein levels for known targets. Of these, one for Ad12 E1B-55kDa (Figure 3.2B, Panel 3) and one for p53 (Figure 3.1B, Panel 2) are shown. The actin blots provided (Figure 3.1A, Panel 9; Figure 3.1B, Panel 4) indicated that loading was equivalent in all samples tested.



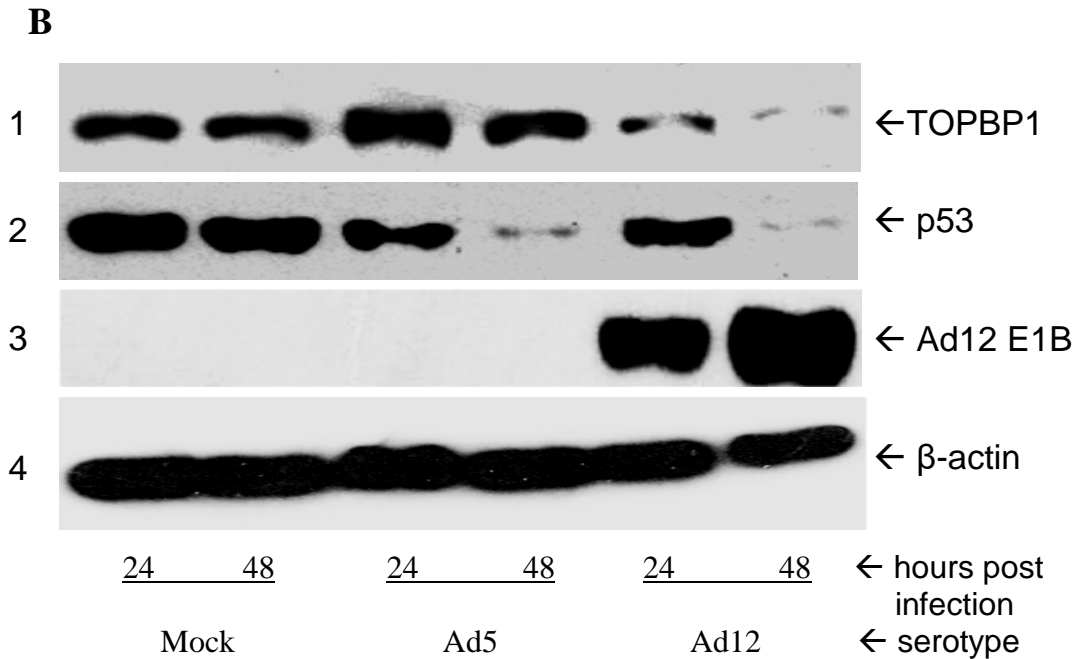


Figure 3.1A and B: Western blots showing the absolute levels of specified proteins over time following Ad5, Ad12, or mock (serum free DMEM) infection of A549 cells at time=zero. Cells were lysed in urea buffer and lysate volumes equivalent to 50 μ g total protein were resolved using SDS-PAGE. Proteins were transferred to nitrocellulose membrane and this was probed with suitable primary and secondary antibodies and finally developed as described in text.

Previous findings by this lab showing the degradation of TIF1 γ following infection of cultured cells with Ad5 or Ad12 were reproduced here. Whilst Western blotting allowed for gross changes in TIF1 γ levels over time to be observed, it did not give any indication of what mechanisms underlay the change.

3.2 Interaction of E1B-55kDa with TIF1 γ and other cellular proteins

E1B-55kDa interacts with a variety of cellular proteins and can cause their relocation within the cell. In some cases it has been shown to present specific proteins to the adenoviral E3 ubiquitin ligase that can then mediate their degradation by the 26S proteasome. Having established that absolute TIF1 γ levels fall following infection with Ad5 or Ad12, it was decided to investigate whether or not TIF1 γ co-immunoprecipitated with the E1B-55kDa protein.

In order to avoid the loss of protein that would occur following actual infection, the IPs were carried out using non-infected HEK293 (Figure 3.2A) and HER2 cells (Figure 3.2B), neither of which express E4orf3 or E4orf6. The resultant lysates were then subjected to protein quantification, resolved via SDS-PAGE, transferred to nitrocellulose membrane and finally

assayed using Western blotting. As it has previously been shown that Mre11 and p53 both interact with E1B-55kDa, blots were also carried out for these proteins as positive internal controls (Figure 3.2A, panels 2 and 3; Figure 3.2B, panels 2 and 3).

Interactions were seen between TIF1 γ and both Ad12 (Figure 3.2B, panel 1) and, although to a lesser extent, Ad5 (Figure 3.2A, panel 1) large E1B.

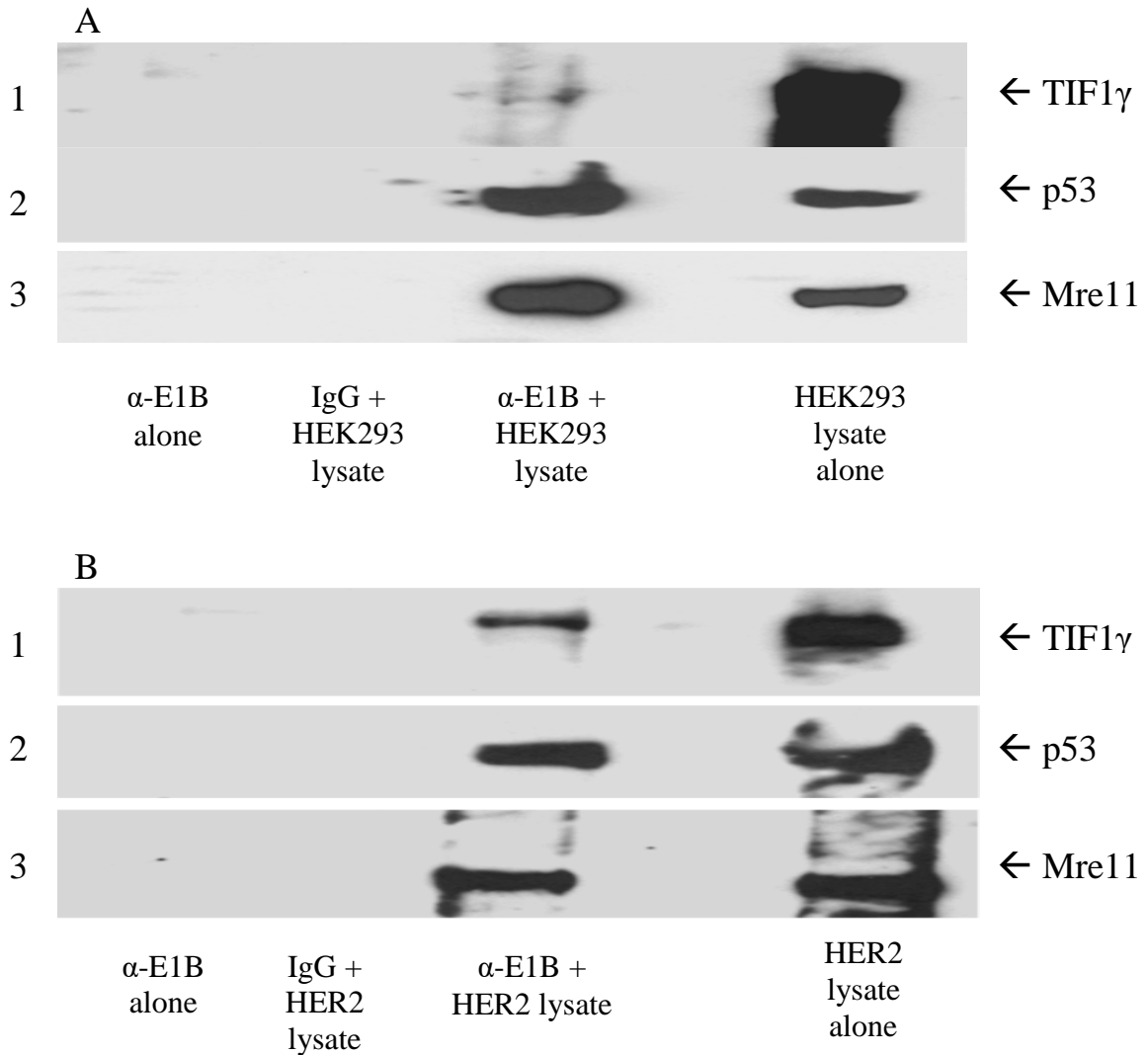


Figure 3.2: co-immunoprecipitation of named proteins with; A) Ad5 large E1B in HEK293 cells, or B) Ad12 large E1B in HER2 cells. Cells were harvested in HiLo buffer and volumes equating to 50 μ g total protein were run in each lysate alone lane. Control lanes contained anything pulled down by Protein G from either the respective anti-large E1B antibodies (α -E1B) in HiLo, or the respective cell lysates containing control mouse IgG.

TIF1 γ showed a clear interaction with E1B-55kDa in adenovirus E1 region transformed cells in culture. The pull-down data however, said nothing about the subcellular location of the interaction.

3.3 Demonstration of TIF1 γ and E1B-55kDa co-localisation using immunofluorescence microscopy

It was known from the literature that E1B-55kDa localises mainly to cytoplasmic aggresome-type structures when expressed in Ad5 or Ad12 transformed cells. It was also known to interact with p53 which co-localises with it in these structures. It was not, however, known whether or not TIF1 γ localises to these structures. Owing to the interaction previously demonstrated between E1B-55kDa and TIF1 γ , it seemed reasonable to investigate whether or not this was the case.

Although E1B and TIF1 γ were shown to interact in HEK293/HER2 cells (Figure 3.2), it was understood that no inferences could be drawn as to the function of the interaction in the context of adenoviral infection. At this point it was considered useful to obtain further evidence of the interaction in a whole cell setting. As the pulldowns in the previous section had been carried out using HEK293 and HER2 cells, initial immunofluorescence images were obtained using these cells.

Confocal microscopy revealed, as expected, that E1B was mainly found localised in the discrete regions of the nucleus and neighbouring cytoplasm (Figure 3.3A). It exhibited remarkable consistency of co-localisation with p53 in discrete cytoplasmic flecks that were particularly pronounced in the HER2 images (Figure 3.3A, panels 1 and 2).

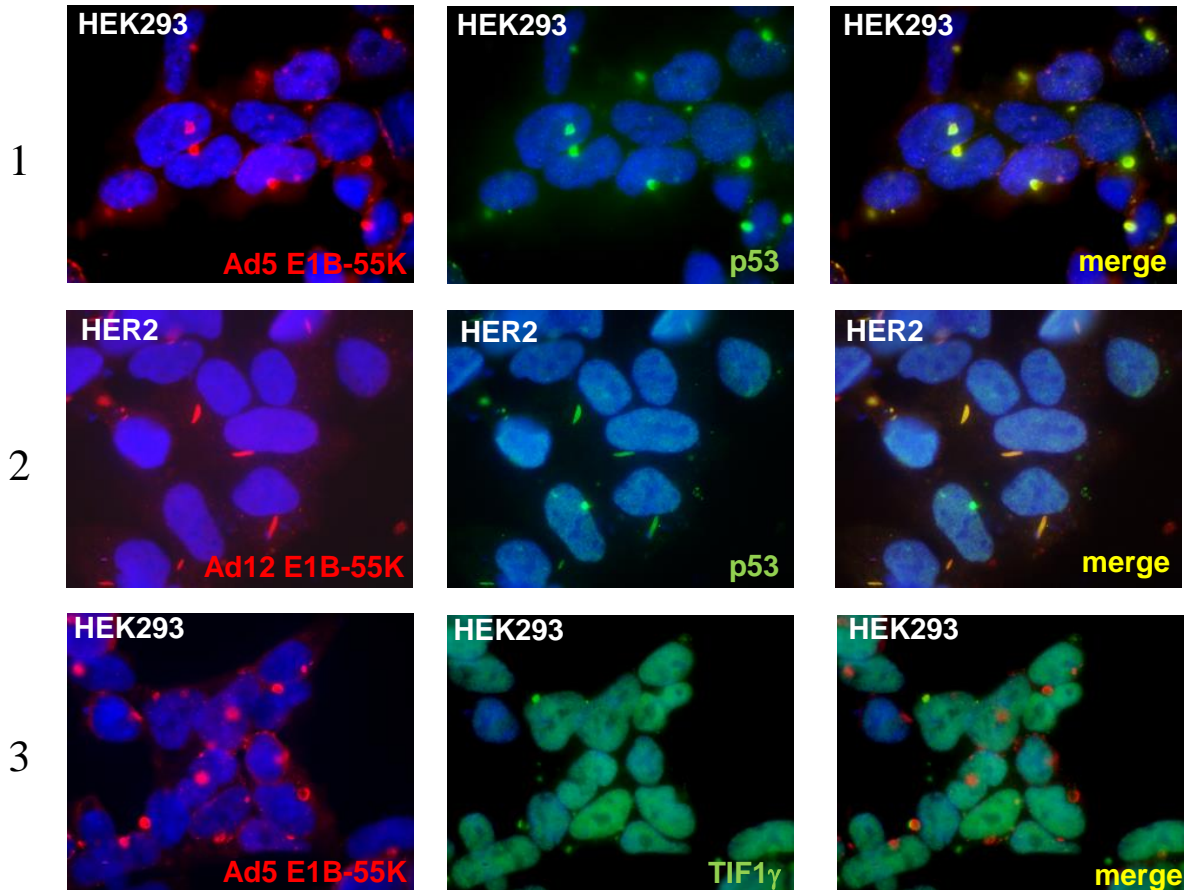
Ad5 infection had been documented as causing the active re-localisation of a variety of tumour suppressor proteins, such as p53 and Mre11, to pericentrisomal E1B-55kDa containing cytoplasmic aggresomes. Ad12 infection had been shown to have similar effects. Although the cells used here were not virally infected and did not express a full complement of early region viral gene products, certain E1B-55kDa binding proteins were still found to reside in these structures.

There appeared to be less E1B expressed in HER2s than in HEK293s, although it should be noted that different α -E1B antibodies were used.

TIF1 γ had a more diffuse distribution pattern in and around the nucleus (Figure 3.3A, panel 3; Figure 3.3B), contrary to earlier findings implying an exclusively nuclear localisation in *Xenopus laevis* cells that were not infected with adenovirus (Dupont *et al.*, 2005). Although it also clearly demonstrated some co-localisation with E1B, a much smaller fraction did so than was the case with p53 and some E1B containing flecks did not contain any TIF1 γ (Figure 3.3B). This may have been due to differences in expression levels between p53 and TIF1 γ ,

differential regulation of discrete cellular pools of TIF1 γ , or both. The higher magnification images (Figure 3.3B) clearly show large cytoplasmic aggregates to which E1B and TIF1 γ co-localise.

A



B

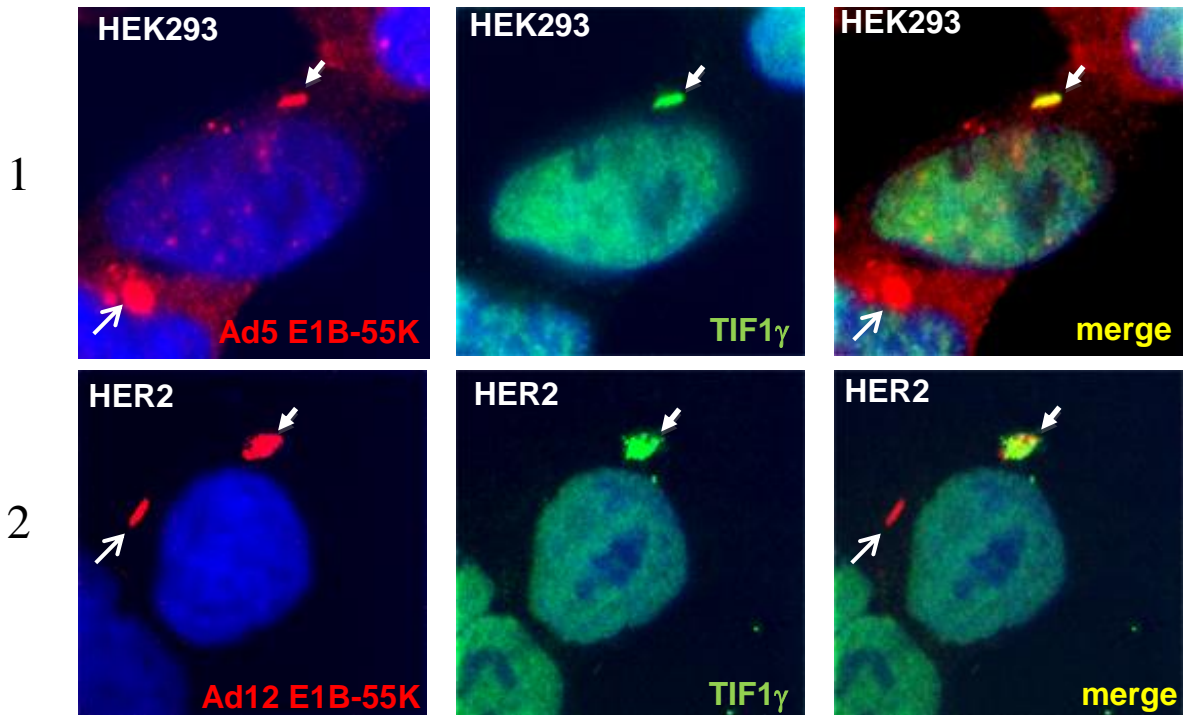


Figure 3.3: Immunofluorescence confocal microscopy images showing staining for either Ad5 or Ad12 E1B-55kDa (red) in conjunction with either p53 or TIF1 γ (both green), as labelled. Nuclei are stained blue with the DNA-binding fluorescent stain DAPI. Images in 3.3B are at higher magnification than those shown in 3.3A. White arrows with closed heads show E1B containing structures that also contain TIF1 γ . White arrows with open heads show E1B containing structures that do not contain a detectable level of TIF1 γ .

TIF1 γ was shown to co-localise with E1B-55kDa in structures that resemble cytoplasmic aggresomes. It is likely that the interaction observed in section 3.2 was occurring within these structures prior to cell lysis.

3.4 Demonstration of TIF1 γ and PML/E4orf3 co-localisation using immunofluorescence microscopy

It was noted previously that TIF1 γ co-localised with E1B-55kDa in some, but not all, E1B-55kDa-containing cytoplasmic flecks. As both TIF1 γ and E1B have been shown to possess pleiotropic functions, this observation could be explained if either or both proteins existed in discrete pools in which they possessed different binding partners. E1B-55kDa was also known to co-localise with E4orf3 in nuclear tracks formed following the E4orf3-dependent restructuring of PODs. Certain tumour suppressor proteins, such as Mre11, have been shown to be localised to these nuclear tracks prior to being exported from the nucleus with E1B-55kDa – a process made more efficient by the presence of either E4orf3 or E4orf6. It seemed reasonable to explore whether or not TIF1 γ was also to be found in these nuclear tracks.

To address the question of whether or not E4orf3 could be a player in the reduction of TIF1 γ observed on adenoviral infection, further immunofluorescence images were obtained using HeLa cells that had been infected with Ad5 or Ad12 to provide them with a full complement of adenoviral proteins (Figure 3.4i; Figure 3.4iiA).

Unfortunately, a lack of Ad12 E4orf3 antibody precluded direct attempts to co-stain for Ad12 E4orf3 and TIF1 γ in infected cells. Therefore two indirect methods were devised to compare E4orf3 and TIF1 γ co-localisation on Ad5 and Ad12 infection.

In the first, staining was carried out for TIF1 γ and PML on the basis that E4orf3 is well documented as co-localising with PML in nuclear tracks (Figure 3.4i).

In the second, direct co-staining for E4orf3 and TIF1 γ during Ad5 infection was carried out (Figure 3.4iiA) and, for comparison, slides were made following tag staining for HA-tagged E4orf3 and FLAG-tagged TIF1 γ in monoclonal HeLa cells that were formed by co-transfection of the plasmid constructs containing the two genes (Figure 3.4iiB).

PML exhibited some co-localisation with TIF1 γ (Figure 3.4i, panels 1 and 2) but not as much as for direct E4orf3/TIF1 γ co-localisation as seen in the Ad5 infection images (Figure 3.4iiA).

The Ad12 transfection images (Figure 3.4iiB) were quite different to the Ad5 infection image (Figure 3.4iiA). This was mainly due to more intense and widespread staining for HA-E4orf3 than for Ad5 E4orf3, presumably due to plasmid expression being under a strong promoter or differences due to comparing staining by different antibodies. Nevertheless, co-localisation of FLAG-TIF1 γ and HA-E4orf3 was still apparent.

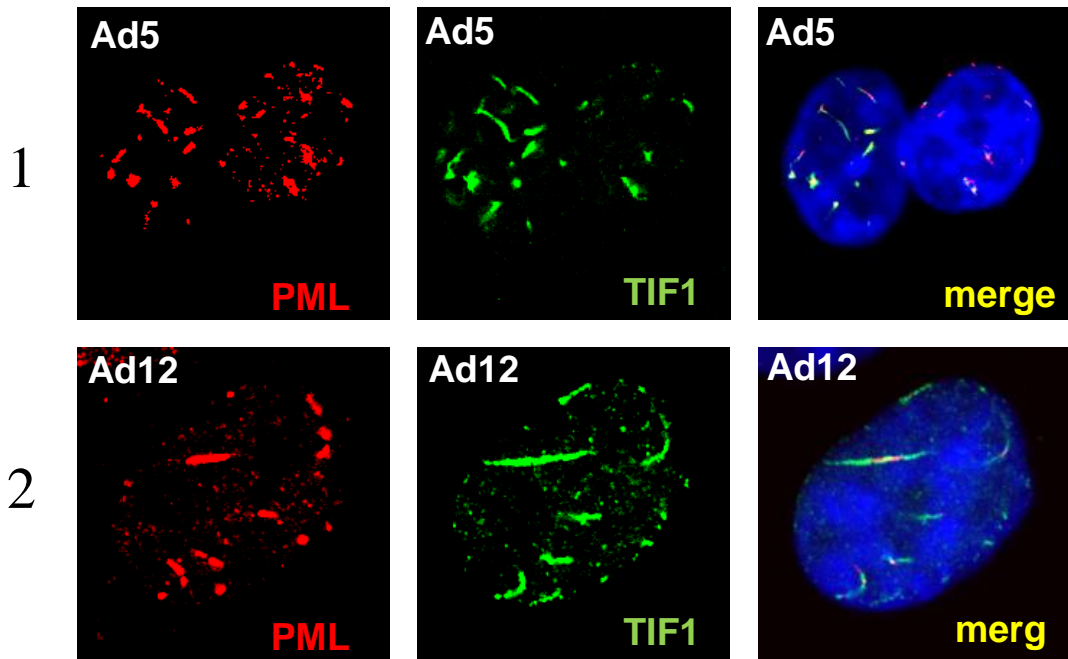


Figure 3.4i: Immunofluorescence confocal microscopy images of HeLa cells showing staining for PML (red) and TIF1 γ (green), as labelled. Nuclei are stained blue with the DNA-binding fluorescent stain DAPI. Images were taken from cells fixed and stained 18 hours post infection with 10pfu per cell of Ad5 (panel 1) or Ad12 (panel 2).

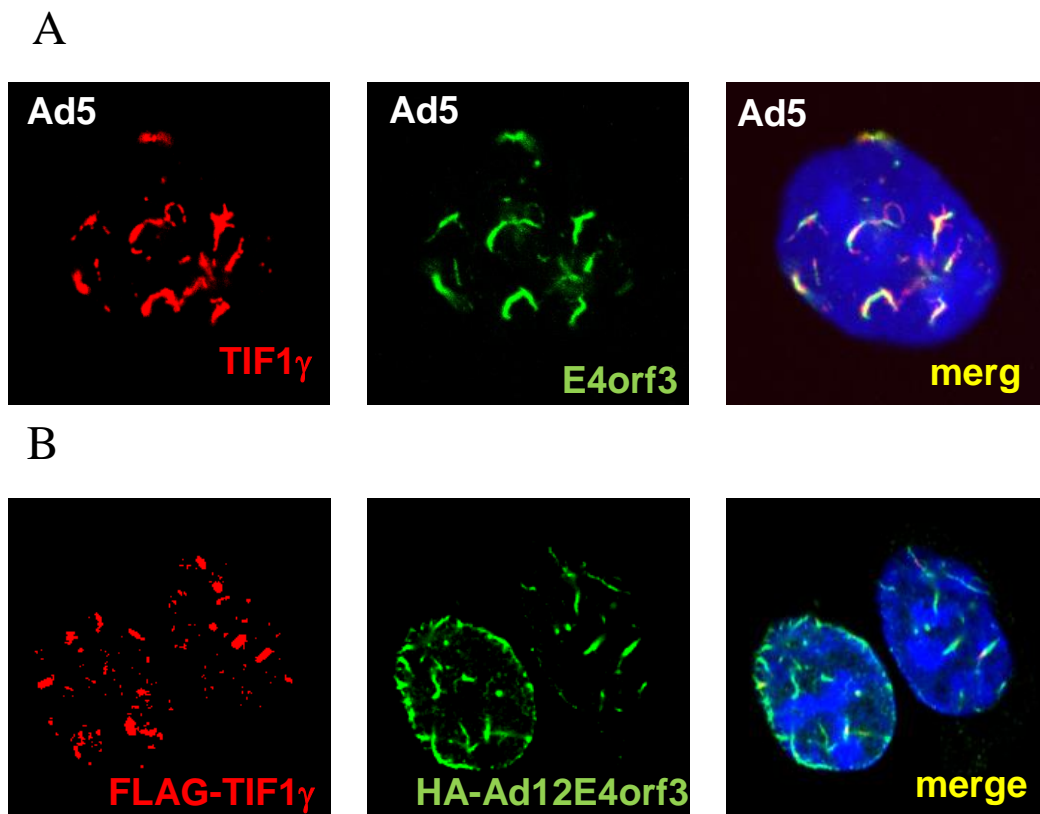


Figure 3.4ii Immunofluorescence confocal microscopy images of HeLa cells showing staining for TIF1 γ or FLAG (both red) and Ad5 E4orf3 or HA (both green), as labelled. Nuclei are stained blue with the DNA-binding fluorescent stain DAPI. Images in 3.4iiA were

taken from cells fixed and stained 18 hours post infection with 10pfu per cell of Ad5. Images in 3.4iiB were taken using a monoclonal cell line generated by co-transfection of plasmid constructs containing genes encoding the tagged proteins.

These figures demonstrated a clear spatiotemporal connection between E4orf3 and TIF1 γ in the nucleus during Ad5 infection, and supported the suggestion that E4orf3 may be involved in the reduction in TIF1 γ levels seen during adenoviral infection.

3.5 E4orf3 is necessary for the reduction in TIF1 γ levels seen following Ad5 infection in A549 cells

During the course of this investigation, an Ad5 mutant virus that does not express E4orf3 was generated by the Dobner group (University of Hamburg, Germany). In conjunction with an E4orf3/E4orf6 mutant that had previously been created, this allowed for direct examination of the effects of E4orf3 and E4orf6 on the reduction in TIF1 γ levels seen on wild type Ad5 infection of cultured cells.

E1B-55kDa has been shown to interact with TIF1 γ and is known to interact with both E4orf3 and E4orf6. Both E4 proteins could potentially be involved in the Ad5-mediated reduction in TIF1 γ levels.

Evidence produced so far in this investigation has shown co-localisation between TIF1 γ and E4orf3. It could be postulated that this interaction results in the translocation of TIF1 γ to aggresomes to await ubiquitylation by the adenoviral E3 ligase. This has not been demonstrated however. Indeed, no evidence has been provided to suggest that E4orf3 need be necessary for the drop in TIF1 γ levels. Mre11, for example, has been shown to migrate to aggresomes with E1B in the absence of E4orf3/E4orf6, albeit at a slower rate. In contrast, E4orf6 has been well documented as an integral part of the adenoviral E3 ubiquitin ligase that can directly reduce the cellular level of a protein by targeting it for degradation by the 26S proteasome.

The availability of the new E4orf3 mutant Ad5 allowed for a series of Western blots to be designed in order to ascertain if E4orf3 is necessary for the reductions in TIF1 γ following Ad5 infection. A549s were infected with wild type Ad5, a mutant Ad5 that lacks E4orf3 expression, a mutant Ad5 that lacks E4orf3 and E4orf6 expression, or mock (serum free DMEM). Cells were then harvested after 24 and 48 hours. The resultant lysates were subjected to protein quantification, resolved via SDS-PAGE and used to generate blots for TIF1 γ and a number of different controls (Figure 3.5).

In conjunction with the actin blot loading control (Figure 3.5, panel 6), the E4orf3 (Figure 3.5, panel 4) and E4orf6 (Figure 3.5, panel 5) blots demonstrated that the infections has worked and that the mutant viruses were expressing as expected. E1B-55kDa levels were fairly constant between infections (Figure 3.5, panel 3). This blot was important to show that it was present to act in concert with the E4orf6 containing E3 ligase and/or E4orf3 and that its levels were not significantly altered in the mutant Ad5 infections with respect to wild type infection. Finally a blot for p53 was performed to allow comparison between TIF1 γ and a protein known to be ubiquitylated by the E4orf6 containing E3 ligase (Figure 3.5, panel 2). This blot clearly showed that E4orf3 was not involved in the degradation of p53. It even appeared to stabilise it a little as the E4orf3 null mutant virus degraded host p53 quicker than wild type. It also confirmed a major role for E4orf6 in p53 degradation following Ad5 infection.

Most directly important for this investigation, E4orf3 was shown to be a major player in the degradation of TIF1 γ during Ad5 infection (Figure 3.5, panel 1). This finding was a little challenging as the literature does not provide much information on E4orf3 acting alone to cause a drop in cellular protein levels on Ad5 infection.

Two possibilities were considered as possible explanations for this and further avenues of investigation. Firstly, there was the possibility that E4orf3 and E4orf6 have a mutually dependent relationship. The data did not preclude the possibility that the Ad5 E3 ligase was necessary but not sufficient for the ubiquitylation and subsequent proteasomal degradation of TIF1 γ . Should E4orf3 be absolutely required for the translocation of TIF1 γ to the ligase, then it would also be necessary but not sufficient. The lack of an E4orf6- Ad5 mutant was unfortunate as it could have cleared up this issue. Lack of time precluded both the design and ordering of an siRNA to knockdown the protein and another experiment using a proteasome inhibitor.

The other possibility considered was based on the recent finding by Soria *et al* (2010) that E4orf3 could transcriptionally repress p53 responsive genes by causing selective promoter methylation. Should E4orf3 be able to cause downregulation of TIF1 γ , then that would clearly push the TIF1 γ protein turnover equilibrium towards increased catabolism and could mechanistically explain how Ad5 reduces TIF1 γ levels in infected cells.

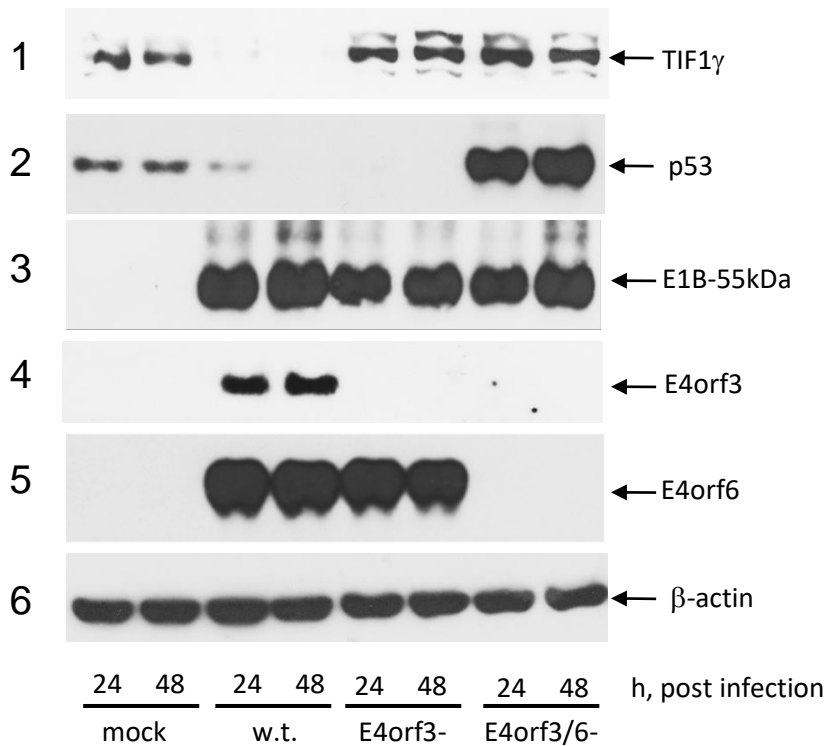


Figure 3.5: Western blots showing the absolute levels of specified proteins over time following wild type Ad5, E4orf3- mutant Ad5, E4orf3-/E4orf6- mutant Ad5 or mock (serum free DMEM) infection of A549 cells at time=zero. Cells were lysed in urea buffer and lysate volumes equivalent to 50µg total protein were resolved using SDS-PAGE. Proteins were transferred to nitrocellulose membrane and this was probed with suitable primary and secondary antibodies and finally developed as described in text.

E4orf3 was shown to be necessary for the fall in TIF1γ levels seen during viral infection with Ad5. The nuclear co-localisation between the two proteins may be important in this process, or it may be a red herring if downregulation due to E4orf3-dependent promoter methylation is responsible for the drop.

3.6 **Repression of p53-dependent transcription by Ad5 E4orf3 is not necessary to instigate the reduction in TIF1γ levels seen following infection**

TIF1γ levels are stable in non-infected cells (Figure 3.1A, Panel 1) and fall post-infection with various adenoviral serotypes, including Ad5 (Figure 3.1A, Panel 1). The fall does not occur in the absence of Ad5 E4orf3. Therefore E4orf3 must mediate TIF1γ degradation, expression or both. Given the necessary role for Ad5 E4orf3 in the attenuation of TIF1γ levels during infection, it was decided to investigate if prevention of p53 dependent transcription is required to allow this to occur in the context of infection.

The question being addressed is subtle. It is possible that p53 dependent transcription does indeed affect TIF1 γ levels. It is even possible that the mechanism by which E4orf3 abates TIF1 γ levels relies on its ability to downregulate p53-responsive genes (see section 4.5). The only point to be considered here, however, is whether E4orf3 repression of p53-dependent transcription is necessary to start a process that ultimately leads to the reduction in absolute TIF1 γ levels seen during Ad5 infection. To be necessary, there has to be basal p53 transcription present prior to infection.

To explore this issue, the A549 data from section 3.1 was to be compared with equivalent data obtained using the p53-null H1299 cell line. If transcriptional repression is required for TIF1 γ levels to fall on infection, then E4orf3 should not be able to attenuate TIF1 γ levels in H1299. That is because there was assumed to be no basal p53 transcription to repress. The same procedures were employed as in section 3.1 except:

- 1) H1299 cells were used, not A549
- 2) Cells were harvested at 12 and 24 hours post-infection
- 3) Only TIF1 γ , actin and certain early region adenoviral proteins were blotted.

Western blot analysis showed TIF1 γ levels to fall post-infection with wild type Ad5 (Figure 3.6). This categorically disproved a necessary role for the repression of p53-dependent transcription in the attenuation of TIF1 γ levels seen within the context of wild type Ad5 infection.

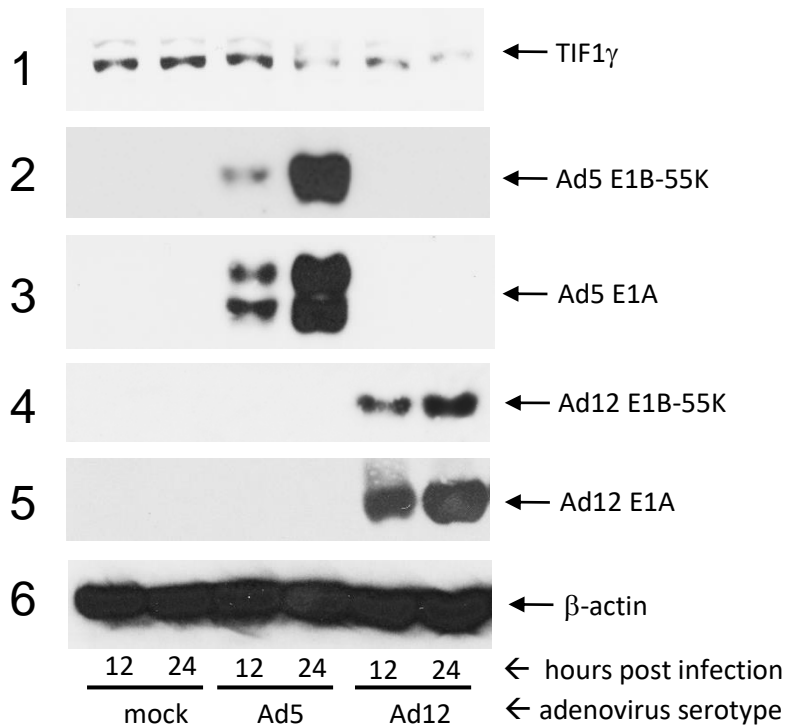


Figure 3.6: Western blots showing the absolute levels of specified proteins over time following Ad5, Ad12, or mock (serum free DMEM) infection of H1299 cells at time=zero. Cells were lysed in urea buffer and lysate volumes equivalent to 50 μ g total protein were resolved using SDS-PAGE. Proteins were transferred to nitrocellulose membrane and this was probed with suitable primary and secondary antibodies and finally developed as described in text.

3.7 Mass spectrometry data suggests that Ad5 E4orf3 interacts with a ubiquitin E3/E4 ligase that could potentially mediate TIF1 γ degradation

In the absence of an E4orf6-null mutant Ad5 or the time to instigate a knock-down experiment, mass spectrometry was carried out on HA-tagged Ad5 or Ad12 E4orf3 expressing clonal cell lines that had previously been generated during the course of this investigation (see section 2.2.2). This was done in the hope of finding novel E4orf3 interactors that could possibly be involved in the attenuation of TIF1 γ levels that occurs during the course of infection with Ad5 or Ad12.

To validate that the clonal HA-E4orf3 HEK293 cell lines were maintaining the expression of E4orf3 prior to performing IPs for mass spectrometry, a second Western blot was undertaken (Figure 3.7A).

A

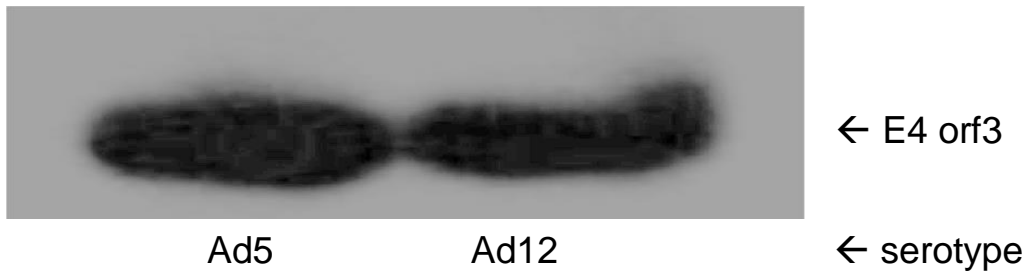


Figure 3.7A: Western blot confirming the continued expression of HA-tagged E4orf3 in the clonal cell lines generated previously (see section 2.2.2; Figure 2.1). Cells were lysed in urea buffer and lysate volumes equivalent to 50 μ g total protein were resolved using SDS-PAGE. Proteins were transferred to nitrocellulose membrane and this was probed with an anti-HA-tag primary antibody and suitable secondary antibody and finally developed as described in text.

Having established that the cell line was continuing to express the desired proteins (Figure 3.7A), an immunoprecipitation experiment was devised using an anti-HA antibody. Twenty confluent dishes each of Ad5 and Ad12 HA-E4orf3 expressing HEK293 cells were harvested using HiLo buffer, processed and then run on a 12% acrylamide gel as shown (Figure 3.7B). The gel was then stained using Coomassie Brilliant Blue dye, destained and prepared for mass spectrometry.

B

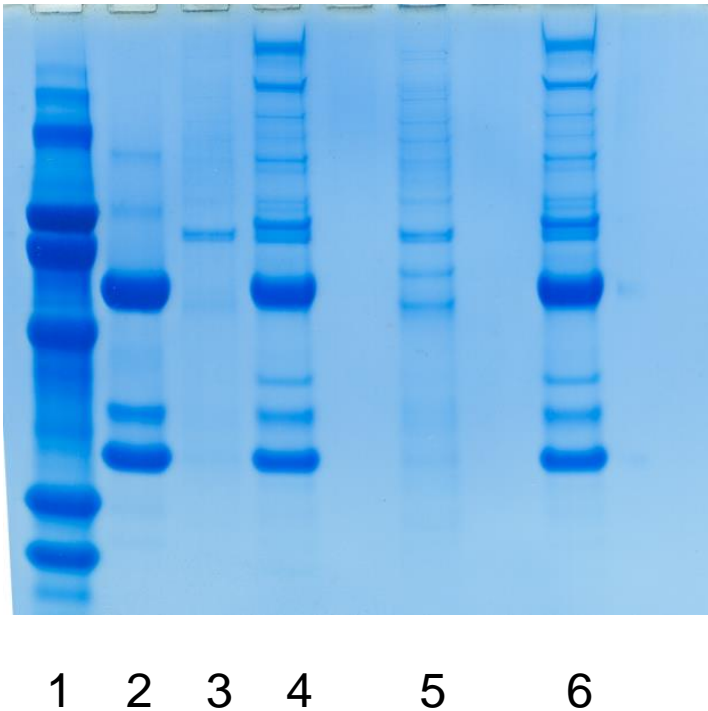


Figure 3.7B: Image of gel used in mass spectrometry experiment following destaining. Lane 1 was a molecular weight marker lane, Lane 2 was α -HA antibody alone, Lane 3 was a Protein G (PrG) control with HA-tagged Ad5 E4orf3 lysate, Lane 4 was α -HA with HA-tagged Ad5 E4orf3 lysate, Lane 5 was a PrG control with HA-tagged Ad12 E4orf3 lysate and Lane 6 was α -HA with HA-tagged Ad12 E4orf3 lysate.

Following trypsinisation of the proteins, the peptides were separated using high performance liquid chromatography (HPLC) and eluted peptides were introduced to a time of flight/time of flight tandem mass spectrometer by an electrospray method. The data obtained were subjected to analysis against the SwissProt protein database using the manufacturer's software.

Across the four lanes, 245 peptides were identified as constituents of named proteins (data not shown). A search was also carried out against a decoy database which found 10 of the 245 to be significant hits, giving a false discovery rate of around 4% (data not shown). All false discoveries from the decoy database were single hits (data not shown), implying that proteins with more than 1 peptide hit were unlikely to be false positives.

The proteins identified as possible E4orf3 interacting proteins are presented in Table 3.1. The protein Mascot scores, as calculated by the ProteinScope software, are the sum of the scores for its individual peptides. Only unique hits were counted. Representative peptide mass spectra are shown in Figure 3.7C. Additional data pertaining to the database search, and

sequence coverage maps, are included in Appendix 1 (Ad5 E4orf3 pulldown data) and Appendix 2 (Ad12 E4orf3 pulldown data).

Table 3.1A: Putative Ad5 E4orf3 interacting proteins suggested by mass spectrometry

<u>Protein</u>	<u>RMM (kDa)</u>	<u>Hits</u>	<u>Mascot Score</u>	<u>coverage (%)</u>
Pro-low-density lipoprotein receptor-related protein 1	504.2	26	933.3	6.8
Tyrosine-protein phosphatase non-receptor type 13	276.7	35	1266.9	18.4
Kinase D-interacting substrate of 220 kDa	196.4	8	255.9	5.5
Ubiquitin conjugation factor E4 A	122.5	11	392.3	11.3
Exportin-7	123.8	3	81.8	2.9
Conserved oligomeric Golgi complex subunit 5	92.7	9	317	12.5
Conserved oligomeric Golgi complex subunit 7	86.3	8	258.1	13
LETM1 and EF-hand domain-containing protein 1	83.3	20	877.1	30.9
Eukaryotic translation initiation factor 3 subunit J	29	7	244.5	27.9

Table 3.1B: Putative Ad12 E4orf3 interacting proteins suggested by mass spectrometry

<u>Protein</u>	<u>RMM (kDa)</u>	<u>Hits</u>	<u>Mascot Score</u>	<u>Coverage (%)</u>
Pro-low-density lipoprotein receptor-related protein 1	504.2	25	858	6.7
Tyrosine-protein phosphatase non-receptor type 13	276.7	36	1272.6	18.8
Kinase D-interacting substrate of 220 kDa	196.4	7	218.4	4.7
Ubiquitin conjugation factor E4 A	122.5	9	330.2	10.1
Exportin-7	123.8	4	99.5	3.9
Conserved oligomeric Golgi complex subunit 5	92.7	11	354.9	14.4
Conserved oligomeric Golgi complex subunit 7	86.3	10	340.2	16.8
LETM1 and EF-hand domain-containing protein 1	83.3	26	1315.5	36.8
Eukaryotic translation initiation factor 3 subunit J	29	7	283.2	27.9

These proteins will all be considered in the discussion, but the UBE4A protein is of considerable interest here. It belongs to a group of U-box containing proteins that are present across all metazoan species. These proteins have been shown to function as E3 ubiquitin ligases, E4 ubiquitin ligases and also to mediate proteasomal degradation. In such, it is undoubtedly the most likely candidate E4orf3 interactor to play a direct role in TIF1 γ degradation.

C

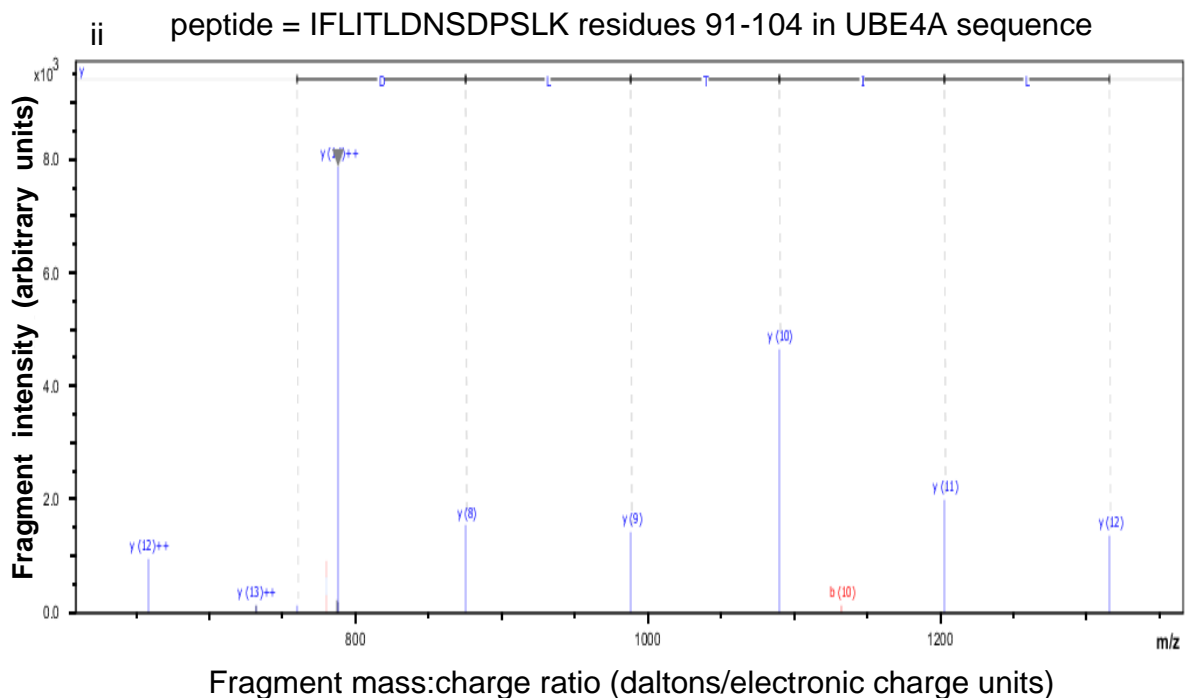
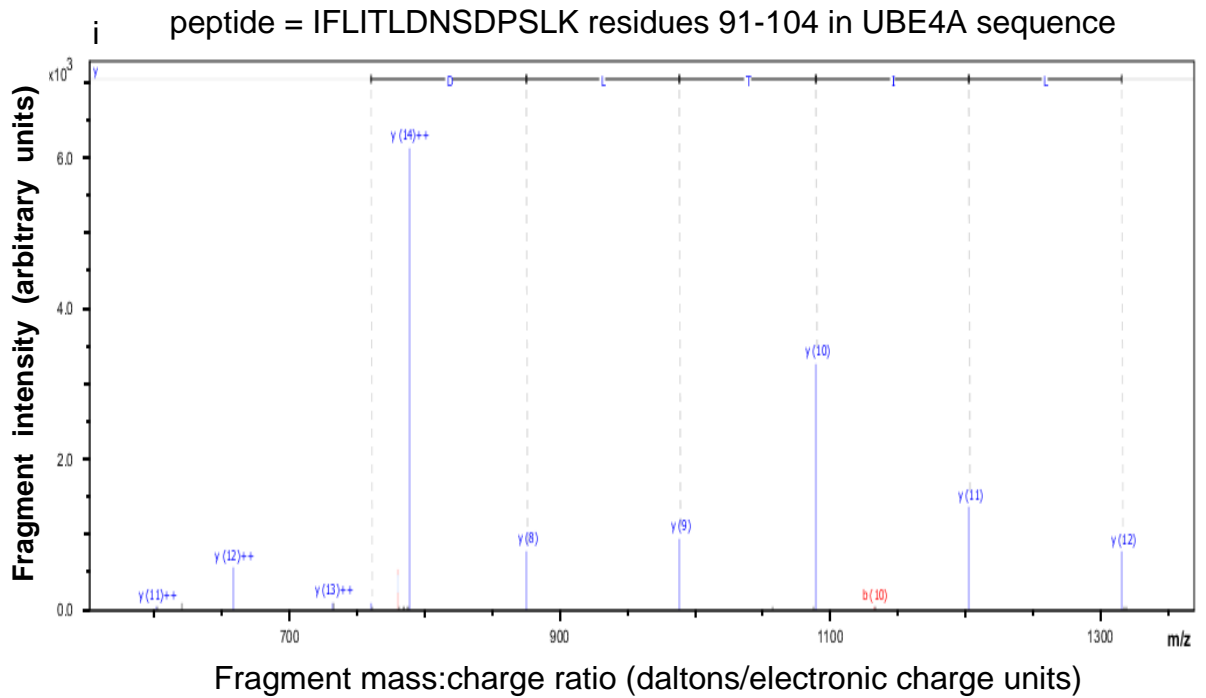


Figure 3.7C: MS/MS spectra generated following the fragmentation of a peptide of sequence IFLITLDNSDPSLK that had formed during the tryptic digest of proteins pulled down with either; i) Ad5 E4orf3 or, ii) Ad12 E4orf3. A Mascot search, using the SwissProt database, suggested that the peptide originated from the UBE4A protein. The location of the sequence within UBE4A is shown above each spectrum. In each figure, blue lines refer to positive y ions. Red lines refer to positive b ions. The horizontal lines above the peaks are divided by dashed vertical lines. The latter refer to projected singly charged fragment peaks if the amino acids named on the former are removed in a right to left direction.

3.8: Summary of results

These findings confirmed earlier observations that showed a fall in absolute cellular TIF1 γ levels post-infection with Ad5 or Ad12 (Figure 3.1A, Panel 1). They imply that this drop is specific to TIF1 γ , as levels of the closely related TIF1 β protein did not show a similar drop (Figure 3.1A, Panel 2). TIF1 γ was shown to interact with both Ad5 (Figure 3.2A, Panel 1) and Ad12 (Figure 3.2B, Panel 1) E1B-55kDa. Spatial insights into this interaction were provided showing that the two proteins co-localise to cytoplasmic structures located close to the nucleus in adenovirus-transformed cells in culture (Figure 3.3B). TIF1 γ was also shown to co-localise with the related PML protein during both Ad5 and Ad12 infection (Figure 3.4i) and with E4orf3 following Ad5 infection (Figure 3.4iiA). This implied a link to E4orf3 nuclear tracks, and subsequent investigation showed that E4orf3 was necessary for TIF1 γ levels to fall following Ad5 or Ad12 infection (Figure 3.5, Panel 1). E4orf3-dependent downregulation of p53-specific genes was not implicated in its modulation of TIF1 γ levels (Figure 3.5, Panels 1 and 2; Figure 3.6, Panel 1). Whilst it is a strong possibility that E4orf3 interacts with other adenoviral proteins in mediating the degradation of TIF1 γ , mass spectrometry data suggested that E4orf3 also interacts with UBE4A, a protein that can mediate the proteasomal degradation of cellular proteins by ubiquitin dependent and independent pathways. UBE4A is therefore a candidate for acting in concert with E4orf3 to result in TIF1 γ degradation. No evidence is provided for it playing such a role, however, and further work will be needed to clarify this issue.

Chapter 4: Discussion

4.1: Initial observations and considerations

It was clear from the initial Western blot data that TIF1 γ levels do fall following infection with Ad5 or Ad12 in adenovirus-transformed cell lines. This was in keeping with previous unpublished findings made by the Turnell group.

TIF1 family members share several domains in common (Figure 1.6), but they also possess other motifs that confer specific functions to each member (Khetchoumian *et al.*, 2004). There are also differences in expression patterns. TIF1 δ , for example, is only expressed in the testes (Khetchoumian *et al.*, 2004). As TIF1 β levels did not fall during adenoviral infection as with TIF1 γ , this implied that adenovirus has evolved to specifically target TIF1 γ whilst leaving certain other closely related proteins unaffected.

This raised a couple of interesting questions – why does adenovirus specifically target TIF1 γ , and how does it do it? It was clear that TIF1 γ had a function that made it more of a danger to adenovirus than the closely related TIF1 β protein. As for how it does it, one theory that had initially been considered was that adenovirus could affect the fat facets in mammals (FAM) protein. Considering the evidence that pointed to TIF1 γ being involved in signalling through SMAD4 (Dupont *et al.*, 2005), it was decided to investigate the effects of infection on the deubiquitylase that antagonises TIF1 γ -mediated ubiquitylation (Dupont *et al.*, 2009).

Absolute FAM levels were unaffected as a result of Ad5 or Ad12 infection (Figure 3.1A, Panel 3). Immunofluorescence work examined the cellular localisation of FAM to see if that changed on Ad5 or Ad12 infection. Unfortunately, no usable data was obtained.

Making the rather bold and unsubstantiated assumption that adenovirus targets TIF1 γ because of its role in TGF- β signalling, it is quite possible that FAM would also be subject to modulation by adenoviral proteins. FAM was shown to be epistatic to TIF1 γ (Dupont *et al.*, 2009), being necessary to switch on signalling through SMAD4. Background FAM levels may be sufficient to instigate downstream signalling, especially in the context of reduced TIF1 γ seen during adenoviral infection. It may also be deleterious for adenovirus to target FAM due to possible functions independent of signalling through SMAD4. Further investigation of this area could prove insightful. While it may not elucidate how adenovirus regulates TIF1 γ , it may nevertheless give some functional insight into why adenovirus regulates TIF1 γ .

4.2: Reflections on the TIF1 γ -large E1B interaction

The observation that TIF1 γ interacts with E1B-55kDa was thought provoking. It was known, for example, that E1B-55kDa could deliver substrates such as p53 to the adenoviral E3 ubiquitin ligase in infected cells. The possibility that the ligase does play a role in reducing TIF1 γ levels was neither fully confirmed nor repudiated here, so the possibility must remain.

An alternative mechanism of action that was considered at this point related to the finding that E1B-55kDa could function as an E3 SUMO ligase (Pennella *et al.*, 2010). SUMOylation of TIF1 γ could potentially result in a change in its function or localisation.

The fact that the TIF1 γ amino acid sequence (Venturini *et al.*, 1999) contains several putative aKXE SUMOylation consensus sequences (where a is an aliphatic amino acid and K is the lysine to be SUMOylated) (Melchior, 2000) (Table 4.1), had been noticed in the lab (Turnell, unpublished observations).

Table 4.1: Possible SUMOylation sites within the TIF1 γ protein

Sequence	Location (based on sequence in Venturini <i>et al.</i> , 1999)
KKKE	Type 2 B-box
VKQE	HP1 box
GKSE	around 25-30 residues N-terminal of the plant homeodomain
SKPE and KKTE	between plant homeodomain and bromo-domain
RKCE, SKPE and IKLE	Bromo-domain
PKPE	around 10-15 residues C-terminal of the bromo-domain

Considering that adenovirus was known to target PODs, whose function is regulated by SUMOylation, attempts were made to express FLAG-tagged SUMO1 or SUMO2 in U2OS cells and then infect them with Ad5, Ad12 or mock virus (serum free DMEM). Cells were harvested and immunoprecipitated with an anti-FLAG primary antibody followed by blotting for TIF1 γ . Unfortunately no usable data was forthcoming. It would still be useful to learn if SUMOylation is involved in the regulation of TIF1 γ levels by adenovirus, and future work could readdress the issue.

It was noted incidentally that the rate of loss of TIF1 γ increases with increasing E1B-55kDa levels (Figure 3.1A). E1B-55kDa is one of the first viral proteins to be expressed and it is not unexpected that viral protein expression in general would be temporally linked to the cellular symptoms of infection.

4.3: Considerations following immunofluorescence findings

The finding that some TIF1 γ co-localised with E1B-55kDa in cytoplasmic structures near the nucleus (Figure 3.3B) was interesting. As these findings were carried out in adenovirus-transformed cells, the findings are perhaps not exactly as would be found in infection. For example, it is possible that E1B-55kDa causes TIF1 γ to relocate to cytoplasmic structures to instigate a process leading to adenoviral E3 ubiquitin ligase-dependent degradation.

TIF1 γ possesses chromatin remodelling PHD and bromo-domains. E1B-55kDa is known to function to repress p53-dependent transcription. The possibility that they play antagonistic roles in transcription suggests a function for E1B-55kDa sequestering TIF1 γ outside the nucleus, although that may be coincidental. In the natural context of infection, any TIF1 γ functions potentially deleterious to adenovirus could be independent of E1B-55kDa.

In infection, viral transcription and ultimate translation occur in a well choreographed manner. In these cells, E1A and E1B proteins are constitutively expressed. How these proteins function and interact with cellular proteins without the co-ordination of the rest of the viral genome is uncertain, and it is possible that these findings are a function of the experimental conditions as opposed to a function of the adenoviral proteins per se.

Possibly more intriguing still was the finding that TIF1 γ closely co-localises with E4orf3 in Ad5 infected cells (Figure 3.4iiA), and may well also do so in Ad12 infected cells based in particular on PML/TIF1 γ co-localising on infection (Figure 3.4i, Panel 2). The lack of pronounced FLAG-TIF1 γ /Ad12 HA-E4orf3 nuclear co-localisation in co-transfected HeLa cells was not taken to disprove a spatiotemporal relationship in the context of infection.

The viral infection confocal images give a snapshot of TIF1 γ prior to its E4orf3-dependent dissipation. It is intriguing that they co-localise in the nucleus 18 hours post-Ad5 infection when levels will have already started to fall.

Combined, the E1B-55kDa/TIF1 γ and E4orf3/TIF1 γ data are reminiscent of how Ad5 targets Mre11 for degradation (Stracker *et al.*, 2005). Firstly it is sequestered away from viral replication centres in nuclear tracks by interaction with E4orf3. Later it is exported from the nucleus to aggresomes/aggresome-like structures with E1B-55kDa in conjunction with E4orf3 or E4orf6. The ultimate fate of Mre11 is proteasomal degradation secondary to ubiquitylation by the adenoviral E3 ligase. It could well be that TIF1 γ is similarly regulated.

It would be interesting to examine E1B-55kDa and TIF1 γ during infection in another cell type, such as A549, to see if E1B does indeed co-localise with TIF1 γ to cytoplasmic structures on infection.

Transfecting cells with an siRNA-resistant wild type TIF1 γ -green fluorescent protein (GFP) construct whilst knocking down their endogenous TIF1 γ with a suitably designed siRNA could be useful. The cells could then be infected and recorded by confocal microscopy for 48 hours post infection. Any change in localisation or concentration could then be observed in real time using computer software to calculate changes in GFP signal intensity over time.

4.4: Implications of mutant virus data

E4orf3 was shown to be a necessary factor in the reduction in cellular TIF1 γ levels seen post-infection with Ad5, whereas that was not the case for p53 degradation (Figure 3.5), making it clear that Ad5 regulates the two proteins differently.

It could be that Ad5 E4orf3 is directly involved in the reduction of cellular TIF1 γ following infection to the exclusion of the adenoviral E3 ubiquitin ligase. The effective degradation of p53 during E4orf3- mutant Ad5 infection implied that the ligase remained functional whilst TIF1 γ levels remained constant. Concluding that the ligase is not involved in TIF1 γ degradation could be spurious, however, as it remains possible that E4orf3 has a necessary role in transporting mediating their interaction.

It is unfortunate that a mutant Ad5 lacking E4orf6 alone was not available as this could have either proven that the Ad5 E3 ubiquitin ligase is not involved, or alternatively strongly imply that it does play a role. This is an area for future investigation. It would also be useful to develop similar mutant viruses representative of other species and repeat the experiment with them. Serotype-specific differences in the regulation of other proteins by adenovirus suggest that it would be unfair to induce that E4orf3 is necessary to reduce TIF1 γ levels following infection with Ad12, for example.

Whilst the underlying mechanism remained enigmatic, E4orf3 was clearly necessary for adenovirus to abate TIF1 γ during Ad5 infection.

Three possible explanations were considered of which the first has been discussed here and the second will be explored in the next section.

- 1) E4orf3 is necessary to mediate TIF1 γ ubiquitylation by the adenoviral E3 ligase.
- 2) E4orf3-mediated repression of p53-dependent genes is necessary to abate TIF1 γ
- 3) Some other E4orf3-mediated mechanism is involved

4.5: E4orf3-dependent regulation of TIF1 γ is p53-independent

Ad5 E4orf3 had recently been shown to selectively cause promoter methylation of p53-responsive genes (Soria *et al.*, 2010). As the E4orf3- mutant Ad 5 had shown TIF1 γ stabilisation, it was useful to examine whether that was due to E4orf3 no longer being present to repress p53-dependent transcription.

It was clearly shown that p53-dependent transcription is not required for E4orf3 to be able to abate TIF1 γ levels in wild type Ad5 infection (Figure 3.6, Panel 1; cf. Figure 3.1A, Panel 1 and Figure 3.5, Panel 1). This by no means proves that p53-dependent transcription is not involved in the process, however. The issue arises when addressing the levels of p53 present in A549s during Ad5 infection.

As a major difference between the wild type and E4orf3- mutant Ad5 infections (Figure 3.5, Panel 1) involved the relative abilities of the viruses to repress p53-dependent transcription, a hypothesis could be made stating that p53-transcription results in the stabilisation of TIF1 γ in the absence of Ad5 E4orf3. This idea is explored in Figure 4.1.

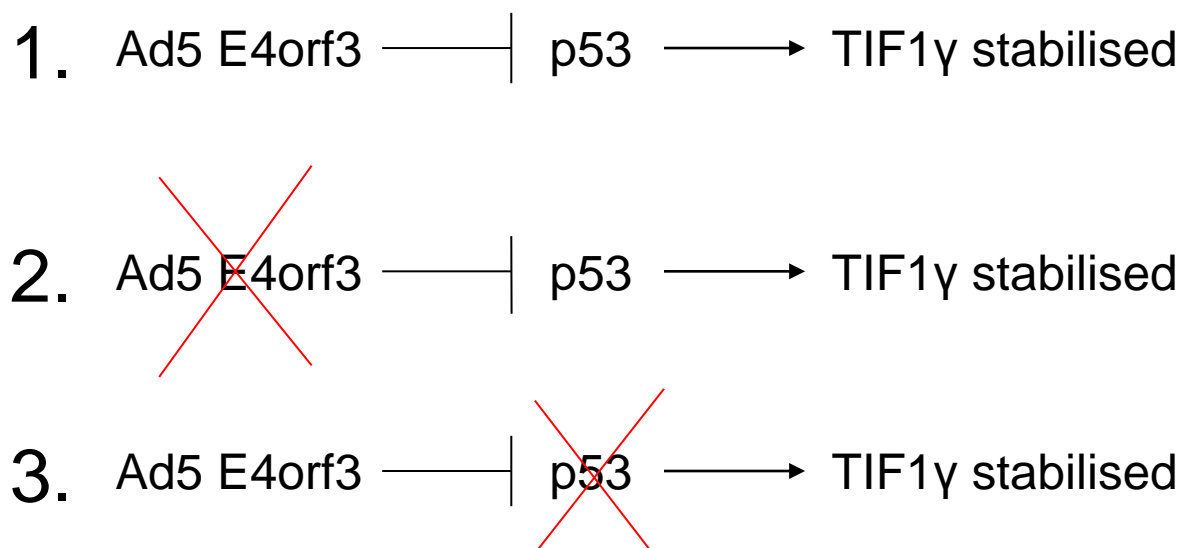


Figure 4.1: Effects of different experiments on the hypothetical ability of p53 to stabilise TIF1 γ levels in a transcription-dependent manner. p53 stabilises TIF1 γ and Ad5 E4orf3 antagonises that by transcriptional repression of p53-dependent promoters. A red cross denotes a step that is missing. 1) Wild type Ad5 infection of wild type p53 cells. p53 is unable to stabilise TIF1 γ [Figure 3.1A, Panel 1]. 2) E4orf3- mutant Ad5 infection of wild type p53 cells. p53 stabilises TIF1 γ in the absence of E4orf3 [Figure 3.5, Panel 1]. 3) Wild type Ad5 infection of p53-null cells. p53 is not present to stabilise TIF1 γ [Figure 3.6, Panel 1].

A further experiment using the E4orf3- mutant Ad5 to infect H1299 cells could be useful. It would address whether p53 transcription was involved in regulating TIF1 γ . In TIF1 γ levels were stabilised; as in Figure 4.1, Panel 2, then p53 cannot be regulate TIF1 γ levels downstream of E4orf3. If TIF1 γ fell, however, then that would imply that p53 was involved on some level as the major difference between that and Figure 4.1, Panel 2 would be p53 status. Any role for p53 seems unlikely based on subsequent analysis in this section, but the experiment would give clarity to the situation in the same way an E4orf6- mutant Ad5 could disprove a role for the adenoviral E3 ligase in TIF1 γ attenuation.

Although the underlying mechanism of action of E4orf3 is interesting in itself, adenovirus should be considered as a gestalt. E4orf3 does not function alone in Ad5 infection and the finding that it is p53-dependent promoter methylation is not necessary for TIF1 γ attenuation is a very important finding worth consideration.

The literature presently points to two unique E4orf3 functions that can modulate of cellular protein levels. One is to mediate transport to the viral E3 ubiquitin ligase (as with Mre11) and the other involves selectively repressing p53-dependent transcription. By formally removing one of these as a sine qua non for TIF1 γ levels to fall during Ad5 infection, only two options remain. Either the E4orf3 protein is absolutely necessary for allowing the Ad5 E3 ubiquitin ligase to mediate TIF1 γ degradation or, more excitingly perhaps, there is a novel E4orf3-dependent mechanism of selectively modulating protein levels.

Whilst a non-necessary role for E4orf3 in the attenuation of TIF1 γ through transcriptional repression of p53-dependent genes has not been disproven, the data suggest that the process is p53-independent. Even assuming that p53-dependent transcription continues when the p53 levels are sub-detectable by Western blotting, comparison of Figures 3.5 and 3.6 shows that the reduction in TIF1 γ is p53-independent.

Table 4.2: Effect of E4orf3/p53 status on TIF1 γ levels 24 hours post-Ad5 infection

Reference	Ad5	p53 present?	E4orf3 expressed?	TIF1 γ present?	Remarks
Fig 3.5, wt	Wild type	+	YES	-	p53 degraded
Fig 3.6, Ad5	Wild type	-	YES	++	p53 null
Fig3.5	E4orf3-	-	NO	++++	p53 degraded
Fig3.5	E4orf3- /E4orf6-	+++++++	NO	++++	p53 stabilised

Number of '+' is relative to absolute cellular levels of p53 or TIF1 γ

TIF1 γ levels did not appear to vary with p53 levels when E4orf3 was absent. Whilst the deleterious, and possibly confounding, effects of the loss of both E4orf6 and E4orf3 can not be completely ignored, TIF1 γ levels were the same 24 hours post-infection whether there was no detectable p53 present, or levels around 4 times base level. As E4orf3 was not present in either case it was not able to repress p53 responsive promoters. Levels of another known transcriptional repressor of p53-responsive genes, E1B-55kDa, were similar in both cases. This should have led to a difference in p53-dependent expression levels, yet there was no resultant difference in TIF1 γ levels (Table 4.2). This could be explained in terms of an extremely low level of p53 being sufficient for TIF1 γ stability in Ad5-infected cells in the absence of E4orf3.

However, when E4orf3 was present, a small amount of p53 corresponded to no detectable TIF1 γ (Figure 3.5, Panels 2 and 1; Table 4.2) whereas zero detectable p53 corresponded to some TIF1 γ remaining (Figure 3.6, Panel 1; Table 4.2).

It could then be argued that p53 can lead to the degradation of TIF1 γ in the presence of E4orf3 but that is unlikely and involves making more ad hoc assumptions.

A more parsimonious explanation can be provided by looking at the data in terms of E4orf3 expression against TIF1 γ levels. When E4orf3 was expressed, TIF1 γ levels were low or zero. When E4orf3 was not expressed, TIF1 γ levels were stabilised. This seemed completely independent of p53.

More exotic ideas could be postulated involving novel functions for E4orf3, but whilst a novel function is certainly a possibility, there is no evidence to suggest what that function might be.

4.6: Discussion of mass spectrometry results

4.6.1: Validity of data

A selection process was used that involved ignoring all keratins and other proteins present in the control lanes. According to the finding that 10 of the 245 peptides discovered were also flagged as significant in the decoy database search, and that each of those were single hits, it was further decided to ignore all suggested proteins for which there was only one peptide found.

It is interesting, and not altogether irrelevant, to consider that the Mascot scores calculated for the peptides, thereafter used to define significance, are directly related to the size of the database. The score is calculated based on the formula:

$$\text{Mascot Score} = -10\log_{10}(\text{probability of peptide being a false positive})$$

This leads to two related concerns, assuming that the algorithm used to calculate the probability is fair and unbiased;

- 1) As the database increases in size, so does the likelihood of a given set of peptides sharing the same sequences with multiple proteins. This will increase the general probability of finding false positives and lower the output score. Extrapolating into the future, peptides presently considered significant hits may not be in the future and this may skew the search results when the software has to decide on the most probable identity of a protein when two or more have similar scores. This issue mainly concerns proteins with low overall scores, such as Exportin-7.
- 2) Mass spectrometry is a powerful tool that often finds new proteins that have not yet entered into a given database. Should any proteins have been pulled down in the IPs that were not in the SwissProt database, then they would have been missed or come up as false positives.

Concerns about validity of the results aside, all proteins that passed the selection process were similarly flagged up as interacting with Ad5 E4orf3 and Ad12 E4orf3 (Table 3.1A and B; Appendices 1 and 2). This is in some ways expected as the proteins are well conserved at the amino acid level (Weitzman, 2005). The complete lack of differences is also surprising, however, due to previously reported differences in their functions and binding partners

(Stracker *et al.*, 2005; Greer *et al.*, 2011). Three things should be noted when considering this issue;

- 1) The cells had been generated by transfection as opposed to infection. Therefore the natural interactions that occur in the presence of the full complement of adenoviral proteins may not be seen.
- 2) It should be noted that the clonal lines were generated using HEK293 cells. These cells have neural characteristics and express a different complement of proteins to the epithelial cells that are normally targeted by adenovirus.
- 3) As HEK293 expresses Ad5 E1A and E1B proteins, interactions between E1B and Ad5 E4orf3 may be closer to those found in infection than E1B-Ad12 E4orf3 interactions. It should further be noted that Ad5 E1B-55kDa may have indirectly recruited Ad5-only interacting proteins to Ad12 E4orf3. Attempts to transfect HA-tagged Ad12 E4orf3 into HER2 and HER10 cells by electroporation were not successful (data not shown). In hindsight, attempts to transfect those cell lines with lipofectamine could have been undertaken. Alternatively, non-virally transformed cell lines could have been transfected with constructs encoding a variety of E4orf3/E1B-55kDa combinations.

Other things were surprising. As an example, E1B-55kDa had been well documented as interacting with E4orf3, yet neither it nor E4orf3 itself were recorded as present in the results. Previous mass spectrometry experiments in the Turnell lab using adenoviral E4 transcription unit proteins had also failed to flag either the E4 proteins themselves or other adenoviral proteins as having been present (data not shown). This was in spite of the fact that the proteins are supposedly in the database. This could have to do with the sequence of the proteins or with the fact that, in the case of E4orf3, the protein is very small.

Likewise proteins such as Mre11 or, interestingly, TIF1 α did not show up in the data. These omissions give further cause for concern and any discussion of the data should be treated cautiously. Reciprocal IPs would have clarified the validity of any suggested interactions, but unfortunately there was not enough time to carry out these experiments.

4.6.2: Function of putative E4orf3 interacting proteins/protein complexes

(protein names as pulled from database)

4.6.2.i: Ubiquitin conjugation factor E4 A (UBE4A)

Perhaps the most initially exciting putative E4orf3 interactor pulled down was the *UBE4A* gene product, Ubiquitin conjugation factor E4A. U-box containing ubiquitin E4 ligases such as this are extremely well conserved throughout the metazoa (Marín, 2010) and have been shown to function in a number of ways. They can mediate the polyubiquitylation of oligoubiquitylated proteins in the presence of E1, E2 and E3 enzymes (Koegl *et al.*, 1999). They can also function as E3 ligases in conjunction with E1 and E2 enzymes (Hatakeyama *et al.*, 2001). As well as targeting proteins for ubiquitin-dependent proteasomal degradation, they have also been shown to regulate the function of target proteins and even target them for proteasomal degradation in a ubiquitin-independent manner (Hosoda *et al.*, 2005). Whereas p73 degradation was enhanced by UBE4A (Hosoda *et al.*, 2005), a usually cisplatin-sensitive isoform of p63 was stabilised by it in the presence of the drug (Chatterjee *et al.*, 2008). The same protein has been shown to be targeted during apoptosis (Mahony *et al.*, 2002). Although many proteins are targeted during apoptosis, this has nevertheless led some to speculate that it is an important regulator of apoptosis (Chatterjee *et al.*, 2008). That could explain why adenovirus would evolve to modulate its function in some way. It has also been suggested to be involved in growth and differentiation and to possess both nuclear and cytoplasmic functions (Contino *et al.*, 2004). It is clear that UBE4A is a multifunctional protein.

Given the links between this protein family and proteasomal degradation, it is probably the strongest contender for being involved in the adenoviral-induced reduction in TIF1 γ level out of all the proteins pulled down with E4orf3. Unfortunately, time considerations prevented further work in that area being undertaken as part of this investigation.

Given sufficient time, it would have been useful to confirm the interaction by performing reciprocal IPs. If the interaction was confirmed, then it would be useful to investigate the role of the U-box in TIF1 γ regulation. A suggestion for how this could be done would be:

- 1) Generate a siRNA resistant UBE4A gene, insert it into a plasmid and transfect that, or a non-expressing control plasmid, into a given cell line.
- 2) Engineer an siRNA against the endogenous mRNA. Treat the cells with this to check for viability.

- 3) If cells tolerate that, then generate a series of U-box mutant genes and transfect those, or non-expressing control plasmids, into the same cell line and again knock down endogenous expression.

That should tell if the U-box is important in mediating the reduction in TIF1 γ levels. It is important to test a variety of mutants as E4 proteins are known to have a variety of functions and loss of the U-box, or specific residues from it, could theoretically affect other non-U-box related functions. Finally, if the U-box is deemed to be important, the following experiments could be carried out:

- 1) Carry out a ubiquitylation assay on TIF1 γ to ascertain if UBE4A can ubiquitylate it and on which lysine residues this can occur.
- 2) Generate a siRNA resistant TIF1 γ that, say, has target lysines exchanged for arginines. Then express this and knock down endogenous expression as before.

From those experiments the following should be ascertained:

- a) If UBE4A interacts with E4orf3
- b) If the UBE4A U-box is involved in reducing TIF1 γ levels
- c) If UBE4A can ubiquitylate TIF1 γ
- d) If such ubiquitylation is involved in TIF1 γ degradation

4.6.2.ii: Conserved Oligomeric Golgi Complex

This is involved in Golgi apparatus stabilisation, tethering vesicles to the Golgi, protein glycosylation within the Golgi and inter-Golgi transport (Smith and Lupashin, 2008). Whilst an interaction between this complex and E4orf3 could be involved in the post-translational modification of both viral and host proteins and is worth pursuing in that context, it is unlikely to be involved in the regulation of TIF1 γ in infection.

4.6.2.iii: Eukaryotic translation initiation factor 3 (eIF3)

eIF3 is involved in the initiation of translation (Pestova *et al.*, 2001). In such, sequestering it away from sites of translation could potentially result in the reduction in TIF1 γ observed during adenoviral infection. This is unlikely, however, as any effects would be likely to be global and not all cellular protein levels show the same reduction. It could potentially aid in the late stage host cell shutdown process, assuming that a mechanism existed to allow for

continued translation of late viral proteins and is possibly worth further investigation in that context.

4.6.2.iv: Exportin 7

Exportin 7 is involved in the Ran-GTPase dependent shuttling of certain proteins out of the nucleus through nuclear pore complexes. Importantly, these include 14-3-3 proteins (Mingot *et al.*, 2004). 14-3-3 proteins are involved in regulating a plethora of cellular events from growth to apoptosis, and are known to be involved in several signalling pathways related to cancer (Morrison, 2009). There is no record in the literature of Exportin 7 acting as a cargo receptor for TIF1 γ . Nevertheless, it is possible that E4orf3 can mediate the export of TIF1 γ out of the nucleus in conjunction with Exportin 7. This would enable adenovirus to reduce the ability of TIF1 γ to act as a transcriptional repressor and concentrate it in cytoplasmic structures for efficient ubiquitylation by the adenoviral E3 ligase. This possibility is worth investigating further.

4.6.2.v: Tyrosine-protein phosphatase non-receptor type 13 (FAP-1)

Tyrosine-protein phosphatase non-receptor type 13, also known as Fas-associated phosphatase 1 (FAP-1) and a variety of other names (Abaan and Toretsky, 2008), has been shown to reduce the expression of the apoptosis-inducing Fas receptor on the cell membrane (Ivanov *et al.*, 2003). It has also been implicated in the development of cancer (Abaan and Toretsky, 2008). As adenoviral proteins often target tumour suppressor and apoptotic pathways, these findings make FAP-1 a likely target for adenovirus – especially when the large Mascot scores (Table 3.1A and B) are considered. No evidence currently exists proving a role for FAP-1 in the modulation of TIF1 γ levels during adenoviral infection, however, and more work would be required before such a role could be considered.

4.6.2.vi: Kinase D-interacting substrate of 220 kDa (Kidins220)

Kidins220 is an integral transmembrane protein expressed in certain neural cells that is phosphorylated by protein kinase D (Inglesias *et al.*, 2000). It is responsible for regulating dendritic spine branching (Wu *et al.*, 2009). Given its selective expression in neural cells, adenoviruses that habitually infect epithelial cells are unlikely to have evolved to target this protein in nature and it seems unlikely to be involved in regulating TIF1 γ levels.

4.6.2.vii: Prolow-density lipoprotein receptor-related protein 1 (LRP1)

This protein, also known as CD91 or low density lipoprotein receptor-related protein 1 has a wide variety of functions. These include cell signalling (Lutz *et al.*, 2002), endocytosis

(Willnow *et al.*, 1999), reducing matrix metalloproteinase activity (Hahn-Dantona *et al.*, 2001), transport across the blood-brain barrier (Pflanzner *et al.*, in press) and mediating the internalisation of viral or tumour antigens by immune cells that subsequently co-present them with MHC Class I antigens (Stebbing *et al.*, 2004). Overexpression has been noted as a negative prognostic factor linked to increased proliferation and invasiveness in at least one form of cancer (Catasus *et al.*, in press).

In that it can potentially mediate the instigation of an anti-viral immune response, it is a likely target for adenovirus. It could also benefit adenovirus to manipulate LRP1 into altering output through various signalling pathways. It is questionable as to whether any gain or loss of function of LRP1 could directly affect TIF1 γ levels, however.

4.6.2.viii: LETM1 and EF-hand domain-containing protein 1 (LETM1)

The genome-encoded LETM1 and EF-hand domain-containing protein 1 (LETM1) protein is located exclusively in the inner mitochondrial membrane (IMM) and functions as an electrogenic Ca²⁺/H⁺ antiporter that can possibly work in either direction depending on the electrochemical gradients across the IMM (Jiang *et al.*, 2009). It is only one of several calcium transporters in the IMM (Santo-Domingo and Demarex, 2010). In terms of maintaining cytoplasmic calcium homeostasis, there are also several points at which this can occur (Carafoli, 1987; Várnai *et al.*, 2009). On the other hand, there is much evidence that calcium signalling depends on localised pools (Parekh, 2008), so it is not inconceivable that modulation of LETM1 levels and localisation by adenovirus could have major effects on the cell. Indeed, deletion of one copy of the gene is associated with Wolf-Hirschhorn syndrome, a disease characterised by, among other things, microcephaly and mental retardation (Akhtar, 2008). Its location in the mitochondrion raises the possibility that it could be involved in apoptosis by mediating the electrochemical gradient across the IMM and that affecting the likelihood of MOMP occurring. What effect, if any, a possible interaction between E4orf3 and LETM1 could have on TIF1 γ levels is unknown and further study is needed initially to verify the interaction, prior to further exploration of its function.

4.6.3: Conclusions from mass spectrometry data

Due to their very high Mascot scores, it would seem likely that FAP-1 and LETM1 and EF-hand domain-containing protein 1 are genuine E4orf3 interacting proteins. Whilst they were unlikely to be relevant to this investigation, they may ultimately prove to be useful lines of investigation in terms of elucidating more about the adenoviral life cycle and its effects on

cellular tumour suppressor pathways. The relatively low scores for Exportin-7, coupled with the low number of unique peptides found for it, would make that finding more dubious.

It must be reiterated that verification by molecular biology techniques, such as reciprocal immunoprecipitations, would be required before any of these putative interactions could be categorically accepted.

4.7: Overall conclusions and suggestions for further work

It is clear from this work that cellular TIF1 γ levels fall following infection with Ad5 and Ad12 in a number of cultured cell lines. It is also clear that E4orf3 has a necessary role in this process in Ad5 infected cells. The precise mechanism by which E4orf3 mediates the loss of TIF1 γ remains enigmatic. It is not clear whether it functions alone, in concert with the E4orf6-containing E3 ubiquitin ligase or with some other, as yet unknown, proteins. Transcriptional repression of p53-dependent expression is not necessary for TIF1 γ levels to fall during Ad5 infection. As Ad5 E1B-55kDa is known to independently repress p53 transcriptional activity, the possibility arises that it could function together with E4orf3 in transcriptional modulation. This possibility, and any likely impact on TIF1 γ expression levels, is worth investigation. As TIF1 γ possesses chromatin interacting domains and was shown to closely co-localise with E4orf3 in nuclear tracks, it is even possible that they functionally interact modulate transcription in the early stages of infection. It is likely that any TIF1 γ transcriptional activity is deleterious to adenovirus, however, given that E4orf3 mediates a reduction in its cellular concentration during infection and E1B-55kDa sequesters it outside the nucleus in adenovirus-transformed cells. It is of pressing concern to confirm or exclude a role for the adenoviral E3 ubiquitin ligase in that process. Confirmation would all but resolve the issue. Exclusion could be much more exciting; however, as it would imply that there is a novel and potentially important new E4orf3 function that has not yet been discovered. The possibility of E4orf3 interacting with and manipulating U-box containing E3/E4 proteins is intriguing. There could represent an entirely new mechanism by which adenovirus targets proteins for degradation. To put that in context, there could be a whole array of undiscovered tumour suppressor proteins that adenovirus inactivates in a similar way to TIF1 γ , just waiting to be discovered by anyone pursuing this line of investigation. Even if the reality is more mundane and E4orf3 simply targets TIF1 γ to the adenoviral E3 ubiquitin ligase, this investigation may still have contributed a little new knowledge to the field. The putative interactions suggested in the mass spectrometry data require validation by conventional protein biochemical and cell biological studies prior to further work exploring possible mechanisms of action. For example, if the probable interactions between E4orf3 and LETM1/FAP-1 are investigated and confirmed in the future, then initial findings from this investigation may still come to shed

some new light on novel cellular targets for adenovirus that may function as tumour suppressors.

References

- Abaan, O. D., & Toretsky, J. A. (2008). PTPL1: A large phosphatase with a split personality. *Cancer Metastasis Reviews*, 27(2), 205-214.
- Ablack, J. N. G., Pelka, P., Yousef, A. F., Turnell, A. S., Grand, R. J. A., & Mymryk, J. S. (2010). Comparison of E1A CR3-dependent transcriptional activation across six different human adenovirus subgroups. *The Journal of Virology*, 84(24), 12771-12781.
- Akhtar, N. (2008). Wolf-hirschhorn syndrome. *Journal of the College of Physicians and Surgeons--Pakistan : JCPSP*, 18(4), 254-256.
- Aucagne, R., Droin, N., Paggetti, J., Lagrange, B., Largeot, A., Hammann, A., et al. (2011). Transcription intermediary factor 1gamma is a tumor suppressor in mouse and human chronic myelomonocytic leukemia. *The Journal of Clinical Investigation*, 121(6), 2361-2370.
- Babiss, L. E., & Ginsberg, H. S. (1984). Adenovirus type 5 early region 1b gene product is required for efficient shutoff of host protein synthesis. *The Journal of Virology*, 50(1), 202-212.
- Banerjee, A. C., Recupero, A. J., Mal, A., Piotrkowski, A. M., Wang, D. M., & Harter, M. L. (1994). The adenovirus E1A 289R and 243R proteins inhibit the phosphorylation of p300. *Oncogene*, 9(6), 1733-1737.
- Bennett, E. M., Bennink, J. R., Yewdell, J. W., & Brodsky, F. M. (1999). Cutting edge: Adenovirus E19 has two mechanisms for affecting class I MHC expression. *Journal of Immunology (Baltimore, Md.: 1950)*, 162(9), 5049-5052.
- Bernards, R., Schrier, P. I., Houweling, A., Bos, J. L., van der Eb, A. J., Zijlstra, M., et al. (1983). Tumorigenicity of cells transformed by adenovirus type 12 by evasion of T-cell immunity. *Nature*, 305(5937), 776-779.
- Blackford, A. N., Patel, R. N., Forrester, N. A., Theil, K., Groitl, P., Stewart, G. S., et al. (2010). Adenovirus 12 E4orf6 inhibits ATR activation by promoting TOPBP1 degradation. *Proceedings of the National Academy of Sciences of the United States of America*, 107(27), 12251-12256.

- Blanchette, P., Cheng, C. Y., Yan, Q., Ketner, G., Ornelles, D. A., Dobner, T., et al. (2004). Both BC-box motifs of adenovirus protein E4orf6 are required to efficiently assemble an E3 ligase complex that degrades p53. *Molecular and Cellular Biology*, 24(21), 9619-9629.
- Boulanger, P. A., & Blair, G. E. (1991). Expression and interactions of human adenovirus oncoproteins. *The Biochemical Journal*, 275 (Pt 2), 281-299.
- Boyd, J. M., Subramanian, T., Schaeper, U., La Regina, M., Bayley, S., & Chinnadurai, G. (1993). A region in the C-terminus of adenovirus 2/5 E1a protein is required for association with a cellular phosphoprotein and important for the negative modulation of T24-ras mediated transformation, tumorigenesis and metastasis. *The EMBO Journal*, 12(2), 469-478.
- Byrd, P. J., Chia, W., Rigby, P. W. J., & Gallimore, P. H. (1982). Cloning of DNA fragments from the left end of the adenovirus type 12 genome: Transformation by cloned early region 1. *Journal of General Virology*, 60(2), 279-293.
- Carafoli, E. (1987). Intracellular calcium homeostasis. *Annual Review of Biochemistry*, 56, 395-433.
- Catusus, L., Gallardo, A., Llorente-Cortes, V., Escuin, D., Muñoz, J., Tibau, A., et al. Low-density lipoprotein receptor-related protein 1 is associated with proliferation and invasiveness in her-2/neu and triple-negative breast carcinomas. *Human Pathology, In Press, Corrected Proof*
- Chatterjee, A., Upadhyay, S., Chang, X., Nagpal, J. K., Trink, B., & Sidransky, D. (2008). U-box-type ubiquitin E4 ligase, UFD2a attenuates cisplatin mediated degradation of DeltaNp63alpha. *Cell Cycle (Georgetown, Tex.)*, 7(9), 1231-1237.
- Chen, Z. J., & Sun, L. J. (2009). Nonproteolytic functions of ubiquitin in cell signaling. *Molecular Cell*, 33(3), 275-286.
- Cheng, C. Y., Gilson, T., Dallaire, F., Ketner, G., Branton, P. E., & Blanchette, P. (2011). The E4orf6/E1B55K E3 ubiquitin ligase complexes of human adenoviruses exhibit heterogeneity in composition and substrate specificity. *The Journal of Virology*, 85(2), 765-775.

- Chipuk, J. E., Moldoveanu, T., Llambi, F., Parsons, M. J., & Green, D. R. (2010). The BCL-2 family reunion. *Molecular Cell*, *37*(3), 299-310.
- Contino, G., Amati, F., Pucci, S., Pontieri, E., Pichiorri, F., Novelli, A., et al. (2004). Expression analysis of the gene encoding for the U-box-type ubiquitin ligase UBE4A in human tissues. *Gene*, *328*, 69-74.
- Davison, A. J., Benko, M., & Harrach, B. (2003). Genetic content and evolution of adenoviruses. *Journal of General Virology*, *84*(11), 2895-2908.
- de Jong, R. N., van der Vliet, P. C., & Brenkman, A. B. (2003). Adenovirus DNA replication: Protein priming, jumping back and the role of the DNA binding protein DBP. *Current Topics in Microbiology and Immunology*, *272*, 187-211.
- de Stanchina, E., McCurrach, M. E., Zindy, F., Shieh, S. Y., Ferbeyre, G., Samuelson, A. V., et al. (1998). E1A signaling to p53 involves the p19(ARF) tumor suppressor. *Genes & Development*, *12*(15), 2434-2442.
- Doerfler, W. (2007). Human adenovirus type 12: Crossing species barriers to immortalize the viral genome. *Methods in Molecular Medicine*, *131*, 197-211.
- Dupont, S., Zacchigna, L., Cordenonsi, M., Soligo, S., Adorno, M., Rugge, M., et al. (2005). Germ-layer specification and control of cell growth by ectodermin, a Smad4 ubiquitin ligase. *Cell*, *121*(1), 87-99.
- Dupont, S., Mamidi, A., Cordenonsi, M., Montagner, M., Zacchigna, L., Adorno, M., et al. (2009). FAM/USP9x, a deubiquitinating enzyme essential for TGFbeta signaling, controls Smad4 monoubiquitination. *Cell*, *136*(1), 123-135.
- Ferreira, L., Giordano, M., Martinez, L., Isa, M. B., Barril, P., Masachessi, G., et al. (2010). A novel human adenovirus hexon protein of species D found in an AIDS patient. *Archives of Virology*, *155*(1), 27-35.
- Forrester, N. A., Sedgwick, G. G., Thomas, A., Blackford, A. N., Speiseder, T., Dobner, T., et al. (2011). Serotype-specific inactivation of the cellular DNA damage response during adenovirus infection. *The Journal of Virology*, *85*(5), 2201-2211.

- Freeman, A. E., Black, P. H., Vanderpool, E. A., Henry, P. H., Austin, J. B., & Huebner, R. J. (1967). Transformation of primary rat embryo cells by adenovirus type 2. *Proceedings of the National Academy of Sciences of the United States of America*, 58(3), 1205-1212.
- Gallimore, P. H., & Turnell, A. S. (2001). Adenovirus E1A: Remodelling the host cell, a life or death experience. *Oncogene*, 20(54), 7824-7835.
- Gallimore, P., Lecane, P., Roberts, S., Rookes, S., Grand, R., & Parkhill, J. (1997). Adenovirus type 12 early region 1B 54K protein significantly extends the life span of normal mammalian cells in culture. *The Journal of Virology*, 71(9), 6629-6640.
- Ge, R., Kralli, A., Weinmann, R., & Ricciardi, R. P. (1992). Down-regulation of the major histocompatibility complex class I enhancer in adenovirus type 12-transformed cells is accompanied by an increase in factor binding. *The Journal of Virology*, 66(12), 6969-6978.
- Grabham, P. W., Grand, R. J. A., & Gallimore, P. H. (1989). Purification of a serum factor which reverses dibutyl cAMP induced differentiation. *Cellular Signalling*, 1(3), 269-281.
- Graham, F. L., Smiley, J., Russell, W. C., & Nairn, R. (1977). Characteristics of a human cell line transformed by DNA from human adenovirus type 5. *Journal of General Virology*, 36(1), 59-72.
- Grand, R. J., & Gallimore, P. H. (1986). Modulation of the level of expression of cellular genes in adenovirus 12-infected and transformed human cells. *The EMBO Journal*, 5(6), 1253-1260.
- Greer, A. E., Hearing, P., & Ketner, G. The adenovirus E4 11 k protein binds and relocalizes the cytoplasmic P-body component Ddx6 to aggresomes. *Virology*, *In Press, Corrected Proof*
- Hahn-Dantona, E., Ruiz, J. F., Bornstein, P., & Strickland, D. K. (2001). The low density lipoprotein receptor-related protein modulates levels of matrix metalloproteinase 9 (MMP-9) by mediating its cellular catabolism. *Journal of Biological Chemistry*, 276(18), 15498-15503.
- Hanahan, D., & Weinberg, R. A. (2000). The hallmarks of cancer. *Cell*, 100(1), 57-70.

- Hanahan, D., & Weinberg, R. A. (2011). Hallmarks of cancer: The next generation. *Cell*, *144*(5), 646-674.
- Hatakeyama, S., Yada, M., Matsumoto, M., Ishida, N., & Nakayama, K. (2001). U box proteins as a new family of ubiquitin-protein ligases. *Journal of Biological Chemistry*, *276*(35), 33111-33120.
- He, W., Dorn, D. C., Erdjument-Bromage, H., Tempst, P., Moore, M. A., & Massague, J. (2006). Hematopoiesis controlled by distinct TIF1gamma and Smad4 branches of the TGFbeta pathway. *Cell*, *125*(5), 929-941.
- Herquel, B., Ouararhni, K., Khetchoumian, K., Ignat, M., Teletin, M., Mark, M., et al. (2011). Transcription cofactors TRIM24, TRIM28, and TRIM33 associate to form regulatory complexes that suppress murine hepatocellular carcinoma. *Proceedings of the National Academy of Sciences of the United States of America*, *108*(20), 8212-8217.
- Hilger-Eversheim, K., & Doerfler, W. (1997). Clonal origin of adenovirus type 12-induced hamster tumors: Nonspecific chromosomal integration sites of viral DNA. *Cancer Research*, *57*(14), 3001-3009.
- Hoppe, A., Beech, S. J., Dimmock, J., & Leppard, K. N. (2006). Interaction of the adenovirus type 5 E4 Orf3 protein with promyelocytic leukemia protein isoform II is required for ND10 disruption. *The Journal of Virology*, *80*(6), 3042-3049.
- Hosoda, M., Ozaki, T., Miyazaki, K., Hayashi, S., Furuya, K., Watanabe, K., et al. (2005). UFD2a mediates the proteasomal turnover of p73 without promoting p73 ubiquitination. *Oncogene*, *24*(48), 7156-7169.
- Hough, R., Pratt, G., & Rechsteiner, M. (1986). Ubiquitin-lysosome conjugates. identification and characterization of an ATP-dependent protease from rabbit reticulocyte lysates. *Journal of Biological Chemistry*, *261*(5), 2400-2408.
- Iglesias, T., Cabrera-Poch, N., Mitchell, M. P., Naven, T. J., Rozengurt, E., & Schiavo, G. (2000). Identification and cloning of Kidins220, a novel neuronal substrate of protein kinase D. *The Journal of Biological Chemistry*, *275*(51), 40048-40056.
- Ivanov, V. N., Bergami, P. L., Maulit, G., Sato, T., Sassoon, D., & Ronai, Z. (2003). FAP-1 association with fas (apo-1) inhibits fas expression on the cell surface. *Molecular and Cellular Biology*, *23*(10), 3623-3635.

- Javier, R. T. (1994). Adenovirus type 9 E4 open reading frame 1 encodes a transforming protein required for the production of mammary tumors in rats. *The Journal of Virology*, 68(6), 3917-3924.
- Jiang, D., Zhao, L., & Clapham, D. E. (2009). Genome-wide RNAi screen identifies Letm1 as a mitochondrial Ca²⁺/H⁺ antiporter. *Science (New York, N.Y.)*, 326(5949), 144-147.
- Johnston, J. A., Ward, C. L., & Kopito, R. R. (1998). Aggresomes: A cellular response to misfolded proteins. *The Journal of Cell Biology*, 143(7), 1883-1898.
- Khetchoumian, K., Teletin, M., Mark, M., Lerouge, T., Cerviño, M., Oulad-Abdelghani, M., et al. (2004). TIF1δ, a novel HP1-interacting member of the transcriptional intermediary factor 1 (TIF1) family expressed by elongating spermatids. *Journal of Biological Chemistry*, 279(46), 48329-48341.
- Klugbauer, S., & Rabes, H. M. (1999). The transcription coactivator HTIF1 and a related protein are fused to the RET receptor tyrosine kinase in childhood papillary thyroid carcinomas. *Oncogene*, 18(30), 4388-4393.
- Koegl, M., Hoppe, T., Schlenker, S., Ulrich, H. D., Mayer, T. U., & Jentsch, S. (1999). A novel ubiquitination factor, E4, is involved in multiubiquitin chain assembly. *Cell*, 96(5), 635-644.
- Lallemand-Breitenbach, V., & de Thé, H. (2010). PML nuclear bodies. *Cold Spring Harbor Perspectives in Biology*, 2(5)
- Lenaerts, L., De Clercq, E., & Naesens, L. (2008). Clinical features and treatment of adenovirus infections. *Reviews in Medical Virology*, 18(6), 357-374.
- Leppard, K. N., & Everett, R. D. (1999). The adenovirus type 5 E1b 55K and E4 Orf3 proteins associate in infected cells and affect ND10 components. *Journal of General Virology*, 80(4), 997-1008.
- Lewis, A. M., & Cook, J. L. (1982). Spectrum of tumorigenic phenotypes among adenovirus 2-, adenovirus 12-, and simian virus 40-transformed syrian hamster cells defined by host cellular immune-tumor cell interactions. *Cancer Research*, 42(3), 939-944.
- Li, W., & Ye, Y. (2008). Polyubiquitin chains: Functions, structures, and mechanisms. *Cellular and Molecular Life Sciences : CMLS*, 65(15), 2397-2406.

- Lin, H., Eviner, V., Prendergast, G., & White, E. (1995). Activated H-ras rescues E1A-induced apoptosis and cooperates with E1A to overcome p53-dependent growth arrest. *Molecular and Cellular Biology*, *15*(8), 4536-4544.
- Liu, Y., Shevchenko, A., Shevchenko, A., & Berk, A. J. (2005). Adenovirus exploits the cellular aggresome response to accelerate inactivation of the MRN complex. *The Journal of Virology*, *79*(22), 14004-14016.
- Logan, J. S., & Shenk, T. (1982). Transcriptional and translational control of adenovirus gene expression. *Microbiological Reviews*, *46*(4), 377-383.
- Lombard, D. B., & Guarente, L. (2000). Nijmegen breakage syndrome disease protein and MRE11 at PML nuclear bodies and meiotic telomeres. *Cancer Research*, *60*(9), 2331-2334.
- Lowe, S. W., & Ruley, H. E. (1993). Stabilization of the p53 tumor suppressor is induced by adenovirus 5 E1A and accompanies apoptosis. *Genes & Development*, *7*(4), 535-545.
- Lutz, C., Nimpf, J., Jenny, M., Boecklinger, K., Enzinger, C., Utermann, G., et al. (2002). Evidence of functional modulation of the MEKK/JNK/cJun signaling cascade by the low density lipoprotein receptor-related protein (LRP). *Journal of Biological Chemistry*, *277*(45), 43143-43151.
- Lutz, P., Rosa-Calatrava, M., & Kedinger, C. (1997). The product of the adenovirus intermediate gene IX is a transcriptional activator. *The Journal of Virology*, *71*(7), 5102-5109.
- Mahoney, J. A., Odin, J. A., White, S. M., Shaffer, D., Koff, A., Casciola-Rosen, L., et al. (2002). The human homologue of the yeast polyubiquitination factor Ufd2p is cleaved by caspase 6 and granzyme B during apoptosis. *The Biochemical Journal*, *361*(Pt 3), 587-595.
- Marin, I. (2010). Ancient origin of animal U-box ubiquitin ligases. *BMC Evolutionary Biology*, *10*(1), 331.
- Matsumoto, M. L., Wickliffe, K. E., Dong, K. C., Yu, C., Bosanac, I., Bustos, D., et al. (2010). K11-linked polyubiquitination in cell cycle control revealed by a K11 linkage-specific antibody. *Molecular Cell*, *39*(3), 477-484.

- McBride, W. D., & Wiener, A. (1964). In vitro transformation of hamster kidney cells by human adenovirus type 12. *Proceedings of the Society for Experimental Biology and Medicine*. Society for Experimental Biology and Medicine (New York, N.Y.), 115, 870-874.
- Melchior, F. (2000). SUMO--nonclassical ubiquitin. *Annual Review of Cell and Developmental Biology*, 16, 591-626.
- Mellor, J. (2006). It takes a PHD to read the histone code. *Cell*, 126(1), 22-24.
- Meroni, G., & Diez-Roux, G. (2005). TRIM/RBCC, a novel class of ?single protein RING finger? E3 ubiquitin ligases. *BioEssays*, 27(11), 1147-1157.
- Mingot, J. M., Bohnsack, M. T., Jakle, U., & Gorlich, D. (2004). Exportin 7 defines a novel general nuclear export pathway. *The EMBO Journal*, 23(16), 3227-3236.
- Moore, M., Horikoshi, N., & Shenk, T. (1996). Oncogenic potential of the adenovirus E4orf6 protein. *Proceedings of the National Academy of Sciences*, 93(21), 11295-11301.
- Morrison, D. K. (2009). The 14-3-3 proteins: Integrators of diverse signaling cues that impact cell fate and cancer development. *Trends in Cell Biology*, 19(1), 16-23.
- Morsut, L., Yan, K., Enzo, E., Aragona, M., Soligo, S. M., Wendling, O., et al. (2010). Negative control of smad activity by ectodermin/Tif1 γ patterns the mammalian embryo. *Development*,
- Muller, S., Matunis, M. J., & Dejean, A. (1998). Conjugation with the ubiquitin-related modifier SUMO-1 regulates the partitioning of PML within the nucleus. *The EMBO Journal*, 17(1), 61-70.
- Nevels, M., Tauber, B., Kremmer, E., Spruss, T., Wolf, H., & Dobner, T. (1999). Transforming potential of the adenovirus type 5 E4orf3 protein. *The Journal of Virology*, 73(2), 1591-1600.
- Nevels, M., Tauber, B., Spruss, T., Wolf, H., & Dobner, T. (2001). "Hit-and-run" transformation by adenovirus oncogenes. *The Journal of Virology*, 75(7), 3089-3094.
- Nevins, J. R. (1987). Regulation of early adenovirus gene expression. *Microbiological Reviews*, 51(4), 419-430.

- Nevins, J. R. (1982). Induction of the synthesis of a 70,000 dalton mammalian heat shock protein by the adenovirus E1A gene product. *Cell*, 29(3), 913-919.
- Ohh, M., Kim, W. Y., Moslehi, J. J., Chen, Y., Chau, V., Read, M. A., et al. (2002). An intact NEDD8 pathway is required for cullin-dependent ubiquitylation in mammalian cells. *EMBO Reports*, 3(2), 177-182.
- Parekh, A. B. (2008). Ca²⁺ microdomains near plasma membrane Ca²⁺ channels: Impact on cell function. *The Journal of Physiology*, 586(13), 3043-3054.
- Pennella, M. A., Liu, Y., Woo, J. L., Kim, C. A., & Berk, A. J. (2010). Adenovirus E1B-55K is a p53-SUMO1 E3 ligase that represses p53 and stimulates its nuclear export through interactions in PML-nuclear bodies. *The Journal of Virology*,
- Pestova, T. V., Kolupaeva, V. G., Lomakin, I. B., Pilipenko, E. V., Shatsky, I. N., Agol, V. I., et al. (2001). Molecular mechanisms of translation initiation in eukaryotes. *Proceedings of the National Academy of Sciences of the United States of America*, 98(13), 7029-7036.
- Pflanzner, T., Janko, M. C., André-Dohmen, B., Reuss, S., Weggen, S., Roebroek, A. J. M., et al. LRP1 mediates bidirectional transcytosis of amyloid- β across the blood-brain barrier. *Neurobiology of Aging*, *In Press, Corrected Proof*
- Querido, E., Blanchette, P., Yan, Q., Kamura, T., Morrison, M., Boivin, D., et al. (2001). Degradation of p53 by adenovirus E4orf6 and E1B55K proteins occurs via a novel mechanism involving a cullin-containing complex. *Genes & Development*, 15(23), 3104-3117.
- Ransom, D. G., Bahary, N., Niss, K., Traver, D., Burns, C., Trede, N. S., et al. (2004). The zebrafish moonshine gene encodes transcriptional intermediary factor 1gamma, an essential regulator of hematopoiesis. *PLoS Biology*, 2(8), E237.
- Rao, L., Debbas, M., Sabbatini, P., Hockenbery, D., Korsmeyer, S., & White, E. (1992). The adenovirus E1A proteins induce apoptosis, which is inhibited by the E1B 19-kDa and bcl-2 proteins. *Proceedings of the National Academy of Sciences*, 89(16), 7742-7746.
- Riedl, S. J., & Salvesen, G. S. (2007). The apoptosome: Signalling platform of cell death. *Nature Reviews.Molecular Cell Biology*, 8(5), 405-413.

- Rowe, W. P., Huebner, R. J., Gilmore, L. K., Parrott, R. H., & Ward, T. G. (1953). Isolation of a cytopathogenic agent from human adenoids undergoing spontaneous degeneration in tissue culture. *Proceedings of the Society for Experimental Biology and Medicine. Society for Experimental Biology and Medicine (New York, N.Y.)*, 84(3), 570-573.
- Santo-Domingo, J., & Demarex, N. (2010). Calcium uptake mechanisms of mitochondria. *Biochimica Et Biophysica Acta (BBA) - Bioenergetics*, 1797(6-7), 907-912.
- Schreiner, S., Wimmer, P., Sirma, H., Everett, R. D., Blanchette, P., Groitl, P., et al. (2010). Proteasome-dependent degradation of daxx by the viral E1B-55K protein in human adenovirus-infected cells. *The Journal of Virology*, 84(14), 7029-7038.
- Schwickart, M., Huang, X., Lill, J. R., Liu, J., Ferrando, R., French, D. M., et al. (2010). Deubiquitinase USP9X stabilizes MCL1 and promotes tumour cell survival. *Nature*, 463(7277), 103-107.
- Shaw, G., Morse, S., Ararat, M., & Graham, F. L. (2002). Preferential transformation of human neuronal cells by human adenoviruses and the origin of HEK 293 cells. *The FASEB Journal : Official Publication of the Federation of American Societies for Experimental Biology*, 16(8), 869-871.
- Sherr, C. J. (2001). The INK4a/ARF network in tumour suppression. *Nature Reviews. Molecular Cell Biology*, 2(10), 731-737.
- Shi, D., Pop, M. S., Kulikov, R., Love, I. M., Kung, A. L., & Grossman, S. R. (2009). CBP and p300 are cytoplasmic E4 polyubiquitin ligases for p53. *Proceedings of the National Academy of Sciences*, 106(38), 16275-16280.
- Sieber, T., & Dobner, T. (2007). Adenovirus type 5 early region 1B 156R protein promotes cell transformation independently of repression of p53-stimulated transcription. *The Journal of Virology*, 81(1), 95-105.
- Smith, R. D., & Lupashin, V. V. (2008). Role of the conserved oligomeric golgi (COG) complex in protein glycosylation. *Carbohydrate Research*, 343(12), 2024-2031.
- Soria, C., Estermann, F. E., Espantman, K. C., & O'Shea, C. C. (2010). Heterochromatin silencing of p53 target genes by a small viral protein. *Nature*, 466(7310), 1076-1081.

- Stebbing, J., Savage, P., Patterson, S., & Gazzard, B. (2004). All for CD91 and CD91 for all. *The Journal of Antimicrobial Chemotherapy*, 53(1), 1-3.
- Stracker, T. H., Carson, C. T., & Weitzman, M. D. (2002). Adenovirus oncoproteins inactivate the Mre11-Rad50-NBS1 DNA repair complex. *Nature*, 418(6895), 348-352.
- Stracker, T. H., Lee, D. V., Carson, C. T., Araujo, F. D., Ornelles, D. A., & Weitzman, M. D. (2005). Serotype-specific reorganization of the Mre11 complex by adenoviral E4orf3 proteins. *The Journal of Virology*, 79(11), 6664-6673.
- Teodoro, J. G., Shore, G. C., & Branton, P. E. (1995). Adenovirus E1A proteins induce apoptosis by both p53-dependent and p53-independent mechanisms. *Oncogene*, 11(3), 467-474.
- Thrower, J. S., Hoffman, L., Rechsteiner, M., & Pickart, C. M. (2000). Recognition of the polyubiquitin proteolytic signal. *The EMBO Journal*, 19(1), 94-102.
- Torii, S., Egan, D. A., Evans, R. A., & Reed, J. C. (1999). Human daxx regulates fas-induced apoptosis from nuclear PML oncogenic domains (PODs). *The EMBO Journal*, 18(21), 6037-6049.
- Trentin, J. J., Yabe, Y., & Taylor, G. (1962). The quest for human cancer viruses. *Science*, 137(3533), 835-841.
- Turnell, A. S. (2008). Adenoviruses: Malignant transformation and oncology. In B.W.J. Mahy, & M.H.V. van Regenmortel (Eds.), *Encyclopedia of virology* (pp. 9-16). Oxford: Academic Press.
- Várnai, P., Hunyady, L., & Balla, T. (2009). STIM and orai: The long-awaited constituents of store-operated calcium entry. *Trends in Pharmacological Sciences*, 30(3), 118-128.
- Venturini, L., You, J., Stadler, M., Galien, R., Lallemand, V., Koken, M. H., et al. (1999). TIF1gamma, a novel member of the transcriptional intermediary factor 1 family. *Oncogene*, 18(5), 1209-1217.
- Vetter, I., & Lewis, R. J. (2010). Characterization of endogenous calcium responses in neuronal cell lines. *Biochemical Pharmacology*, 79(6), 908-920.

- Vincent, D. F., Yan, K. P., Treilleux, I., Gay, F., Arfi, V., Kaniewski, B., et al. (2009). Inactivation of TIF1gamma cooperates with kras to induce cystic tumors of the pancreas. *PLoS Genetics*, 5(7), e1000575.
- Walz, J., Erdmann, A., Kania, M., Typke, D., Koster, A. J., & Baumeister, W. (1998). 26S proteasome structure revealed by three-dimensional electron microscopy. *Journal of Structural Biology*, 121(1), 19-29.
- Weiden, M. D., & Ginsberg, H. S. (1994). Deletion of the E4 region of the genome produces adenovirus DNA concatemers. *Proceedings of the National Academy of Sciences*, 91(1), 153-157.
- Weinberg, R. A. (2006). *The biology of cancer* Garland Science.
- Weitzman, M. D. (2005). Functions of the adenovirus E4 proteins and their impact on viral vectors. *Frontiers in Bioscience : A Journal and Virtual Library*, 10, 1106-1117.
- White, E., Sabbatini, P., Debbas, M., Wold, W. S., Kusher, D. I., & Gooding, L. R. (1992). The 19-kilodalton adenovirus E1B transforming protein inhibits programmed cell death and prevents cytolysis by tumor necrosis factor alpha. *Molecular and Cellular Biology*, 12(6), 2570-2580.
- Whyte, P., Buchkovich, K. J., Horowitz, J. M., Friend, S. H., Raybuck, M., Weinberg, R. A., et al. (1988). Association between an oncogene and an anti-oncogene: The adenovirus E1A proteins bind to the retinoblastoma gene product. *Nature*, 334(6178), 124-129.
- Wileman, T. (2007). Aggresomes and pericentriolar sites of virus assembly: Cellular defense or viral design? *Annual Review of Microbiology*, 61(1), 149-167.
- Willnow, T. E., Nykjaer, A., & Herz, J. (1999). Lipoprotein receptors: New roles for ancient proteins. *Nature Cell Biology*, 1(6), E157-62.
- Wold, W. S., & Gooding, L. R. (1991). Region E3 of adenovirus: A cassette of genes involved in host immunosurveillance and virus-cell interactions. *Virology*, 184(1), 1-8.
- Woo, J. L., & Berk, A. J. (2007). Adenovirus ubiquitin-protein ligase stimulates viral late mRNA nuclear export. *The Journal of Virology*, 81(2), 575-587.

- Wu, S. H., Arévalo, J. C., Sarti, F., Tessarollo, L., Gan, W., & Chao, M. V. (2009). Ankyrin repeat-rich membrane Spanning/Kidins220 protein regulates dendritic branching and spine stability in vivo. *Developmental Neurobiology*, 69(9), 547-557.
- Yang, X., Khosravi-Far, R., Chang, H. Y., & Baltimore, D. (1997). Daxx, a novel fas-binding protein that activates JNK and apoptosis. *Cell*, 89(7), 1067-1076.
- Yew, P. R., Liu, X., & Berk, A. J. (1994). Adenovirus E1B oncoprotein tethers a transcriptional repression domain to p53. *Genes & Development*, 8(2), 190-202.
- Yondola, M. A., & Hearing, P. (2007). The adenovirus E4 ORF3 protein binds and reorganizes the TRIM family member transcriptional intermediary factor 1 alpha. *The Journal of Virology*, 81(8), 4264-4271.

APPENDICES

Appendix 1

Mass spectrometry protein data and sequence coverage maps (Ad5 E4orf3 pulldown)

**Prolow-density lipoprotein receptor-related protein 1 OS=Homo sapiens GN=LRP1
PE=1 SV=1**

Accession: LRP1_HUMAN

Score: 933.3

Database: SwissProtDecoy(SwissProt_Decoy.fasta)

MW [kDa]: 504.2

Database Date: 2011-03-29

pI: 5.0

Modification(s): Carbamidomethyl, Oxidation

Sequence Coverage [%]: 6.8

No. of unique Peptides: 26

**Tyrosine-protein phosphatase non-receptor type 13 OS=Homo sapiens GN=PTPN13
PE=1 SV=2**

Accession: PTN13_HUMAN

Score: 1266.9

Database: SwissProtDecoy(SwissProt_Decoy.fasta)

MW [kDa]: 276.7

Database Date: 2011-03-29

pI: 6.0

Modification(s): Carbamidomethyl, Oxidation

Sequence Coverage [%]: 18.4

No. of unique Peptides: 35

**Kinase D-interacting substrate of 220 kDa OS=Homo sapiens GN=KIDINS220 PE=1
SV=3**

Accession: KDIS_HUMAN

Score: 255.9

Database: SwissProtDecoy(SwissProt_Decoy.fasta)

MW [kDa]: 196.4

Database Date: 2011-03-29

pI: 6.2

Sequence Coverage [%]: 5.5

No. of unique Peptides: 8

Ubiquitin conjugation factor E4 A OS=Homo sapiens GN=UBE4A PE=1 SV=2
Accession: UBE4A_HUMAN
Score: 392.3
Database: SwissProtDecoy(SwissProt_Decoy.fasta)
MW [kDa]: 122.5
Database Date: 2011-03-29
pI: 5.0
Modification(s): Carbamidomethyl, Oxidation
Sequence Coverage [%]: 11.3
No. of unique Peptides: 11

Exportin-7 OS=Homo sapiens GN=XPO7 PE=1 SV=3
Accession: XPO7_HUMAN
Score: 81.8
Database: SwissProtDecoy(SwissProt_Decoy.fasta)
MW [kDa]: 123.8
Database Date: 2011-03-29
pI: 5.9
Sequence Coverage [%]: 2.9
No. of unique Peptides: 3

Conserved oligomeric Golgi complex subunit 5 OS=Homo sapiens GN=COG5 PE=1 SV=2
Accession: COG5_HUMAN
Score: 317.0
Database: SwissProtDecoy(SwissProt_Decoy.fasta)
MW [kDa]: 92.7
Database Date: 2011-03-29
pI: 6.1
Modification(s): Carbamidomethyl, Oxidation
Sequence Coverage [%]: 12.5
No. of unique Peptides: 9

Conserved oligomeric Golgi complex subunit 7 OS=Homo sapiens GN=COG7 PE=1 SV=1
Accession: COG7_HUMAN
Score: 258.1
Database: SwissProtDecoy(SwissProt_Decoy.fasta)
MW [kDa]: 86.3
Database Date: 2011-03-29
pI: 5.2
Modification(s): Carbamidomethyl
Sequence Coverage [%]: 13.0
No. of unique Peptides: 8

LETM1 and EF-hand domain-containing protein 1, mitochondrial OS=Homo sapiens
GN=LETM1 PE=1 SV=1
Accession: LETM1_HUMAN **Score:** 877.1
Database: SwissProtDecoy(SwissProt_Decoy.fasta)
MW [kDa]: 83.3
Database Date: 2011-03-29
pI: 6.3
Modification(s): Carbamidomethyl, Oxidation
Sequence Coverage [%]: 30.9
No. of unique Peptides: 20

Eukaryotic translation initiation factor 3 subunit J OS=Homo sapiens GN=EIF3J PE=1
SV=2
Accession: EIF3J_HUMAN
Score: 244.5
Database: SwissProtDecoy(SwissProt_Decoy.fasta)
MW [kDa]: 29.0
Database Date: 2011-03-29
pI: 4.6
Modification(s): Carbamidomethyl, Oxidation
Sequence Coverage [%]: 27.9
No. of unique Peptides: 7

Coverage map for Prolow-density lipoprotein receptor-related protein 1

10	20	30	40	50	60	70	80
MLTPPELLLLL	PLLSALVAAA	IDAPKTCSPK	QFACRDQITC	ISKGWRCDGE	RDCPDGSDEA	FEICPQSKAQ	RCQPNEHNCL
90	100	110	120	130	140	150	160
GTELCVPMRS	LCNGVQDCMD	GSDEGPHCRE	LQG NCS RLGC	QHHCVP TL DLG	PTCYC NSS FQ	LQADGKTKCD	FDECSVYGTG
170	180	190	200	210	220	230	240
SQLCTNTDGS	FICGCVEGYL	LQPD NRS SCKA	KNEPVDRPPV	LLIANSQNIL	ATYLSGAQVS	TITPTSTRQT	TAMDFS YANE
250	260	270	280	290	300	310	320
T VCWVHVGD	AAQTQLKCAR	MPGLKGFVDE	HTIN ISL SLH	HVEQMAIDWL	TGNFYFVDDI	DDRIFVCNRN	GDTCVTLLDL
330	340	350	360	370	380	390	400
ELYNPKGIAL	DPAMG VFFT	DY Q QIP KVER	CDMDG QNR TK	LVDSKIVFPH	GITL DL VSRL	VYWADAYLDY	IEVV VD YEGKG
410	420	430	440	450	460	470	480
RQTIIQGLLI	EHLYGLTVFE	NYLYATNSDN	ANAQQKTSVI	RVNR FNS TEY	QVVTRVDKGG	ALHIYQRRQ	PRVRSHACEN
490	500	510	520	530	540	550	560
DQYKPGGCS	DICLLANSHK	ARTCRCSGF	SLGSDGK SK CK	KPEHELFLVY	GKGRPGIIRG	MDMGAKVPEDE	HMPIENLMN
570	580	590	600	610	620	630	640
PRALDFHAET	GFIYFADTTS	YLIGRQKIDG	TERETILKDG	IHNVEGVAVD	WMGDNLYWTD	DGPKK TI SVVA	RLEKAAQTRK
650	660	670	680	690	700	710	720
TLIEGKMTHP	RAIVVDPLNG	WMYWDWEED	PKDSRRGRLE	RAWMDGSHRD	IFVTSKTVLW	PNGLSLDIPA	GRLYWVDAFY
730	740	750	760	770	780	790	800
DRIETILL NG	T DRKIVYEGP	ELNHAFGLCH	HGNYLFWTEY	RSGSVYRLER	G V G G A P P T V T	L L R SERPPIF	E IR M Y D A Q Q Q
810	820	830	840	850	860	870	880
Q V G T N KCRVN	NGGCSLCLLA	TPGSRQCACA	EDQVLADAGV	TCLAN PS YVP	PPQCQ P GEFA	CANSRCIQER	WKCDGNDCL
890	900	910	920	930	940	950	960
DNSDEAPALC	HQHTCPDRF	KCENNRCPIN	RWLCDGDND	GNSEDES NAT	CSARTCPPNQ	FSCASGRICIP	ISWTCDLDD
970	980	990	1000	1010	1020	1030	1040
CGDRSDESAS	CAYPTCFPLT	QFTCNNGRCI	NINWRCDNDN	DCGDN S DEAG	CSHSCSSTQF	KCNSGRCPICE	HWTCDGDND
1050	1060	1070	1080	1090	1100	1110	1120
GDYSDETHAN	C T N QATRPPG	GCHTDEFQCR	LDGLCIPLRW	RCDGD T DCMD	SSDEKSCEGV	THVCDPSVKF	GCKDSARCIS
1130	1140	1150	1160	1170	1180	1190	1200
KAWVCDGND	CEDNSDEENC	ESLACRPPSH	PCAN NTS VCL	PPDKLCDGND	DCGDG S DEGE	LCDQC S LNG	GC S H N C S VAP
1210	1220	1230	1240	1250	1260	1270	1280
GEGIVCSCPL	GME L GP D N H T	CQIQSYCAKH	LKCSQKCDQN	KFSVKCSCYE	GWVLEPDGES	CRSLDPFKPF	IIFSNRHEIR
1290	1300	1310	1320	1330	1340	1350	1360
RIDLHKGDYS	VLVPLRNTI	ALDFHLSQSA	LYWTDVVEDK	IYRGLLDNG	ALTSFEVVIQ	YGLATPEGLA	VDWIAGNIYW
1370	1380	1390	1400	1410	1420	1430	1440
VESNLDQIEV	AKLDGTL RT	L L A G D I E H P R	AIALDPRDGI	LFWTDWDASL	P R I E A A S M S G	A G R T V H R E T	GSGGWPNGLT
1450	1460	1470	1480	1490	1500	1510	1520
VDYLEKRILW	IDARSDAIYS	ARYDGS G HME	VLRGHEFLSH	PFAVTLYGGE	VYWTDWRTNT	LAKANKWTGH	N V T V V Q R T N T
1530	1540	1550	1560	1570	1580	1590	1600
QPFDLQVYHP	SRQPMAPNPC	EANGGQGPCS	HLCLIN N R T	VSCACPHLMK	LHKD N T T CYE	FKKFLLYARQ	MEIRGVDLDA
1610	1620	1630	1640	1650	1660	1670	1680
PYINYIISFT	VPDID N V T VL	DYDAREQRVY	WSDVRTQAIK	RAF I NG T GVE	TVVSADLPNA	HGLAVDWVSR	N L F W T S Y D T N
1690	1700	1710	1720	1730	1740	1750	1760
K K Q INVARLD	GSFK N A V V Q G	L E Q P H G L V V H	P L R G K L Y WTD	GD N I S MANMD	GS N R T LLFSG	Q K G P V G L A I D	F P E S K L Y WIS
1770	1780	1790	1800	1810	1820	1830	1840
SG N H T INRCN	LDGSGLEVID	AMRSQ L GKAT	ALAIMGDKLW	WADQVSEKMG	TCSK A D G S G S	V V L R N S T TLV	M H M K V Y D E S I
1850	1860	1870	1880	1890	1900	1910	1920
Q L D H K GTNPC	SVNNGDCSQL	CLPTSETTRS	CMCTAGYSLR	SGQQACEGVG	SFLLYSVHEG	IRGIPLDPND	KSDALVPVSG
1930	1940	1950	1960	1970	1980	1990	2000
TSLAVGIDFH	A E N D T IYWVD	MGLSTISRAK	RDQ T WREDVV	TNGIGRVEGI	AVDWIAGNIY	WTDQGFVDIE	VARL N G S FRY
2010	2020	2030	2040	2050	2060	2070	2080
V V I S Q GLDKP	RAITVHPEKG	YLFWTEWGQY	PRIERSRLDG	TERVVLV N VS	ISWPNGISVD	YQDGKLYWCD	ARTDKIERID
2090	2100	2110	2120	2130	2140	2150	2160
LETGENREVV	LSSNM D MFS	VSVFEDFIYW	SDR T H A NGSI	KRGSK D NATD	SVPLRTGIGV	QLKDIKVFNR	DRQKGTNVCA
2170	2180	2190	2200	2210	2220	2230	2240

Coverage for Tyrosine-protein phosphatase non-receptor type 13

10	20	30	40	50	60	70	80
MHVSIAEAE	VRGGPLQEE	IWAVLNQSAE	SLQELFRKVS	LADPAALGFI	ISFWSLLLLP	SGSVSFTDEN	ISNQDLRAFT
90	100	110	120	130	140	150	160
APEVLQNSL	TSLSDVKEIH	IYSLGMTLYW	GADYEVFQSQ	PIKLGDLHNS	ILLGMCEDVI	YARVSVRTVL	DACSAHIRNS
170	180	190	200	210	220	230	240
NCAPSFYSVK	HLVKLVLGNL	SGTDQLSCNS	EQKPDRSQAI	RDRLRGKGLP	TGRSSTSDVL	DIQKPPLSHQ	TFLNKGLSKS
250	260	270	280	290	300	310	320
MGFLSIKDTQ	DENYFKDILS	DNSGREDSEN	TFSPYQFKTS	GPEKKPIPGI	DVLSKKKIWA	SSMDLLCTAD	RDFSSETAT
330	340	350	360	370	380	390	400
YRRCHPEAVT	VRTSTTPRKK	EARYSDGSIA	LDIFGPOKMD	PIYHTRELPT	SSAISSALDR	IRERQKQLQV	LREAMNVEEP
410	420	430	440	450	460	470	480
VRRYKTYHGD	VFSTSSSEPS	IISSESDFRQ	VRRSEASKRF	ESSSGLPGVD	ETLSQGQSQR	PSRQYETPFE	GNLNIQEIML
490	500	510	520	530	540	550	560
KRQEEELMQL	QAKMALRQSR	LSLYPGDTIK	ASMLDITRDP	LREIALETAM	TQRKLRNFFG	PEFVKMTIEP	FISLDLPRSI
570	580	590	600	610	620	630	640
LTKKGKNEEDN	RRKVNIMLLN	GQRLELCTDT	KTICKDVFDL	VVAHIGLVEH	HLFALATLKD	NEYFFVDDDL	KLTKVAPEGW
650	660	670	680	690	700	710	720
KEEPKKTKA	TVNFTLFFRI	KFFMDDVSLI	QHTLTCHQYY	LQLRKDILEE	RMHCDDDSL	LLASLALQAE	YGDYQPEVHG
730	740	750	760	770	780	790	800
VSYFRMEHYL	PARVMEKLDL	SYIKEELPKL	HNTYVGASEK	ETEFLEFLKVC	QRLTEYGVHF	HRVHPEKKSQ	TGILLGVCSK
810	820	830	840	850	860	870	880
GVLVFEVHNG	VRTLVLRFPW	RETKKISFSK	KKITLQNTSD	GIKHGFQTDN	SKICQVLLHL	CSYQHKFQLQ	MRARQSNQDA
890	900	910	920	930	940	950	960
QDIERASFPS	LNLQAESVRG	FNMGRAISTG	SLASSTLNKL	AVRPLSVQAE	ILKRLSCSEL	SLYQFLQNS	KEKNDKASWE
970	980	990	1000	1010	1020	1030	1040
EKPREMSKSY	HDLSQASLYP	HRKNVIVNME	PPPQTVAELV	GKPSHQMSRS	DAESLAGVTK	LNSKSVASL	NRSPERRKHE
1050	1060	1070	1080	1090	1100	1110	1120
SDSSSIEDPG	QAYVLGMTMH	SSGNSSSQVP	LKENDVLHKK	WSIVSSPERE	ITLVNLKKA	KYGLGFQIIG	GEKMGRLDLG
1130	1140	1150	1160	1170	1180	1190	1200
IFISSVAPGG	PADLDGCLKP	GDRLISVNSV	SLEGVSHHAA	IEILQNAPEL	VTLVISQPKL	KISKVPSTPV	HLTNEMKNYM
1210	1220	1230	1240	1250	1260	1270	1280
KKSSYMQDSA	IDSSSKDHHW	SRGTLRHISE	NSFGPSGGLR	EGSLSSQDSR	TESASLSQSQ	VNGFFASHLG	DQTWQESQHG
1290	1300	1310	1320	1330	1340	1350	1360
SPSPSVISKA	TEKETPTDSN	QSKTKKPGIS	DVTDYSDRGD	SDMDEATYSS	SQDHQTPKQE	SSSSVNTSNK	MNFKTFSSSP
1370	1380	1390	1400	1410	1420	1430	1440
PKPGDIFEVE	LAKNDNSLGI	SVTGGVNTSV	RHGIIYKAV	IPQGAESDQ	RIHKGDRVLA	VNGVLELAT	HKQAVETLRN
1450	1460	1470	1480	1490	1500	1510	1520
TGQVVHLLLE	KGQSPTSKEH	VPVTPQCTLS	DQNAQGGPE	KVKKTQVKD	YSFVTEENTF	EVKLFKNSSG	LGFSSREDN
1530	1540	1550	1560	1570	1580	1590	1600
LIPEQINASI	VRVKLFPQG	PAESGKIDV	GDVILKNGA	SLKGLSQEV	ISALRGTAPE	VFLLLCRPPP	GVLPEIDTAL
1610	1620	1630	1640	1650	1660	1670	1680
LTPLQSPAQV	LPNSSKDSQ	PSCVEQSTSS	DENEMSDKSK	KQCKSPSRD	SYSDSSGSGE	DDLVTAPANI	SNSTWSSALH
1690	1700	1710	1720	1730	1740	1750	1760
QTLNMSVQA	QSHHEAPKSQ	EDTICTMFYY	PQKIPNKPEF	EDSNPSPLPP	DMAPGQSYQP	QSESASSSSM	DKYHIHHISE
1770	1780	1790	1800	1810	1820	1830	1840
PTRQENWTPL	KNDLENHLED	FELEVELLIT	LIKSEKSLG	FTVTKGNQRI	GCYVHDVIQD	PAKSDGRLKP	GDRLIKVNDT
1850	1860	1870	1880	1890	1900	1910	1920
DVTNMHTDA	VNLLRAASKT	VRLVIGRVLE	LPRIPMLPHL	LPDITLTCNK	EELGFSLCGG	HDSLYQVVYI	SDINPRVAA
1930	1940	1950	1960	1970	1980	1990	2000
IEGNLQLLDV	IHYVNGVSTQ	GMTLEEVRNA	LDMSLPSLVL	KATRNDLPVV	PSSKRSVAVS	PKSTKNGSY	SVGSCSQPAL
2010	2020	2030	2040	2050	2060	2070	2080
TPNDSFSTVA	GEEINEISYP	KGKCYSTYQIK	GSPNLTLPKE	SYIQEDDIYD	DSQAEVVIQS	LLDVVDEEAQ	LLNENNAAG
2090	2100	2110	2120	2130	2140	2150	2160
YSCGPGTLKM	NGKLEERTE	DTDCDGSPLP	EYFTEATKMN	GCEEYCEEKV	KESLIQKPKQ	EKKTDDEIT	WGNDELPIER
2170	2180	2190	2200	2210	2220	2230	2240
TNHEDSDKDH	SFLTNDLAV	LPVVKVLPSP	KYTGANKSV	IRVLRGLLDQ	GIPSKLENL	QELKPLDQCL	IGQTKENRRK
2250	2260	2270	2280	2290	2300	2310	2320
NRYKNILPYD	ATRVPLGDEG	GYINASFYKI	PVGKEEFVYI	ACQGPLPTTV	GDFWQMIWEQ	KSTVIAMTQ	EVEGEKIKCQ
2330	2340	2350	2360	2370	2380	2390	2400
RYWPNILGKT	TMVSNRLRLA	LVRMQQLKGF	VVRAMTLEDI	QTRVVRHISH	LNFTAWPDHD	TPSQPDDLLT	FISYMRHIHR
2410	2420	2430	2440	2450	2460	2470	2480
SGPIITHCSA	GIGRSGTLIC	IDVVLGLISQ	DLDFDISDLV	RCMRLQRHGM	VQTEDQYIFC	YQVILYVLR	LQAEQKQKQ
2490							
PQLLK							

Coverage map for D kinase-interacting substrate of 220kDa

10	20	30	40	50	60	70	80
MSVLISQSVI	NYVEEENIPA	LKALLEKCKD	VDERNECGQT	PLMIAAEQGN	LEIVKELIKN	GANCNLEDDL	NWTALISASK
90	100	110	120	130	140	150	160
EGHVHIVEEL	LKCGVNLHR	DMGGWTALMW	ACYKGRDQV	ELLLSHGANP	SVTGLYSVYP	IWAAGRGA	DIVHLLQNG
170	180	190	200	210	220	230	240
AKVNCSDKYG	TTPLVWAARK	GHLECVKHL	AMGADVDEG	ANSMTALIVA	VKGGYTQSVK	EILKRNPNVN	LTDKDGNTAL
250	260	270	280	290	300	310	320
MIASKEGHE	IVQDLLDAGT	YVNIPDRSGD	TVLIGAVRGG	HVEIVRALLQ	KYADIDIRGQ	DNKTALYWAV	EKGNATMVRD
330	340	350	360	370	380	390	400
ILQCNPDTEI	CTKDGTEPLI	KATKMRNIEV	VELLLDKGAK	VSAVDKKGDT	PLHAIIRGRS	RKLAELLLRN	PKDGRLLYRP
410	420	430	440	450	460	470	480
NKAGETPYNI	DCSHQKSILT	QIFGARHLSP	TETDGDMLGY	DLYSSALADI	LSEPTMQPPI	CVGLYAQWGS	GKSFLKLE
490	500	510	520	530	540	550	560
DEMKTFAQQ	IEPLFQFSWL	IVFLTLLECG	GLGLLFAFTV	HPNLGIAVSL	SFLALYIF	IVIYFGGRRE	GESWNWAWL
570	580	590	600	610	620	630	640
STRLARHIGY	LELLKLMFV	NPPELPEQTT	KALPVRFLFT	DYNRLSSVGG	ETSLAEMIA	LSDACEREF	FLATRLFRVF
650	660	670	680	690	700	710	720
KTEDTQGRK	WKKTCCLPSE	VIFLFIIGCI	ISGITLLAIF	RVDPKHLTVN	AVLISIASVV	GLAFVLCRT	WWQVLDLNL
730	740	750	760	770	780	790	800
SQRKRLHNA	SKLHLKSE	FMKVLKCEVE	LMARMAKTD	SFTQNOTRLV	VIIDGLDACE	QDKVLQMLDT	VRVLFSGKPF
810	820	830	840	850	860	870	880
IAIFASDPHI	IIKAINQNLN	SVLRDSNNG	HDYMRNIVHL	PVFLNSRGLS	NARKFLVTS	TNGDVPCSDT	TGIQEDADRR
890	900	910	920	930	940	950	960
VSQNSLGEMT	KLGSKTALNR	RDTYRRRQMQ	RTITRQMSFD	LTKLLVTEDW	FSDISPQTM	RLLNIVSVTG	RLLRANQISF
970	980	990	1000	1010	1020	1030	1040
NWDRLASWIN	LTEQPWYR	WLILYLEETE	GIPDQMTLKT	IYERISKNI	TTKDVEPLLE	IDGDIRNFEV	FLSRTPLV
1050	1060	1070	1080	1090	1100	1110	1120
ARDVKVFLPC	TVNLDPKLRE	IIADVRAARE	QISIGGLAYP	PLPLHEGPPR	APSGYSQPPS	VCSSTSFNGP	FAGGVVSPQP
1130	1140	1150	1160	1170	1180	1190	1200
HSSYSGMTG	PQHPFYNRPF	FAPYLYTPRY	YPGGSQHLIS	RPSVKTSLPR	DQNGLEVIK	EDAAEGLSSP	TDSSRGSGPA
1210	1220	1230	1240	1250	1260	1270	1280
PGPVLLNSL	NVDAVCEK	QIEGLDQSM	PQYCTTIKKA	NINGRVLAQC	NIDELKKEM	MNFGDWHLFR	STVLEMRNAE
1290	1300	1310	1320	1330	1340	1350	1360
SHVVPEDPRF	LSESSSGPAP	HGEPARRASH	NELPHTELSS	QTPYTLNFSF	EELNTLGLDE	GAPRHSNLSW	QSQTRTPSL
1370	1380	1390	1400	1410	1420	1430	1440
SSLNSQSSI	EISKLTQKVQ	AEYRDAYREY	IAQMSQLEGG	PGSTTISGRS	SPHSTYYMGQ	SSSGGSIHSN	LEQEKGKDE
1450	1460	1470	1480	1490	1500	1510	1520
PKPDDGRKSF	LMKRGDVIDY	SSSGVSTNDA	SPLDPITEED	EKSDQSGSKL	LPGKKSERS	SLFQTDLKLK	GSLRYQKLP
1530	1540	1550	1560	1570	1580	1590	1600
SDEDESGTEE	SDNTPLLKDD	KDKAEGKVE	RVPKSPESHA	EPIRTFIKAK	EYLSDALDK	KDSSDSGVR	SESSPNHSLH
1610	1620	1630	1640	1650	1660	1670	1680
NEVADDSQLE	KANLIELEDD	SHSGKRGI	SLSGLQDPII	ARMSICSEDK	KSPSECSLIA	SSPEENWPAC	QKAYNLNRT
1690	1700	1710	1720	1730	1740	1750	1760
STVTLNNSA	PANRANQNF	EMEGIRETSQ	VILRPSSPN	PTTIQENL	SMTHKRSQRS	SYTRLKSDPP	ELHAAASSES
1770	1780						
TGFGEERESI	L						

Coverage map for Ubiquitin conjugation factor E4 A

10	20	30	40	50	60	70	80
MTDQENNNNI	SSNPFAALFG	SLADAKQFAA	IQKEQLKQQS	DELPASPDDS	DNSVSESLDE	FDYSVAEISR	SFRSQQEICE
90	100	110	120	130	140	150	160
QLNINHMIQR	IFLITLDNSD	PSLKSGNGIP	SRCVYLEEMA	VELEDQDWLD	MSNVEQALFA	RLLLQDPGNH	LINMTSSTTL
170	180	190	200	210	220	230	240
NLSADDRDAGE	RHIFCYLYSC	FQRAKEEITK	VPENLLPFAV	QCRNLTVSNT	RTVLLTPEIY	VDQNIHEQLV	DLMLEAIQGA
250	260	270	280	290	300	310	320
HFEDVTEFLE	EVIEALILDE	EVRTFPEVMI	PVFDILLGRI	KDLELCQILL	YAYLDILLYF	TRQKDMAKVF	VEYIQPKDPT
330	340	350	360	370	380	390	400
NGQMYQKTL	GVILSISCLL	KTPGVVENHG	YFLNPSRSP	QEIKVQEANI	HQFMAQFHEK	IYQMLKNLLQ	LSPETKHCIL
410	420	430	440	450	460	470	480
SWLGNCLHAN	AGRTKIWANQ	MPEIFFQMYA	SDAFFLNLGA	ALLKLCQPF	KPRSSRLITF	NPTYCALKE	NDEERKIKNV
490	500	510	520	530	540	550	560
HMRGLDKETC	LIPAVQEPKF	PQNYNLVTEN	LALTEYTYL	GFHRLHDQMV	KINQNLHRLQ	VAWRDAQQSS	SPAADNREQ
570	580	590	600	610	620	630	640
FERLMTIYLS	TKTAMTEPQM	LQNCLNLQVS	MAVLLVQLAI	GNEGSQPIEL	TFPLPDGYSS	LAYVPEFFAD	NLGDFLIFLR
650	660	670	680	690	700	710	720
RFADDILETS	ADSLEHVLHF	ITIFTGSIER	MKNPHLRACL	AEVLEAVMPH	LDQTPNPLVS	SVFHRKRVFC	NFYAPQLAE
730	740	750	760	770	780	790	800
ALIKVFVDIE	FTGDPHQFEQ	KFNRYRRPMP	ILRYMWGTDI	YRESIKDLAD	YASKNLEAMN	PPLFLRFLNL	LMNDAIFLLD
810	820	830	840	850	860	870	880
EAIQYLSKIK	IQQIEKDRGE	WDSLTPPEAR	EKEAGLQMG	QLARFHNIMS	NETIGTLAFL	TSEIKSLFVH	PFLAERIISM
890	900	910	920	930	940	950	960
LNYFLQHLVG	PKMGALKVKD	FSEFDKPKQQ	LVSDICTIYL	NLGDEENFCA	TVPKDGRSYS	PTLFAQTVRV	LKKINKPGNM
970	980	990	1000	1010	1020	1030	1040
IMAFSNLAER	IKSLADLQQQ	EEETYADACD	EFLDPIMSTL	MCDPVVLPSS	RVTVDRSTIA	RHLLSDQTD	FNSPLTMDQ
1050	1060	1070					
IRPNTELKEK	IQRWLAERKQ	QKEQLE					

Coverage map for Exportin-7

10	20	30	40	50	60	70	80
MADHVQSLAQ	LENLCKQLYE	TDTTTRLQA	EKALVEFTNS	PDCLSKCQLL	LERGSSSYSQ	LLAATCLTKL	VSR TNNPLPL
90	100	110	120	130	140	150	160
EQR IDIRNYV	LNVLATRPKL	ATFVTQALIQ	LYARITKLGW	FDCQKDDYVF	RNAITDVTRF	LQDSVEYCII	GVTILSQLTN
170	180	190	200	210	220	230	240
EINQADTTHP	LTKHRKIASS	FRDSSLFDIF	TLSCNLLKQA	SGKNLNLNDE	SQHGLLMQLL	KLTHNCLNFD	FIGTSTDESS
250	260	270	280	290	300	310	320
DDLCTVQIPT	SWRSAFLDSS	TLQLFFDLYH	SIPPSFSPLV	LSCLVQIASV	RRSLFNNAER	AKFLSHLVDG	VKRILENPQS
330	340	350	360	370	380	390	400
LSDPNNYHEF	CRLLARLKSN	YQLGELVKVE	NYPEVIRLIA	NET VTSLQHW	EFAPNSVHYL	LSLWQRLAAS	VPYVKATEPH
410	420	430	440	450	460	470	480
MLETYTPPEVT	KAYITSRLES	VHIILRDGLE	DPLEDTGLVQ	QQLDQLSTIG	RCEYEKTCAL	LVQLFDQSAQ	SYQELLSAS
490	500	510	520	530	540	550	560
ASPMIAVQE	GRLTWLVYII	GAVIGGRVSF	ASTDEQDAMD	GELVCRVLQL	MNL TDSRLAQ	AGNEKLELAM	LSFFEQFRKI
570	580	590	600	610	620	630	640
YIGDQVQKSS	KLYRRLSEVL	GLNDETMVLS	VFIGKIITNL	KYWGRCEPIT	SKTLQLLNDL	SIGYSSVRKL	VKLSAVQFML
650	660	670	680	690	700	710	720
N NHTSEHFSF	LGIN NQSNLT	DMRCRTTFYT	ALGRLLMVDL	GEDEDQYEQF	MLPLTAAFEA	VAQMFSTNSF	NEQEAKRTLIV
730	740	750	760	770	780	790	800
GLVRDLRGIA	FAFNAKTSFM	MLFEWIYPSY	MPILQRAIEL	WYHDPACTTP	VLKLMAELVH	NRS QRLQFDV	SSPNGILLFR
810	820	830	840	850	860	870	880
ETSKMITMYG	NRILTLGEVP	KDQVYALKLK	GISICFSQLK	AALSGSYVNF	GVFRLYGDDA	LDNALQTFIK	LLLSIPHSDL
890	900	910	920	930	940	950	960
LDYPKLSQSY	YSLEVLTDQ	HMNFIASLEP	HVIMYILSSI	SEGLTALDTM	VCTGCCCLD	HIVTYLQFKL	SRSTK KRTTP
970	980	990	1000	1010	1020	1030	1040
LNQESDR FLH	IMQQHPEMIQ	QMLSTVLNII	IFEDCRNQWS	MSRPLLGLIL	LNEKYFSDLR	NSIVNSQPPE	KQQAMHL CFE
1050	1060	1070	1080	1090			
NLMGIERNL	LTKNRDRFTQ	NLSA FRREVN	DSMKNST YGV	NSNDMMS			

Coverage map for Conserved oligomeric Golgi complex subunit 5

10	20	30	40	50	60	70	80
MGWVGRRRD	SASPPGRSRS	AADDINPAPA	NMEGGGSVA	VAGLGARGSG	AAAATVRELL	QDGCYSDFLN	EDFDVKTYTS
90	100	110	120	130	140	150	160
QSIHQAVIAE	QLAKLAQGIS	QLDRELHLQV	VARHEDLLAQ	ATGIESLEGV	LQMMQTRIGA	LQGAVDRIKA	KIVEPYNKIV
170	180	190	200	210	220	230	240
ARTAQLARLQ	VACDLLRRII	RILNLSKRLQ	GQLQGGGREI	TKAAQSLNEL	DYLSQGIDLS	GIEVIENDLL	FIARARLEVE
250	260	270	280	290	300	310	320
NQAKRLEQG	LETQNPTQVG	TALQVFYNLG	TLKDTITSVV	DGYCATLEEN	INSALDIKVL	TQPSQSAVRG	GPRSTMPTP
330	340	350	360	370	380	390	400
GNTAALRASL	WTNMEKLMDH	IYAVCGVQH	LQKVLAKKRD	PVSHICFIEE	IVKDGQPEIF	YTFWNSVTQA	LSSQFHMATN
410	420	430	440	450	460	470	480
SSMFLKQAFE	GEYPKLLRLY	NDLWKRLQY	SQHIQGNFNA	SGTTDLVVDL	QHMEDDAQDI	FIPKKPDYDP	EKALKDSLQP
490	500	510	520	530	540	550	560
YEAYLSKSL	SRLEFDPINLV	FPPGGRNPPS	SDELDTIKT	IASELNVAAV	DTNLTAVSK	NVAKTIQLYS	VKSEQLLPTQ
570	580	590	600	610	620	630	640
GDASQVIGPL	TEGQRNVAV	VNSLYKLHQS	VTKAIHALME	NAVQPLTSV	GDAIEAIIIT	MHQEDFGSL	SSSGKPDVPC
650	660	670	680	690	700	710	720
SLYMKELQGF	IARVMSDYFK	HFECLDFVFD	NTEAIAQRAV	ELFIRHASLI	RPLGEGGKMR	LAADFAQMEI	AVGPFCCRVS
730	740	750	760	770	780	790	800
DLGKSYRMLR	SFRPLLQAS	EHVASSPALG	DVIPFSIIQ	FLFTRAPAEI	KSPFQRAEWS	HTRFSQWLDD	HPSEKDRLLL
810	820	830	840				
IRGALEYVQ	SVRSREGKEF	APVYPIMVQL	LQKAMSALQ				

Coverage map for Conserved oligomeric Golgi complex subunit 7

10	20	30	40	50	60	70	80
MDFSKFLADD	FDVKEWINAA	FRAGSKEAAS	GKADGHAATL	VMKLQLFIQE	VNHAVEETSH	QALQNMPKVL	RDVEALKQEA
90	100	110	120	130	140	150	160
SFLKEQMILV	KEDIKKFEQD	TSQSMQVLVE	IDQVKSRMQL	AAESLQEADK	WSTLSADIEE	TFK TQDI AVI	SAK LTGMQNS
170	180	190	200	210	220	230	240
LMMLVDTPDY	SEKCVHLEAL	KNRLEALASP	QIVAAFTSQA	VDQSKVFKV	FTEIDRMPQL	LAYYYKCHKV	QLLAAWQELC
250	260	270	280	290	300	310	320
QSDLSLDRQL	TGLYDALLGA	WHTQIQWATQ	VFQKPHEVVM	VLLIQTLGAL	MPSLPSCLSN	GVER AGPEQE	LTRL LLEFYDA
330	340	350	360	370	380	390	400
TAHFAKGLEM	ALLPHLHEHN	LVK VTEL VDA	VYDPYKPYQL	KY GDMEESNL	LIQMSAVPLE	HGEVIDCVQE	LSHSVNLKLF
410	420	430	440	450	460	470	480
LASAAVDRCV	RFTNGLGTGC	LLSALKSLFA	KYVSDFTSTL	QSIR KKCKLD	HIPPNSLFQE	DWTAFQNSIR	IIATCGELLR
490	500	510	520	530	540	550	560
HCGDFEQQLA	NRILSTAGKY	LSDSCSPRSL	AGFQESILTD	KKNSAKNPWQ	EYNYLQKDNP	AEYASLMEIL	YTLKEKSSN
570	580	590	600	610	620	630	640
HNLLAAPRAA	L TRLNQQA HQ	LAFDSVFLRI	KQQLLLISKM	DSWNTAGIGE	TLTDELPAFS	LTPLEYISNI	GQYIMSLPLN
650	660	670	680	690	700	710	720
LEPFVTQEDS	ALELALHAGK	LFPFPEQGDE	LPELDNMADN	WLGSIARATM	QTYCDAILQI	PELSPHSAKQ	LATDIDYLIN
730	740	750	760	770	780		
VMDALGLQPS	RTLQHI V TLL	KTR PEDYRQV	SKGLPRRLAT	TVATMRSVNY			

Coverage map for LETM1 and EF-hand domain-containing protein 1, mitochondrial

10	20	30	40	50	60	70	80	
MASILLRSCR	GRAPARLPPP	PRYTVPRGSP	GDPAHLSCAS	TLGLRNCLNV	PFGCCTPIHP	VYTSSRGDHL	GCWALRPECL	
90	100	110	120	130	140	150	160	
RIVSRAPWTS	TSVGFVAVGP	QCLPVRGWHS	SRPVRDSSV	EKSLKSLKDK	NKKLEGGPV	YSPPAEVVVK	KSLGQRVLDE	
170	180	190	200	210	220	230	240	
LKHYHGFRL	LWIDTKIAAR	MLWRILNGHS	LTRRERRQFL	RICADLFRLV	PFLVFFVVPF	MEFLLPVAVK	LFPNMLPSTF	
250	260	270	280	290	300	310	320	
ETQSLKEERL	KKELRVKLEL	AKFLQDTIEE	MALKNKAAKG	SATKDFSVFF	QKIRETGERP	SNEEIMRFSK	LFEDELTLDN	
330	340	350	360	370	380	390	400	
LT	TRPQLVALC	KLLELQSIGT	NNFLRFQMTM	RLRSIKADDK	LIAEEGVDSL	NVKELQAACR	ARGMRALGVT	EDRLRGQLKQ
410	420	430	440	450	460	470	480	
WLDLHLHQEI	PTSLILSRA	MYLPDTLSPA	DQLKSTLQTL	PEIVAKEAQV	KVAEVEGEQV	DNKAKLEATL	QEAAIQEH	
490	500	510	520	530	540	550	560	
REKELQKRSE	VAKDFEPERV	VAAPQRPSTE	PQPEMPDTVL	QSETLKDTAP	VLEGLKEEII	TKEEIDILSD	ACSKLQEQQK	
570	580	590	600	610	620	630	640	
SLTKEKEELE	LLKEDVQDYS	EDLQEIKKEL	SKTGEEKYVE	ESKASKRLTK	RVQQMIGQID	GLISQLEMDQ	QAGKLAPANG	
650	660	670	680	690	700	710	720	
MPTGENVISV	AELINAMQV	KHIPESKLT	LAAALDENKD	GKVNIDDLVK	VIELVDKEDV	HISTSQVAEI	VATLEKEEKV	
730	740							
EEKEKAKEKA	EKEVAEVKS							

Coverage map for Eukaryotic translation initiation factor 3, subunit J

10	20	30	40	50	60	70	80
MAAAAAAGD	SDSWDADAFS	VEDPVRKVGG	GGTAGGDRWE	GEDEDEDVKD	NWDDDDDEKK	EEAEVKPEVK	ISEKKKIAEK
90	100	110	120	130	140	150	160
IKEKERQQKK	RQEEIKKRLE	EPEEPKVLTP	EEQLADKLRL	KKLQEESDLE	LAKETFGVNN	AVYGIDAMNP	SSRDDDFTEFG
170	180	190	200	210	220	230	240
KLLKDKITQY	EKSLYYASFL	EVLVRDVCIS	LEIDDLKKIT	NSLTVLCSEK	QKQEKQSKAK	KKKKGVVPGG	GLKATMKDDL
250	260						
ADYGGYDGGY	VQDYEDFM						

Appendix 2

Mass spectrometry protein data and sequence coverage maps (Ad12 E4orf3 pulldown)

**Prolow-density lipoprotein receptor-related protein 1 OS=Homo sapiens GN=LRP1
PE=1 SV=1**

Accession: LRP1_HUMAN

Score: 858.0

Database: SwissProtDecoy(SwissProt_Decoy.fasta)

MW [kDa]: 504.2

Database Date: 2011-03-29

pI: 5.0

Modification(s): Carbamidomethyl, Oxidation

Sequence Coverage [%]: 6.7

No. of unique Peptides: 25

**Tyrosine-protein phosphatase non-receptor type 13 OS=Homo sapiens GN=PTPN13
PE=1 SV=2**

Accession: PTN13_HUMAN

Score: 1272.6

Database: SwissProtDecoy(SwissProt_Decoy.fasta)

MW [kDa]: 276.7

Database Date: 2011-03-29

pI: 6.0

Modification(s): Carbamidomethyl, Oxidation

Sequence Coverage [%]: 18.8

No. of unique Peptides: 36

**Kinase D-interacting substrate of 220 kDa OS=Homo sapiens GN=KIDINS220 PE=1
SV=3**

Accession: KDIS_HUMAN

Score: 218.4

Database: SwissProtDecoy(SwissProt_Decoy.fasta)

MW [kDa]: 196.4

Database Date: 2011-03-29

pI: 6.2

Sequence Coverage [%]: 4.7

No. of unique Peptides: 7

Ubiquitin conjugation factor E4 A OS=Homo sapiens GN=UBE4A PE=1 SV=2

Accession: UBE4A_HUMAN

Score: 330.2

Database: SwissProtDecoy(SwissProt_Decoy.fasta)

MW [kDa]: 122.5

Database Date: 2011-03-29

pI: 5.0

Modification(s): Oxidation

Sequence Coverage [%]: 10.1

No. of unique Peptides: 9

Exportin-7 OS=Homo sapiens GN=XPO7 PE=1 SV=3

Accession: XPO7_HUMAN

Score: 99.5

Database: SwissProtDecoy(SwissProt_Decoy.fasta)

MW [kDa]: 123.8

Database Date: 2011-03-29

pI: 5.9

Sequence Coverage [%]: 3.9

No. of unique Peptides: 4

Conserved oligomeric Golgi complex subunit 5 OS=Homo sapiens GN=COG5 PE=1 SV=2

Accession: COG5_HUMAN

Score: 354.9

Database: SwissProtDecoy(SwissProt_Decoy.fasta)

MW [kDa]: 92.7

Database Date: 2011-03-29

pI: 6.1

Modification(s): Oxidation

Sequence Coverage [%]: 14.4

No. of unique Peptides: 11

Conserved oligomeric Golgi complex subunit 7 OS=Homo sapiens GN=COG7 PE=1 SV=1

Accession: COG7_HUMAN

Score: 340.2

Database: SwissProtDecoy(SwissProt_Decoy.fasta)

MW [kDa]: 86.3

Database Date: 2011-03-29

pI: 5.2

Modification(s): Carbamidomethyl

Sequence Coverage [%]: 16.8

No. of unique Peptides: 10

LETM1 and EF-hand domain-containing protein 1, mitochondrial OS=Homo sapiens GN=LETM1 PE=1 SV=1

Accession: LETM1_HUMAN

Score: 1315.5

Database: SwissProtDecoy(SwissProt_Decoy.fasta)

MW [kDa]: 83.3

Database Date: 2011-03-29

pI: 6.3

Modification(s): Carbamidomethyl, Oxidation

Sequence Coverage [%]: 36.8

No. of unique Peptides: 26

Eukaryotic translation initiation factor 3 subunit J OS=Homo sapiens GN=EIF3J PE=1 SV=2
Accession: EIF3J_HUMAN
Score: 283.2
Database: SwissProtDecoy(SwissProt_Decoy.fasta)
MW [kDa]: 29.0
Database Date: 2011-03-29
pI: 4.6
Modification(s): Carbamidomethyl, Oxidation
Sequence Coverage [%]: 27.9
No. of unique Peptides: 7

Coverage diagrams for proteins pulled down with Ad12 E4orf3

Coverage map for Prolow-density lipoprotein receptor-related protein 1

10	20	30	40	50	60	70	80
MLTPPLLLL	PLLSALVAAA	IDAPKTCSPK	QFACRDQITC	ISKGWRCDGE	RDCPDGSDEA	PEICPQSKAQ	RCQPNEHNCL
90	100	110	120	130	140	150	160
GTELCVPMR	LCNGVQDCMD	GSDEGPHCRE	LQGNCSRLGC	QHHCVPITLDG	PTCYCNSSFQ	LQADGKTCKD	FDECSVYGTC
170	180	190	200	210	220	230	240
SQLCTNTDGS	FICGCVVEYL	LQPDNRSCKA	KNPEVDRPPV	LLIANSQNIL	ATYLSGAQVS	TITPTSTRQT	TAMDFSYANE
250	260	270	280	290	300	310	320
TVCVHVHGD	AAQTQLKCAR	MPGLKGFVDE	HTINISLSLH	HVEQMAIDWL	TGNFYFVDDI	DDRIFVCNRR	GDTCVTLDDL
330	340	350	360	370	380	390	400
ELYNPKGIAL	DPAMGKVFFT	DYGQIPKVER	CDMDGQNRTK	LVDSKIVFFH	GITLDLVSRL	VYWADAYLDY	IEVVDYEGKG
410	420	430	440	450	460	470	480
RQTIIQGILI	EHLYGLTFE	NYLYATNSDN	ANAQQKTSVI	RVNRFNSTEY	QVVTRVDKGG	ALHIYHQRRQ	PRVRSACEN
490	500	510	520	530	540	550	560
DQYKPGGCS	DICLLANSHK	ARTCRCRSGF	SLGSDGKSCK	KPEHELFLVY	GKGRPGIIRG	MDMGAKVPDE	HMIPIENLMN
570	580	590	600	610	620	630	640
PRALDFAET	GFIYFADTTS	YLIGRQKIDG	TERETILKDG	IHNVEGVAVD	WMGDNLWYTD	DGPKKTISSA	RLEKAAQTRK
650	660	670	680	690	700	710	720
TLIEGKMTHP	RAIVVDPLNG	WYWTDWEEED	PKDSRRGRLE	RAWMDGSHRD	IFVTSKTVLW	PNGLSLDIPA	GRLYWDAFY
730	740	750	760	770	780	790	800
DRIETILLNG	TDRKIVYEGP	ELNHAFGLCH	HGNLFWTEY	RSGSVYRLER	GVGGAPPTVT	LLRSERPPIF	EIRMYDAQQQ
810	820	830	840	850	860	870	880
QVGTNKCRVN	NGGCSSLCLA	TPGSRQCACA	EDQVLDADGV	TCLANPSYVP	PPQCQPFGEA	CANSRCIQER	WKCDGDNDCL
890	900	910	920	930	940	950	960
DNSDEAPALC	HQHTCPSDRF	KCENNRCPIN	RWLCDGDND	GNSEDES NAT	CSARTCPPNQ	FSCASGRICIP	ISWTCDLDDD
970	980	990	1000	1010	1020	1030	1040
CGDRSDESAS	CAYPTCFPLT	QFTCNNGRCI	NINWRCDNDN	DCGDNSEAG	CSHSCSSTQF	KCNSGRCIPE	HWTCGDNDNC
1050	1060	1070	1080	1090	1100	1110	1120
GDYSDETHAN	CTNQATRPPG	GCHTDEFQCR	LDGLCIPLRW	RCDGDTDCMD	SSDEKSCEGV	THVCDPSVKF	GCKDSARCIS
1130	1140	1150	1160	1170	1180	1190	1200
KAWVCDGDND	CEDNSDEENC	ESLACRPPSH	PCANNTSVCL	PPDKLCDGND	DCGDGSDEGE	LCDQCSLNGG	GCSHNCSVAP
1210	1220	1230	1240	1250	1260	1270	1280
GEGIVCSPL	GMELGPDNHT	CQIQSYCAKH	LKCSQKCDQN	KFSVKCSCEYE	GWVLEPDGES	CRSLDPFKPF	IIFSRHEIR
1290	1300	1310	1320	1330	1340	1350	1360
RIDLHKGDYS	VLVPLRNTI	ALDFHLSQSA	LYWTDVVEDK	IYRGKLLDNG	ALTSFEVVIQ	YGLATPEGLA	VDWIAGNIYW
1370	1380	1390	1400	1410	1420	1430	1440
VESNLDQIEV	AKLDGTLRRT	LLAGDIEHPR	AIALDPRDGI	LFWTDWDASL	PRIEAASMSG	AGRRTVHRET	GSGGWPNGLT
1450	1460	1470	1480	1490	1500	1510	1520
VDYLEKRILW	IDARSDAIYS	ARYDGS GHME	VLRGHEFLSH	PFAVTLYGGE	VYWTDWRTNT	LAKANKWTGH	NVTVVQRTNT
1530	1540	1550	1560	1570	1580	1590	1600
QPFDLQVYHP	SRQPMAPNPC	EANGGQGPCS	HLCLINYNRT	VSCACPHLMK	LHKDNTTCYE	FKKFLLYARQ	MEIRGVLDLA
1610	1620	1630	1640	1650	1660	1670	1680
PYYNYIISFT	VPDIDNVTVL	DYDAREQRVY	WSDVRTQAIK	RAFINGTGVE	TVVSADLPNA	HGLAVDWVSR	NLFWTSYDTN
1690	1700	1710	1720	1730	1740	1750	1760
KKQINVARLD	GSFKNAVVOG	LEQPHGLVH	PLRGKLYWTD	GDNISMANMD	GSNRTLLFSG	QKGPVGLAID	FPESKLYWIS
1770	1780	1790	1800	1810	1820	1830	1840
SGNHTINRCN	LDGSGLEVID	AMRSQLGKAT	ALAIMGDKLV	WADQVSEKMG	TCSKADGSGS	VVLRNSTTLV	MHMKVYDESI
1850	1860	1870	1880	1890	1900	1910	1920
QLDHKGTNPC	SVNNGDCSQL	CLPTSETTRS	CMCTAGYSLR	SGQQACEGVG	SFLLYSVHEG	IRGIPLDPND	KSDALVFPVSG
1930	1940	1950	1960	1970	1980	1990	2000
TSLAVGIDFH	AENDTIYWVD	MGLSTISRAK	RDQTWREDDV	TNGIGRVEGI	AVDWIAGNIY	WTDQGFVIE	VARLNGSFRY
2010	2020	2030	2040	2050	2060	2070	2080
VVISQGLDKP	RAITVHPEKG	YLFWEWGQY	PRIERSRLDG	TERVVLVNVS	ISWPNGISVD	YQDGKLYWCD	ARTDKIERID
2090	2100	2110	2120	2130	2140	2150	2160
LETGENREVV	LSSNNMDFMS	VSVFEDFIYW	SDRTHANGSI	KRGSKNATD	SVPLRTGIGV	QLKDIKVFNR	DRQKGTNVCA
2170	2180	2190	2200	2210	2220	2230	2240

Coverage map for Tyrosine-protein phosphatase non-receptor type 13

10	20	30	40	50	60	70	80
MHVSIAEAE	VRGGPLQEE	IWAVLNQSAE	SLQELFRKVS	LADPAALGFI	ISFWSLLLLP	SGSVSFTDEN	ISNQDLRAFT
90	100	110	120	130	140	150	160
APEVLQNSL	TSLSDVEKIH	IYSLGMTLYW	GADYEVPSQ	PIKLGDLNS	ILLGMCEVDI	YARVSVRTVL	DACSAHIRNS
170	180	190	200	210	220	230	240
NCAPSFYVK	HLVKLVGLNL	SGTDQLSCNS	EQKPDRSQAI	RDRLRGKGLP	TGRSSTSDVL	DIQKPLPSHQ	TFLNKGLSKS
250	260	270	280	290	300	310	320
MGFLSIKDTQ	DENYFKDILS	DNSGREDSN	TFSPYQFKTS	GPEKKPIPGI	DVLSKKIWA	SSMDLLCTAD	RDFSSGETAT
330	340	350	360	370	380	390	400
YRRCHPEAVT	VRTSTTPRKK	EARYSDGSAI	LDIFGPQKMD	PIYHTRELPT	SSAISSALDR	IRERQKQLQV	LREAMNVEEP
410	420	430	440	450	460	470	480
VRRYKTYHGD	VFSTSSSEPS	IISSEDFRQ	VRRSEASKRF	ESSSGLPGVD	ETLSQGQSQR	PSRQYETPFE	GNLNQEIIML
490	500	510	520	530	540	550	560
KRQEELMQL	QAKMALRQSR	LSLYPGDTIK	ASMLDITRDP	LREIALETAM	TQRKLRNFFG	PEFVKMTIEP	FISLDLPRSI
570	580	590	600	610	620	630	640
LTKKGKNEEDN	RRKVNIMLLN	QORLELCTDT	KTICKDVFDL	VVAHIGLVEH	HLFALATLKD	NEYFFVDPDL	KLTKVAPEGW
650	660	670	680	690	700	710	720
KEEPKKTKA	TVNFTLFFRI	KFFMDDVSLI	QHTLTCHQYY	LQLRKDILEE	RMHCDEETSL	LLASLALQAE	YGDYQPEVHG
730	740	750	760	770	780	790	800
VSYFRMEHYL	PARVMEKLDL	SYIKEELPKL	HNTYVGASEK	ETEFLEFLKVC	QRLTEYGVHF	HRVHPEKKSQ	TGILLGVCSK
810	820	830	840	850	860	870	880
GVLVEEVHNG	VRTLVLRFPW	RETKKISFSK	KKITLQNTSD	GIKHGFQTDN	SKICQYLLHL	CSYQHKFQLQ	MRARQSNQDA
890	900	910	920	930	940	950	960
QDIERASFRS	LNLQAESVRG	FNMGRAISTG	SLASSTLNKL	AVRPLSVQAE	ILKRLSCSEL	SLYQFLQNS	KEKNDKASWE
970	980	990	1000	1010	1020	1030	1040
EKPREMSKSY	HDLSQASLYP	HRKNVIVNME	PPPQTVAELV	GKPSHQMSRS	DAESLAGVTK	LNSKSVASL	NRSPERRKHE
1050	1060	1070	1080	1090	1100	1110	1120
SDSSSIEDPG	QAYVLGMTMH	SSGNSSSQVP	LKENDVLHKK	WSIVSSPERE	ITLVNLKKDA	KYGLGFQIIG	GEKMGRLDLG
1130	1140	1150	1160	1170	1180	1190	1200
IFISSVAPGG	PADLDGCLKP	GDRLISVNSV	SLEGVSHHAA	IEILQNAPEL	VTLVISQPKL	KISKVPSTPV	HLTNEMKNYM
1210	1220	1230	1240	1250	1260	1270	1280
KKSSYMQDSA	IDSSSKDHHW	SRGTLRHISE	NSFGPSGGLR	EGSLSSQDSR	TESASLSQSQ	VNGFFASHLG	DQTWQESQHG
1290	1300	1310	1320	1330	1340	1350	1360
SPSPSVISKA	TEKETFTDSN	QSKTKKPGIS	DVTDYSDRGD	SMDDEATYSS	SQDHQTPKQE	SSSSVNTSNK	MNFKTFSSSP
1370	1380	1390	1400	1410	1420	1430	1440
PKPGDIFEVE	LAKNDNSLGI	SVTGGVNTSV	RHGGIYKAV	IPOGAESDGG	RIHKGDRVLA	VNGVSLGAT	HKQAVETLRN
1450	1460	1470	1480	1490	1500	1510	1520
TGQVVHLLLE	KGQSPTSKEH	VPVTPQCTLS	DQNAQGQGE	KVKKTTQVKD	YSFVTEENTF	EVKLFKNSSG	LGFSSFREDN
1530	1540	1550	1560	1570	1580	1590	1600
LIPEQINASI	VRVKLFPQG	PAESGKIDV	GDVILKVNGA	SLKGLSQQEV	ISALRGTAPE	VFLLLCRPPP	GVLPEIDTAL
1610	1620	1630	1640	1650	1660	1670	1680
LTPLQSPAQV	LPNSSKDSSQ	PSCVEQSTSS	DENEMSDKSK	KQCKSPSRD	SYSDSSGSGE	DDLVTAPANI	SNSTWSSALH
1690	1700	1710	1720	1730	1740	1750	1760
QTLNMQVQA	QSHHEAPKSQ	EDTICTMFYY	PQKIPNKPEF	EDSNPSPLPP	DMAPGQSYQP	QSESASSSSM	DKYHIHHISE
1770	1780	1790	1800	1810	1820	1830	1840
PTRQENWTPL	KNDLENHLED	FELEVELLIT	LIKSEKGLG	FTVTKGNQRI	GCYVHDVIQD	PAKSDGRLKP	GDRLIKVNDT
1850	1860	1870	1880	1890	1900	1910	1920
DVTNMHTHDA	VNLLRAASKT	VRLVIGRVLE	LPRIPMLPHL	LPDITLTCNK	EELGFSLCGG	HDSLYQVVYI	SDINPRSVAA
1930	1940	1950	1960	1970	1980	1990	2000
IEGNLQLLDV	IHYVNGVSTQ	GMTLEEVRNA	LDMSLPSLVL	KATRNDLPVV	PSSKRSVSA	PKSTKNGSY	SVGSCSQPAL
2010	2020	2030	2040	2050	2060	2070	2080
TFNDSFSTVA	GEEINEISYP	KGKCYSTYQIK	GSPNLTLPKE	SYIQEDDIYD	DSQEAQVQIS	LLDVVDEEAQ	LLNENNAAG
2090	2100	2110	2120	2130	2140	2150	2160
YSCGPGTLKM	NGKLSERTE	DTDCDGSPLP	EYFTEATKMN	GCEEYCEEKV	KESLIQKPK	EKKTDDEIT	WGNDELPIER
2170	2180	2190	2200	2210	2220	2230	2240
TNHEDSDKDH	SFLTNDLAV	LPVVKVLPSP	KYTGANLKS	IRVLRGLLDQ	GIPSKELN	QELKPLDQCL	IGQTKENRRK
2250	2260	2270	2280	2290	2300	2310	2320
NRYKNILPYD	ATRVPLGDEG	GYINASFYKI	PVGKEEFVYI	ACQGPLPTTV	GDFWQMIWEQ	KSTVIAMTQ	EVEGEKIKCQ
2330	2340	2350	2360	2370	2380	2390	2400
RYWPNILGKT	TMVSNRLRLA	LVRMQQLKGF	VVRAMTLEDI	QTRVVRHISH	LNFTAWPDHD	TPSQPDDLLT	FISYMRHIHR
2410	2420	2430	2440	2450	2460	2470	2480
SGPIITHCSA	GIGRSGTLIC	IDVVLGLISQ	DLDFDISDLV	RCMRLQRHGM	VQTEDQYIFC	YQVILYVLR	LQAEQKQ
2490							
PQLLK							

Coverage map for D kinase-interacting substrate of 220kDa

10	20	30	40	50	60	70	80
MSVLISQSVI	NYVEENIPA	LKALLEKCKD	VDERNECGQT	PLMIAAEQGN	LEIVKELIKN	GANCNLEDLD	NWT ALISASK
90	100	110	120	130	140	150	160
EGHVHIVEEL	LKCGVNLEHR	DMGGWTALMW	ACYKGRTDVV	ELLLSHGAN P	S VTGLYSVYP	I IWAAGRGA	DIVHLLQNG
170	180	190	200	210	220	230	240
AKV NCS DKYG	TTPLVWAARK	GHLECVKHLL	AMGADVQEG	ANSMTALIVA	VKGGYTQSVK	EILKRNPNVN	LTD KDGNTAL
250	260	270	280	290	300	310	320
MIASKEGHT	IVQDLLDAGT	YVNIPDR SGD	TVLIGAVRGG	HVEIVRALLQ	KYADIDIRGQ	DNKT ALYWAV	EKG NAT MVRD
330	340	350	360	370	380	390	400
ILQCNPDTEI	CTKDGTEPLI	KATKMR NIEV	VELLLDKGAK	VSAVDKKGDT	PLHAIIRGRS	RKLAE LLLRN	PKDGRLLYRP
410	420	430	440	450	460	470	480
NKAGETPYNI	DCSHQ SILT	QIFGARHLSP	TETDGM LG	DLYSSALADI	LSEPTMQPPI	CVGLYAQWGS	GKS FLLK LE
490	500	510	520	530	540	550	560
DEMKT FAGQQ	IEPL FQFSW L	IVFL TLLCG	GLGL FAFTV	HPNLGIAVSL	SFLALYIF	IVIY FGRRE	GESWN WAWL
570	580	590	600	610	620	630	640
STRLARHIGY	LELLLLMFV	NPELPEQTT	KALPVRFLFT	DYNRLSSVGG	ETSLAEMIA	LSDACEREF	FLATRLFRVF
650	660	670	680	690	700	710	720
KTEDTQ GK K	WKKTCCLP SF	VIFLFIIGCI	ISGITLLAIF	RVDPKHLTVN	AVLISIASVV	GLAFV LNCR T	WWQV LD SLN
730	740	750	760	770	780	790	800
SQRKRLHNA	SKLHLK SE G	FMKVLK CE VE	LMARMA TTID	SFTQ NOTRLV	VIIDGLDACE	QDKVLQ MLD T	VRVLF SKG PF
810	820	830	840	850	860	870	880
IAIFASDPHI	IIK AINQ LN	SVLR DSNING	HDYMRNIVHL	PVFLNSRGLS	NARKFLV TS A	TNGDVPCSDT	TGIQEDADRR
890	900	910	920	930	940	950	960
VSQNSLGEMT	KLGSKTALNR	RDTYRR RQ MQ	RTITRQMSFD	LTKLLVTE DW	FSDISPQ TMR	RLLNIVSVTG	RLLRANQISF
970	980	990	1000	1010	1020	1030	1040
NWDRLASW IN	LTE QWPYRTS	WLILYLEETE	GIPDQMTLKT	IYERISK NIP	TTKDVE P LE	IDGDIRN F EV	FLSSR TP VLV
1050	1060	1070	1080	1090	1100	1110	1120
ARDVKVFLPC	TVNLDPKLRE	IIADVRAARE	QISIGGLAYP	PLPLHEGPPR	APSGYSQPPS	VCSSTS F NGP	FAGGVVSPQP
1130	1140	1150	1160	1170	1180	1190	1200
HSSYSGMTG	PQHPFYNRPF	FAPYLYTPRY	YPGGSQHLIS	RPSVK TSLPR	DQNNGLE V IK	EDAAEGLSSP	TDSSRGSGPA
1210	1220	1230	1240	1250	1260	1270	1280
PGPVLLNSL	NVDAVCEK LK	QIEGLDQ SML	PQYCTTIK KA	NINGRVLAQ C	NIDELK KEM N	MNFGDWHLFR	STVLE MNAE
1290	1300	1310	1320	1330	1340	1350	1360
SHVVPEDPRF	LSESSSGPAP	HGEPARRASH	NELPHTELSS	QTPYTL NFSF	EELNTLGLDE	GAPRHS NLSW	QSQTR RTP SL
1370	1380	1390	1400	1410	1420	1430	1440
SSLNSQDSSI	EISKLT DKVQ	AEYRDAYREY	IAQMSQLEGG	PGSTTISGRS	SPHSTYMGQ	SSSGS SI HSN	LEQEK GK DSE
1450	1460	1470	1480	1490	1500	1510	1520
PKPDDGRKSF	LMKRGDVIDY	SSSGVST NDA	SPLDPITEED	EKSDQSGSKL	LPGKKSSERS	SLFQTDL KL K	G SLR YQKLP
1530	1540	1550	1560	1570	1580	1590	1600
SDEDESGTEE	SDNTPL LKDD	KDRKAEGKVE	RVPK SPE SA	EPIRTFIKAK	EYLS DAL LK	KDSSD S GVRS	SESS P NHSLH
1610	1620	1630	1640	1650	1660	1670	1680
NEVADDSQLE	KANLIELEDD	SHSGKRGIPH	SLSGLQDPII	ARMSICSEDK	KSPSECSLIA	SSPEENWPAC	QKAYLN R TP
1690	1700	1710	1720	1730	1740	1750	1760
STVTLN N NSA	PANRANQ N FD	EMEGIRETSQ	VILRPSS PN	P TTIQ N ENLK	SMTHKRSQ R S	SYTRL S KDPP	ELHAA S SES
1770	1780						
TGFGEERESI	L						

Coverage map for Ubiquitin conjugation factor E4 A

10	20	30	40	50	60	70	80
MTDQENNNNI	SSNPFAALFG	SLADAKQFAA	IQKEQLKQQS	DELPASPDDS	DNSVSESLDE	FDYSVAEISR	SFRSQQEICE
90	100	110	120	130	140	150	160
QLNINHMIQR	IFLITLDNSD	PSLKSGNGIP	SRCVYLEEMA	VELEDQDWLD	MSNVEQALFA	RLLLQDPGNH	LINMTSSTTL
170	180	190	200	210	220	230	240
NLSADDRDAGE	RHIFCYLYSC	FQRAKEEITK	VPENLLPFAV	QCRNLTVSNT	RTVLLTPEIY	VDQNIHEQLV	DLMLEAIQGA
250	260	270	280	290	300	310	320
HFEDVTEFLE	EVIEALILDE	EVRTFPEVMI	PVFDILLGRI	KDLELCQILL	YAYLDILLYF	TRQKDMAKVF	VEYIQPKDPT
330	340	350	360	370	380	390	400
NGQMYQKTLT	GVILSISCLL	KTPGVVENHG	YFLNPSRSP	QEIKVQEANI	HQFMAQFHEK	IYQMLKNLLQ	LSPETKHCIL
410	420	430	440	450	460	470	480
SWLGNCLHAN	AGRTKIWANQ	MPEIFFQMYA	SDAFFLNLGA	ALLKLCQPFC	KPRSSRLITF	NPTYCALKEL	NDEERKIKNV
490	500	510	520	530	540	550	560
HMRGLDKETC	LIPAVQEPKF	PQNYNLVTEN	LALTEYTYL	GFHRLHDQMV	KINQNLHRLQ	VAWRDAQQSS	SPAADNLRQ
570	580	590	600	610	620	630	640
FERLMTIYLS	TKTAMTEPQM	LQNCLNLQVS	MAVLLVQLAI	GNEGSQPIEL	TFPLPDGYSS	LAYVPEFFAD	NLGDFLIFLR
650	660	670	680	690	700	710	720
RFADDILETS	ADSLEHVLHF	ITIFTGSIER	MKNPHLRACL	AEVLEAVMPH	LDQTPNPLVS	SVFHRKRVFC	NFYAPQLAE
730	740	750	760	770	780	790	800
ALIKVFVDIE	FTGDPHQFEQ	KFNRYRRPMP	ILRYMWGTDI	YRESIKDLAD	YASKNLEAMN	PPLFLRFLNL	LMNDAIFLLD
810	820	830	840	850	860	870	880
EAIQYLSKIK	IQQIEKDRGE	WDSLTPPEAR	EKEAGLQMGF	QLARFHNIMS	NETIGTLAFL	TSEIKSLFVH	PFLAERIISM
890	900	910	920	930	940	950	960
LNYFLQHLVG	PKMGALKVKD	FSEFDKPPQ	LVSDICTIYL	NLGEENFCA	TVPKGRSYS	PTLFAQTVRV	LKKINKPGNM
970	980	990	1000	1010	1020	1030	1040
IMAFSNLAER	IKSLADLQQQ	EEETYADACD	EFLDPI MSTL	MCDPVLPS	RVTVDRSTIA	RHLLSDQTD	FNSPLTMDQ
1050	1060	1070					
IRPNTELKEK	IQRWLAERKQ	QKEQLE					

Coverage map for Exportin-7

10	20	30	40	50	60	70	80
MADHVQSLAQ	LENLCKQLYE	TTDTTRLQA	EKALVEFTNS	PDCLSKCQLL	LERGSSSYSQ	LLAATCLTKL	VSR TNNPLPL
90	100	110	120	130	140	150	160
EQR IDIRNYV	LNVLATRPKL	ATFVTQALIQ	LYARITKLGW	FDCQKDDYVF	RNAITDVTRF	LQDSVEYCII	GVTILSQLTN
170	180	190	200	210	220	230	240
EINQADTTHP	LTKHRKIASS	FRDSSLFDIF	TLSCNLLKQA	SGKNLNLNDE	SQHGLLMQLL	KLTHNCLNFD	FIGTSTDESS
250	260	270	280	290	300	310	320
DDLCTVQIPT	SWRSAFLDSS	TLQLFFDLYH	SIPPSFSPLV	LSCLVQIASV	RRSLFNNAER	AKFLSHLVDG	VKRILENPQS
330	340	350	360	370	380	390	400
LSDPNNYHEF	CRLLARLKSN	YQLGELVKVE	NYPEVIRLIA	NETVTSLQHW	EFAPNSVHYL	LSLWQRLAAS	VPYVKATEPH
410	420	430	440	450	460	470	480
MLETYTPPEVT	KAYITSRLES	VHIILRDGLE	DPLEDTGLVQ	QQLDQLSTIG	RCEYEKTCAL	LVQLFDQSAQ	SYQELLSAS
490	500	510	520	530	540	550	560
ASPMIAVQE	GRLTWLVYII	GAVIGGRVSF	ASTDEQDAMD	GELVCRVLQL	MNLTDSRLAQ	AGNEKLELAM	LSFFEQFRKI
570	580	590	600	610	620	630	640
YIGDQVQKSS	KLYRRLSEVL	GLNDETMVLS	VFIGKIITNL	KYWGRCEPIT	SKTLQLLNDL	SIGYSSVRKL	VKLSAVQFML
650	660	670	680	690	700	710	720
NNHT SEHFSF	LGIN NQSNLT	DMRCRTTFYT	ALGRLLMVDL	GEDEDQYEQF	MLPLTAAFEA	VAQMFSTNSF	NEQEAKRTLIV
730	740	750	760	770	780	790	800
GLVRDLRGIA	FAFNAKTSFM	MLFEWIYPSY	MPILQRAIEL	WYHDPACTTP	VKLMAELVH	NRS QRLQFDV	SSPNGILLFR
810	820	830	840	850	860	870	880
ETSKMITMYG	NRILTLGEVP	KDQVYALKLK	GISICFSMLK	AALSGSYVNF	GVFRLYGDDA	LDNALQTFIK	LLLSIPHSDL
890	900	910	920	930	940	950	960
LDYPKLSQSY	YSLEVLTDQ	HMNFIASLEP	HVIMYILSSI	SEGLTALDTM	VCTGCCSCLD	HIVTYLQKQL	SRSTK KRTTP
970	980	990	1000	1010	1020	1030	1040
LNQESDR FLH	IMQQHPEMIQ	QMLSTVLNII	IFEDCRNQWS	MSRPLLGLIL	LNEKYFSDLR	NSIVNSQPPE	KQQAMHL CFE
1050	1060	1070	1080	1090			
NLMEGIERNL	LTKNRDRFTQ	NLSAFRREVN	DSMKNSTYGV	NSNDMMS			

Coverage map for Conserved oligomeric Golgi complex subunit 5

10	20	30	40	50	60	70	80
MGWVGRRRD	SASPPGRSRS	AADDINPAPA	NMEGGGSVA	VAGLGARGSG	AAAATVRELL	QDGCYSDFLN	EDFDVKTYTS
90	100	110	120	130	140	150	160
QSIHQAVIAE	QLAKLAQGIS	QLDRELHLQV	VARHEDLLAQ	ATGIESLEGV	LQMMQTRIGA	LQGAVDRIKA	KIVEPYNKIV
170	180	190	200	210	220	230	240
ARTAQLARLQ	VACDLLRRII	RILNLSKRLQ	GQLQGGSRREI	TKAAQSLNEL	DYLSQGIDLS	GIEVIENDLL	FIARARLEVE
250	260	270	280	290	300	310	320
NQAKRLEQG	LETQNPTQVG	TALQVFYNLG	TLKDTITSVV	DGYCATLEEN	INSALDIKVL	TQPSQSAVRG	GPRSTMPTP
330	340	350	360	370	380	390	400
GNTAALRASL	WTNMEKLMDH	IYAVCGVQH	LQKVLAKKRD	PVSHICFIEE	IVKDGQPEIF	YTFWNSVTQA	LSSQFHMATN
410	420	430	440	450	460	470	480
SSMFLKQAFE	GEYPKLLRLY	NDLWKRLQY	SQHIQGNFNA	SGTTDLVVDL	QHMEDDAQDI	FIPKKPDYDP	EKALKDSLQP
490	500	510	520	530	540	550	560
YEAYLSKSL	SRLFDPINLV	FPPGGRNPPS	SDELDTGIKT	IASELNVAAV	DTNLTAVSK	NVAKTIQLYS	VKSEQLLPTQ
570	580	590	600	610	620	630	640
GDASQVIGPL	TEGQRRNVAV	VNSLYKLHQS	VTKAIHALME	NAVQPLTSTV	GDAIEAIIIT	MHQEDFGSGL	SSSGKPDVPC
650	660	670	680	690	700	710	720
SLYMKELQGF	IARVMSDYFK	HFECLDFVFD	NTEAIAQRAV	ELFIRHASLI	RPLGEGGKMR	LAADFAQMEI	AVGPFRRVRS
730	740	750	760	770	780	790	800
DLGKSYRMLR	SFRPLLQAS	EHVASSPALG	DVIPFSIIIQ	FLFTRAPAEI	KSPFQRAEWS	HTRFSQWLDD	HPSEKDRLLL
810	820	830	840				
IRGALEYVQ	SVRSREGKEF	APVYPIMVQL	LQKAMSALQ				

Coverage map for Conserved oligomeric Golgi complex subunit 7

10	20	30	40	50	60	70	80
MDFSKFLADD	FDVKEWINAA	FRAGSKEAAS	GKADGHAATL	VMKLQLFIQE	VNHAVEETSH	QALQNMPKVL	RDVEALKQEA
90	100	110	120	130	140	150	160
SFLKEQMILV	KEDIKKFEQD	TSQSMQVLVE	IDQVKSQMQL	AAESLQEADK	WSTLSADIEE	TFK TQDI AVI	SAK LTMQNS
170	180	190	200	210	220	230	240
LMLLVDPDY	SEKCVHLEAL	KNR LEALASP	QIVAAFTSQA	VDQSK VFVKV	FTEIDRMPQL	LAYYYKCHKV	QLLAAWQELC
250	260	270	280	290	300	310	320
QSDLSLDRQL	TGLYDALLGA	WHTQIQWATQ	VFQKPHEVVM	VLLIQTLGAL	MPSLPSCLSN	GVER AGPEQE	LTRLLEFYDA
330	340	350	360	370	380	390	400
TAHFAK GLEM	ALLPHLHEHN	LVKVTLELDA	VYDPYKPYQL	KYGDMEESNL	LIQMSAVPLE	HGEVIDCVQE	LSHSVNLKLF
410	420	430	440	450	460	470	480
LASAAVDRCV	RFTNGLGTCG	LLSALKSLFA	KYVSDFTSTL	QSIRK CKCLD	HIPPNSLFQE	DWTAFQNSIR	IATCGELLR
490	500	510	520	530	540	550	560
HCGDFEQQLA	NRILSTAGKY	LSDSCSPRSL	AGFQESILTD	KKNSAKNPWQ	EYNYLQKDNP	AEYASLMEIL	YTLKEKGSN
570	580	590	600	610	620	630	640
HNLLAAPRAA	L TRLNQQAHQ	LAFDSVFLRI	KQQLLLISKM	DSWNTAGIGE	TLTDELPAFS	LTPLEYISNI	GQYIMSLPLN
650	660	670	680	690	700	710	720
LEPFVTQEDS	ALELALHAGK	LFPPEQGDG	LPELDNMDN	WLGSIARATM	QTYCDAILQI	PELSPHSAKQ	LATDIDYLIN
730	740	750	760	770	780		
VMDALGLQPS	RTLQHI VTLL	KTRPEDYRQV	SKGLPRRLAT	TVATMRSVNY			

Coverage map for LETM1 and EF-hand domain-containing protein 1, mitochondrial

10	20	30	40	50	60	70	80
MASILLRSCR	GRAPARLPPP	PRYTVPRGSP	GDPAHLSCAS	TLGLRNCLNV	PFGCCTPIHP	VYTSSRGDHL	GCWALRPECL
90	100	110	120	130	140	150	160
RIVSRAPWTS	TSVGFVAVGP	QCLPVRGWHS	SRPVRDSDSV	EKSLKSLKDK	NK KLEGGPV	YSPPAEVVVK	KSLGQRVLDE
170	180	190	200	210	220	230	240
LKHYYHGFRLL	LWIDTKIAAR	MLWRILNGHS	LTRRERRQFL	RICADLFRLV	PFLVFVVVVPF	MEFLLPVAVK	LFPNMLPSTF
250	260	270	280	290	300	310	320
ETQSLKEERL	KKELRVKLEL	AKFLQDTIEE	MALKNKAAAG	SATKDFSVFF	QKIRETGERP	SNEEIMRFSK	LFEDELTLDN
330	340	350	360	370	380	390	400
LTRPQLVALC	KLLELQSIGT	NNFLRFQLTM	RLRSIKADDK	LIAEEGVDSL	NVKELQAACR	ARGMRALGVT	EDRLRGQLKQ
410	420	430	440	450	460	470	480
WLDLHLHQEI	PTSLILLSRA	MYLPDTLSPA	DQLKSTLQTL	PEIVAKEAQV	KVAEVEGEQV	DNKAKLEATL	QEEAAIQQEH
490	500	510	520	530	540	550	560
REKELQKRSE	VAKDFEPERV	VAAPQRPSTE	PQPEMPDITVL	QSETLKDITAP	VLEGLKEEEI	TKEEIDILSD	ACSKLQEQKK
570	580	590	600	610	620	630	640
SLTKEKEELE	LLKEDVDQYS	EDLQEIKKEL	SKTGEEKYVE	ESKASKRLTK	RVQQMIGQID	GLISQLEMDQ	QAGKLAPANG
650	660	670	680	690	700	710	720
MPTGENVISV	AELINAMQV	KHIPESK LTS	LAAALDENKD	GKVNIDDLVK	VIELVDKEDV	HISTSQVAEI	VATLEKEEKV
730	740						
EKEKAKEKA	EKEVAEVKS						

Coverage map for Eukaryotic translation initiation factor 3, subunit J

10	20	30	40	50	60	70	80
MAAAAAAGD	SDSWDADAFS	VEDPVRKVG	GGTAGGDRWE	GEDEDEDVKD	NWDDDDDEKK	EEAEVKPEVK	ISEKKKIAEK
90	100	110	120	130	140	150	160
IKEKERQKK	RQEEIKR LE	EPEEPKVLTP	EEQLADKLRL	KKLQEE SDLE	LAKETFGVNN	AVYGIDAMNP	SSRDDFTFEG
170	180	190	200	210	220	230	240
KLLDKITQY	EKSLYYASF	EVLVRDVCIS	LEIDDLK KIT	NSLTVLCSEK	QKQEKQSKAK	KKKKGVVPGG	GLKATMKDDL
250	260						
ADYGGYDGGY	VQDYEDFM						